

TE
662
.A3
no.
FHWA-RD-
80-028

Report No. FHWA/RD-80/028

NEW STRUCTURAL SYSTEMS FOR ROAD-MAINTENANCE PAVEMENTS

Vol. 3 Anchored Pavement System Designed for Edens Expressway

August 1980

Final Report



DEPARTMENT OF
TRANSPORTATION

JAN 14 1981

LIBRARY

Document is available to the public through
the National Technical Information Service,
Springfield, Virginia 22161



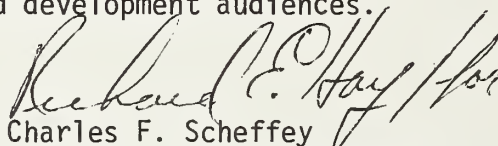
Prepared for
FEDERAL HIGHWAY ADMINISTRATION
Offices of Research & Development
Structures and Applied Mechanics Division
Washington, D.C. 20590

FOREWORD

This report illustrates the analysis and design of the anchored pavement concept to an actual pavement, the Edens Expressway in Chicago. The computer input parameters used in this analysis represented the vehicle loads and the mechanical and thermal properties of materials that could be encountered in future reconstruction of the Edens Expressway. The behavior of the anchored pavement subjected to these typical design values is clearly demonstrated. This illustration will enable the analysis and design of the anchored pavement concept for any set of road design specifications.

This report is the third volume of a set of three final reports resulting from a research contract, "New Structural Systems for Zero-Maintenance Pavements," issued to Dames & Moore by the Office of Research and Development of the Federal Highway Administration. The objective of this research study was to identify and assess the potential of new and innovative structural concepts and systems to serve as "Zero-Maintenance" pavements. An interim report, "Unique Concepts and Systems for Zero Maintenance Pavements," FHWA-RD-77-76, provides an updated state-of-the-art and comprehensive review of each of the three major structural components of a pavement system: the subgrade, the base and subbase, and the pavement surface. The other two volumes in this final set are reports FHWA/RD-80/026, Volume 1: Analytical and Experimental Studies of an Anchored Pavement, and FHWA/RD-80/027, Volume 2: Analysis of Anchored Pavements Using ANSYS. Volume 1 was published and distributed previously.

Copies of Volumes 2 and 3 are being distributed jointly by a single transmittal memorandum primarily to research and development audiences.


Charles F. Scheffey
Director, Office of Research
Federal Highway Administration

NOTICE

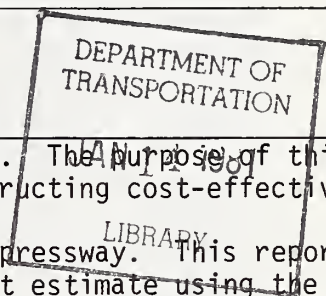
This document is disseminated under the sponsorship of the Department of Transportation in the interest of information exchange. The United States Government assumes no liability for its contents or use thereof.

The contents of this report reflect the views of the Dames & Moore organization which is responsible for the facts and the accuracy of the data presented herein. The contents do not necessarily reflect the official views or policy of the Department of Transportation.

This report does not constitute a standard, specification, or regulation.

The United States Government does not endorse products or manufacturers. Trademarks or manufacturers' names appear herein only because they are considered essential to the object of this document.

1. Report No. FHWA/RD-80/028	2. Government Accession No.	3. Recipient's Catalog No.	
4. Title and Subtitle NEW STRUCTURAL SYSTEMS FOR ZERO-MAINTENANCE PAVEMENTS Volume 3: Anchored Pavement System Designed for Edens Expressway		5. Report Date August 1980	6. Performing Organization Code
7. Author(s) S.K. Saxena and S.G. Militsopoulos		8. Performing Organization Report No.	
9. Performing Organization Name and Address Dames & Moore Illinois Institute of Technology 7101 Wisconsin Avenue Washington, D.C. 20014 and Civil Engineering Department Chicago, Illinois 60616		10. Work Unit No. (TRAIS) FCP 35E2-042	11. Contract or Grant No. DOT-FH-11-9114
12. Sponsoring Agency Name and Address Offices of Research and Development Federal Highway Administration U.S. Department of Transportation Washington, D.C. 20590		13. Type of Report and Period Covered Final Report	
15. Supplementary Notes FHWA Contract Manager: Dr. Floyd J. Stanek, HRS-14 Dames & Moore Project Manager: Dr. Mysore S. Nataraja		14. Sponsoring Agency Code	
<p>16. Abstract New Structural Systems for Zero-Maintenance Pavements. The purpose of this study is to investigate the feasibility of designing and constructing cost-effective "Zero-Maintenance" highways.</p> <p>Volume 3: Anchored Pavement System Designed for Edens Expressway. This report provides an analysis example of an actual pavement and the cost estimate using the anchored system. The actual pavement is the Edens Expressway in Chicago. The report provides the response of the Edens Expressway subjected to mechanical and environmental loads using the anchored pavement concept. The mechanical and thermal properties of materials that could be encountered in future reconstruction of Edens Expressway are presented in a consistent form for computer programming. These properties are viewed as typical design values during investigation of pavement response. The behavior of the anchored pavement under induced temperature loads and weakening of subgrade (by thawing action) is clearly demonstrated. This report will enable application of the anchored pavement concept by any road with heavy traffic. The example problem provides the input parameters of materials and loads for the analysis, the generation of finite element mesh, and the results of the analysis. The computer program ANSYS was used for this study (the manual for the use of this program is presented in Volume 2 of this series of reports).</p> <p>This volume is the third in a series. The others in the series are Volume 1: Analytical and Experimental Studies of an Anchored Pavement, and Volume 2: Analysis of Anchored Pavements Using ANSYS. Abstracts of these volumes are included on page ii.</p>			
17. Key Words Pavement systems Anchored pavement Edens Expressway, Chicago Zero Maintenance		18. Distribution Statement No restrictions. This document is available to the public through the National Technical Information Service, Springfield, Virginia 22161.	
19. Security Classif. (of this report) Unclassified	20. Security Classif. (of this page) Unclassified	21. No. of Pages 120	22. Price



Abstracts of Related Documents

Volume 1: Analytical and Experimental Studies of an Anchored Pavement: A Candidate Zero-Maintenance Pavement

This report documents an investigation of the design feasibility and construction cost-effectiveness of an anchored pavement concept for zero maintenance highways. An analytical model is designed to verify computer program results and to investigate construction methods for a full-scale highway section. The purpose of the analytical study is (1) to present thermal, mechanical, and thermomechanical properties of typical materials in a form easily adaptable to computer programs, and (2) to describe environmental and mechanical properties of a conventional slab and an anchored pavement in both continuous and jointed configurations. The two pavements were subject to heat transfer, thermal stress, and mechanical stress analyses. The anchored pavement offers two distinct advantages over a conventional pavement--deflections are lower and more uniform, and stresses in the soil are lower and distributed more widely by the rigid anchors. Subgrade-related failure is less likely to occur if loads are transmitted deeper within the subgrade. Three-dimensional finite element analysis is considered to be the most efficient technique for examining the significance of environmentally induced stress. The use of the finite element method is anticipated as more advanced analytic techniques are developed.

Volume 2: Analysis of Anchored Pavements Using ANSYS

This report is a manual which provides a set of procedures to evaluate the response of an anchored pavement subjected to vehicle static loads, moisture variation in the subgrade, and/or temperature variation through the surface of the pavement. These procedures include two computer programs known as FEMESH and ANSYS. The FEMESH program generates rectangular meshes in either a two or three dimensional coordinate system for any prespecified number and spacing of nodes. The ANSYS program evaluates the stresses, strains, and deflections at all elements in each material included in the analytical model. The program can be used for any number of different materials in any direction. In the analysis of heat transfer, the program provides the distribution of temperature as a function of time at predesignated points. The program is versatile and capable of solving complex geometrical structures supported on a geologically complex earth mass. The behavior of an anchored pavement section is evaluated with sets of computer programmed mechanistic models. The manual was written to minimize reference to other publications.

TABLE OF CONTENTS

	Page
CHAPTER 1 INTRODUCTION	1
1.1 OBJECTIVE	1
1.2 SCOPE	1
1.3 RELATED DOCUMENTS	2
CHAPTER 2 MATERIAL CHARACTERIZATION	3
2.1 CHICAGO SUBSOIL AND WEATHER	3
2.2 MECHANICAL PROPERTIES	5
2.3 THERMAL PROPERTIES	5
CHAPTER 3 LOAD CHARACTERIZATION	16
3.1 MECHANICAL LOADS	16
3.2 THERMAL LOADS	16
3.3 EFFECT OF CHANGING MOISTURE	16
CHAPTER 4 FINITE ELEMENT MESH GENERATION	20
4.1 EDENS EXPRESSWAY	20
4.2 THREE-DIMENSIONAL MESH	22
4.3 TWO-DIMENSIONAL MESH	25
CHAPTER 5 ANALYSIS OF LOADS	52
5.1 ANALYSIS OF MECHANICAL LOADS	52
5.2 ANALYSIS OF ENVIRONMENTAL LOADS	62
5.2.1 Moisture in Pavement System	62
5.2.2 Heat Transfer Results	63
5.2.3 Thermal Stress Analysis	63
5.3 SUPERPOSITION OF LOADS	83

TABLE OF CONTENTS (continued)

CHAPTER 6	GUIDELINES FOR CONSTRUCTION.	85
6.1	THE SUBGRADE AND BASE COURSE.	85
6.1.1	Excavation.	85
6.1.2	Proofrolling.	85
6.1.3	Backfill.	86
6.1.4	Fill.	86
6.1.5	Crushed Stone Foundation Course.	87
6.1.6	Filter Material.	88
6.2	THE ANCHORED PAVEMENT.	89
6.2.1	Anchors.	89
6.2.2	Slab	89
6.2.3	Joint.	91
CHAPTER 7	CONCLUSION.	93
REFERENCES.	94
APPENDIX A:	Metric Conversion Table*.	96
APPENDIX B:	Summary of Japanese Investigation of Shrinkage Effects.	97
APPENDIX C:	Constuction Costs Estimates.	98

*The units of measurement used in the design and construction of the Edens Expressway are shown in this report; that is, in English units only.

LIST OF TABLES

Table	Page
1. Material properties used in the static analysis.	12
2. Material properties used in the heat transfer model.	13
3. Material properties used in the thermal stress analysis.	15
4. Mesh dimensions in x-y plane	28
5. Material properties numbers in x-y plane	29
6. Clay properties at different layers used in finite element analysis	30
7. Node ordering in three-dimensional mesh.	31-40
8. Element reordering in three-dimensional mesh	41-49
9. Node ordering in two-dimensional mesh.	50
10. Element ordering in two-dimensional mesh	51
11. Metric Conversion Table.	96

LIST OF FIGURES

Figure	Page
1. Results of triaxial compression tests	4
2. Stress-strain curves.	6
3. Grain-size curve of upper clay deposits	7
4. Temperature distribution during January, February, and March 1977 (Chicago).	8
5. Temperature distribution during April, May, and June 1977 (Chicago)	9
6. Temperature distribution during July, August, and September 1977 (Chicago).	10
7. Temperature distribution during October, November, and December 1977 (Chicago)	11
8. Vehicle loading	17
9. Surface temperature input model used in heat transfer analysis	18
10. Effect of traffic on moisture content of subgrade soils (Lytton and Kher 1970).	19
11. Dimensions of Edens Expressway as an anchored pavement.	21
12. Perspective view of three-dimensional mesh.	23
13. Static load configuration and transverse lines where deflections are plotted	24
14. Two-dimensional mesh configuration.	26
15. Transverse surface deflection along line T1-R1.	53
16. Transverse surface deflection along line T2-R2.	54
17. Transverse surface deflection along line T3-R3.	55
18. Transverse surface deflection along line T4-R4.	56

LIST OF FIGURES (cont'd)

Figure	Page
19. Concrete bending stresses in z-direction.	57
20. Ballast vertical stresses	58
21. Ballast maximum shear stresses.	59
22. Soil vertical stress contours	60
23. Soil maximum shear stress contours.	61
24. Summer tautochrones at pavement traffic lane.	64
25. Summer tautochrones at pavement shoulder.	65
26. Summer tautochrones in natural soil	66
27. Winter tautochrones at pavement traffic lane.	67
28. Winter tautochrones at pavement shoulder.	68
29. Winter tautochrones in natural soil	69
30. Deflected shape of the pavement surface (summer condition).	71
31. Concrete bending stresses in x-direction (summer condition).	72
32. Ballast vertical stresses (summer condition).	73
33. Ballast maximum shear stresses (summer condition).	74
34. Soil vertical stress contours (summer condition).	75
35. Soil maximum shear stress contours (summer condition).	76
36. Deflected shape of the pavement surface (winter condition).	77
37. Concrete bending stresses in x-direction (winter condition).	78

LIST OF FIGURES (cont'd)

Figure	Page
38. Ballast vertical stresses (winter condition).	79
39. Ballast maximum shear stresses (winter condition).	80
40. Soil vertical stress contours (winter condition).	81
41. Soil maximum shear stress contours (winter condition).	82
42. Results of surface deflection load superposition. . .	90
43. Edens Expressway as an anchored pavement drainage configuration	90
44. Results of joint response to slab movement analysis. . .	92
45. Drainage Work for Anchored Pavement, Edens Expressway..	105

CHAPTER 1 INTRODUCTION

1.1 OBJECTIVE

The objective of this report is to provide an example for analysis of real life pavement using the anchored system and to provide guidelines for construction. The selected real life pavement is the Edens Expressway of Chicago. The report therefore provides the design engineer with a ready reference of procedures to obtain the response of Edens Expressway (using the anchored pavement concept) subject to mechanical and environmental loads. The construction guidelines are not site specific, but general.

1.2 SCOPE

The basic intent of this study is twofold. First, the mechanical and thermal properties of materials encountered in possible future construction of the Edens Expressway are presented in a consistent form, easily adaptable for input in computer programs. After a comprehensive search, these properties were compiled to ascertain typical actual values. Secondly, the pavement response is investigated.

The mechanical loads consist of vehicles static weight. The environmental loads consist of moisture variation in the subgrade and temperature regimes on the pavement surface. Extreme conditions such as hot summer and cold winter temperature variations are modelled. A heat transfer analysis of the pavement is performed in order to determine temperature distributions within the structural elements and the supporting subgrade.

A thermal stress analysis based upon the temperature distributions derived in the heat transfer analysis is conducted. The results from the mechanical stress analysis is superimposed on the results from the environmental stress analysis so that the relative magnitudes of displacements can be seen. Two-dimensional finite elements are used for heat transfer and thermal stress analysis. Three-dimensional finite elements are used for the static stress analysis. The finite element method is chosen for the analysis because of its versatility. The computer program with the acronym ANSYS for Engineering ANALYSIS SYSTEM developed by Swanson (1976) is used for the analysis.

Finally, the guidelines for construction of the anchored pavement system are presented. The guidelines are not site specific, but general and will have to be improved to provide detailed specifications. The investigation is reported in the following sequence:

1. INTRODUCTION
2. MATERIAL CHARACTERIZATION
3. LOAD CHARACTERIZATION

4. FINITE ELEMENT MESH GENERATION
5. ANALYSIS OF LOADS - MECHANICAL, ENVIRONMENTAL
AND SUPERPOSITION OF BOTH
6. GUIDELINES FOR CONSTRUCTION
7. CONCLUSION

Chapters 2, 3, and 4 describe the necessary steps for data collection, such as material properties, imposed loads, and geometry configuration. Chapter 5 outlines the result displacements and stresses from the mechanical stress, heat transfer, and thermal stress analysis. Chapter 6 describes the guidelines for construction as required for the subgrade, base course, anchors, slab, and joints. Appendix A contains a metric conversion table for the measurements used in this volume. Appendix B is a summary of the Japanese investigation of shrinkage effects. Appendix C contains a construction cost estimate at the current rates for the new anchored pavement concept. The estimate was prepared by a certified estimator who is a member of the American Association of Estimators.

1.3 RELATED DOCUMENTS

This document is developed so that it can be used with a minimal reference to other materials, with the exception of Volume 2: Analysis of Anchored Pavements Using ANSYS which is part of the series of reports entitled New Structural Systems for Zero Maintenance Pavements (Saxena and Militopoulos, 1979).

CHAPTER 2 MATERIAL CHARACTERIZATION

2.1 CHICAGO SUBSOIL AND WEATHER

The subsoil of the Chicago area consists of a series of glacial clays, each somewhat stiffer than the one above.

Beneath the downtown districts of Evanston and Chicago, the clays have very soft to medium consistencies in the top 30 to 50 feet thickness. They are underlain by stiff and hard clays which are usually encountered before bedrock is reached. Deposits of weathering sands and gravel are present near the rock. Beach sands are found above the clays in several areas, particularly within a strip about three miles wide near the lake. In some places, the sands are dense, whereas in others they are loose or of extremely variable relative density.

Almost all of the subsoil in the Chicago area was deposited during the glacial epoch. It consists of large masses of clay that were laid down by the great continental ice sheet. In much of the locality, the clay is overlain by sand deposited when glacial lakes extended over parts of the area. The clay consists of a series of several ground moraines or till sheets lying one on another. Each till sheet represents the clay deposited upon the preexisting surface by the advancing glacier plus that deposited from the melting ice as the glacial front receded. Altogether, six separate till sheets representing six advances and retreats of the ice front have been distinguished in the area.

The subsoil in the vicinity of the Edens Expressway is very soft to medium clay. This is treated as one unit and is designated as "compressible clay." It is convenient to define the compressible clay as that which has an unconfined compressive strength less than 1.0 ton per sq. ft.

The most extensive and precise series of tests for the "compressible clay" was carried out by Arthur Casagrande at Harvard University on samples furnished by the Department of Subways and Superhighways of Chicago. Quick, consolidated-quick, and slow triaxial compression tests were performed. The results are indicated in Figure 1 in the form of the rupture diagrams corresponding to the three test conditions.

The average values of the liquid limit, the plastic limit, the plasticity index and the water content are 32%, 17%, 14%, and 30% respectively. The average coefficient of consolidation was found to be 0.0123 sq. in. per min. with a variation from the average of +50%.

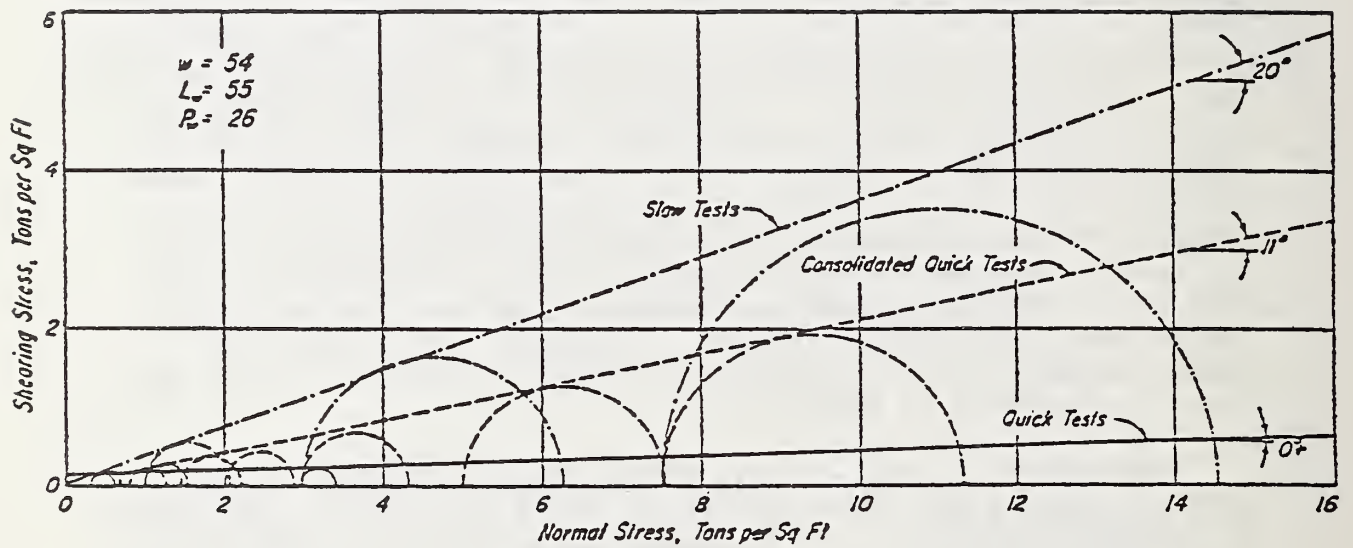


Figure 1. Results of triaxial compression tests

The specific gravity of solids of the "compressible clay" ranges from 2.70 to 2.80, with an average value of about 2.74. The sensitivity of the "compressible clay" is about 4. The stress-strain curves in Figure 2 indicate that the maximum shearing resistance of undisturbed samples is attained at small deformations. K. Terzaghi (1943) reported that the Chicago clay in an undisturbed state behaves like a solid material with a high modulus of elasticity. From Figure 2, the average modulus of elasticity of the "compressible clay" was found to be 500 psi. Figure 3 shows an average grain-size curve of upper "compressible clay" deposits.

In the Chicago area, the weather is highly variable with high winds, changing humidity, and extreme temperatures. Figures 4 thru 7 show the temperature variation for the year 1977 obtained for O'hare Airport. The coldest day was recorded on January 16, having the lowest temperature of -19°F . The hottest day was recorded in July 15, having the highest temperature of $+99^{\circ}\text{F}$. The freeze-thaw cycles, which produce moisture changes in the upper layer of clay, were noticed during the months of March and April. A typical freeze-thaw cycle (April 9) is shown in Figure 5.

2.2 MECHANICAL PROPERTIES

Mechanical strength properties used for ANSYS input (i.e. material properties) are the modulus of elasticity (E), the Poisson's ratio (ν), and the coefficient of linear expansion (α). A summary of the above properties for the fiber reinforced concrete, ballast, and soil (clay) is given in Table 1.

2.3 THERMAL PROPERTIES

Heat transfer is primarily a conduction phenomenon through soils. However, solar radiation and convection through air and liquids at the soil surface as well as convection of heat through vapor, soil, and liquid interfaces within the pore structure do occur.

For the heat transfer analysis, three material properties are required: heat capacity (Cv), conductivity (K), and density (γ). Heat capacity is defined as the quantity of heat necessary to produce a unit change in temperature for a unit mass. Conductivity is a measure of the ease with which heat can flow through a material. Variations of the above properties with temperature are not considered in the present heat transfer analysis. Table 2 summarizes the above properties for the fiber reinforced concrete, ballast, and soil (clay).

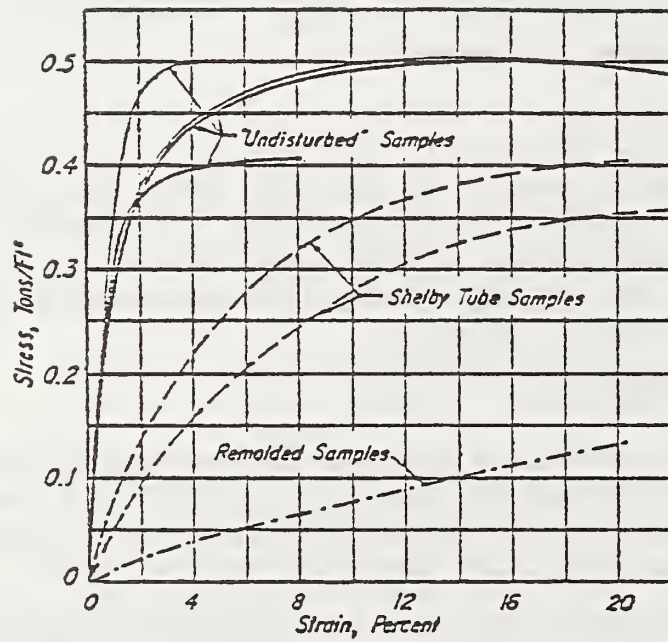


Figure 2. Stress-strain curves

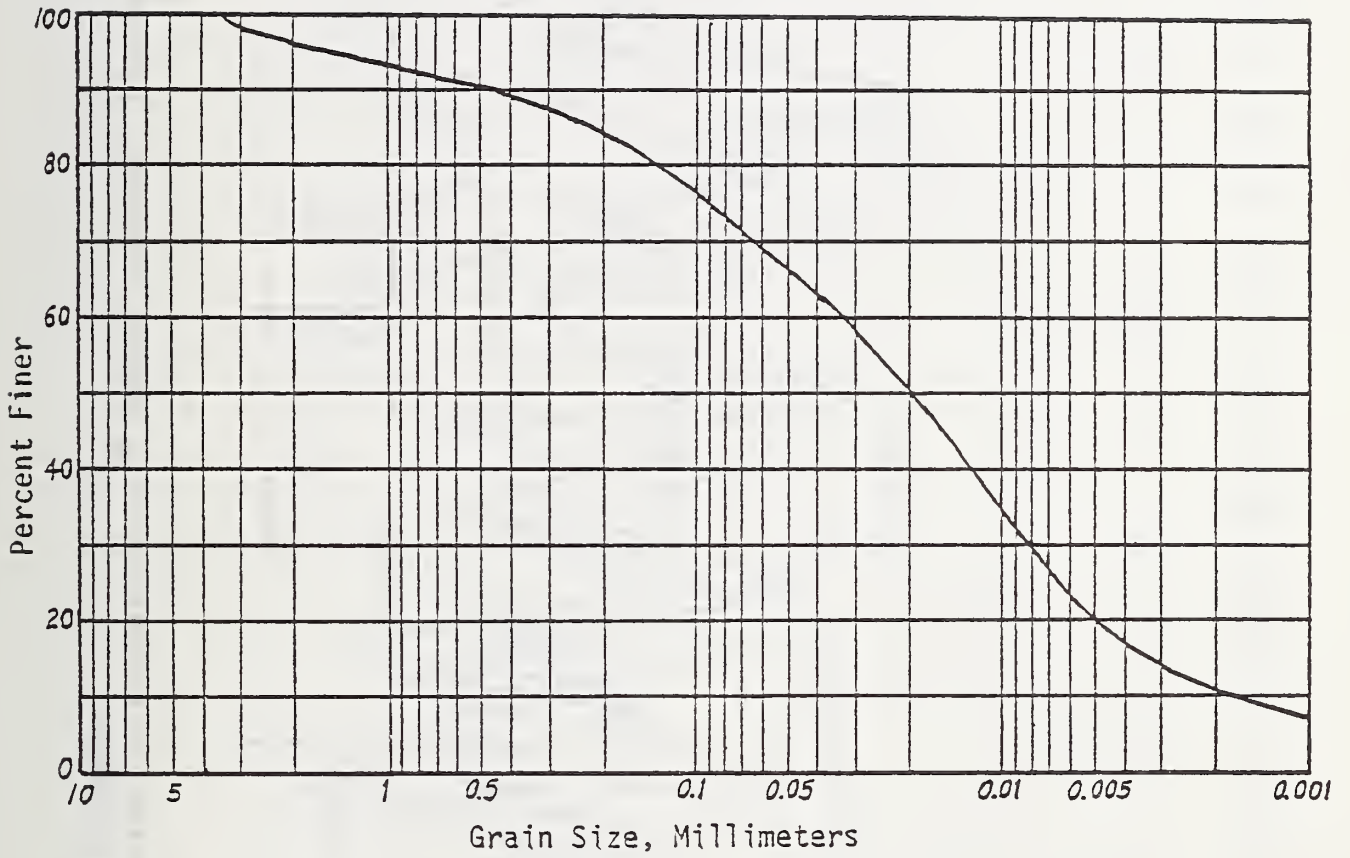


Figure 3. Grain-size curve of upper clay deposits

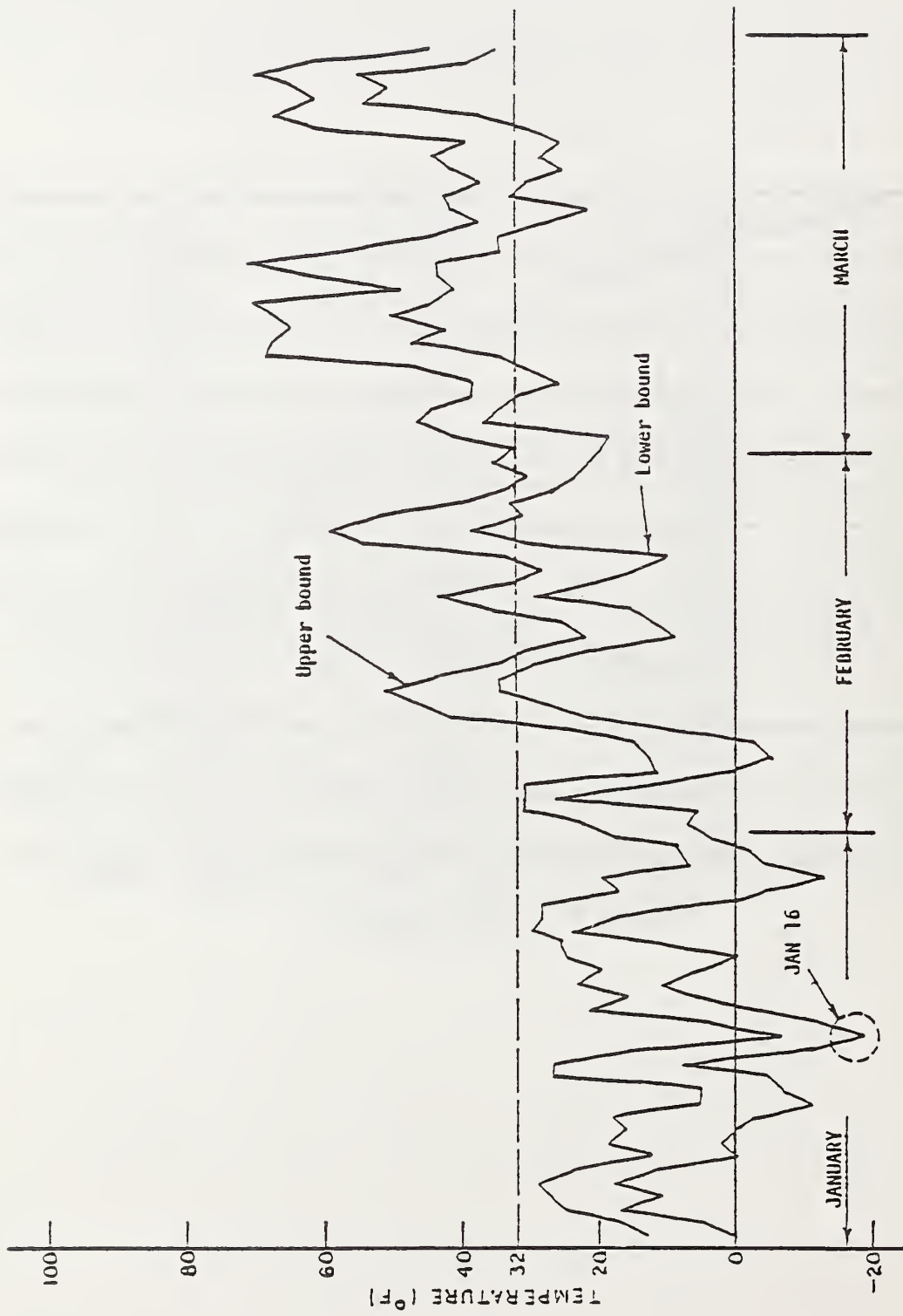


Figure 4. Temperature distribution during January, February, and March 1977 (Chicago)

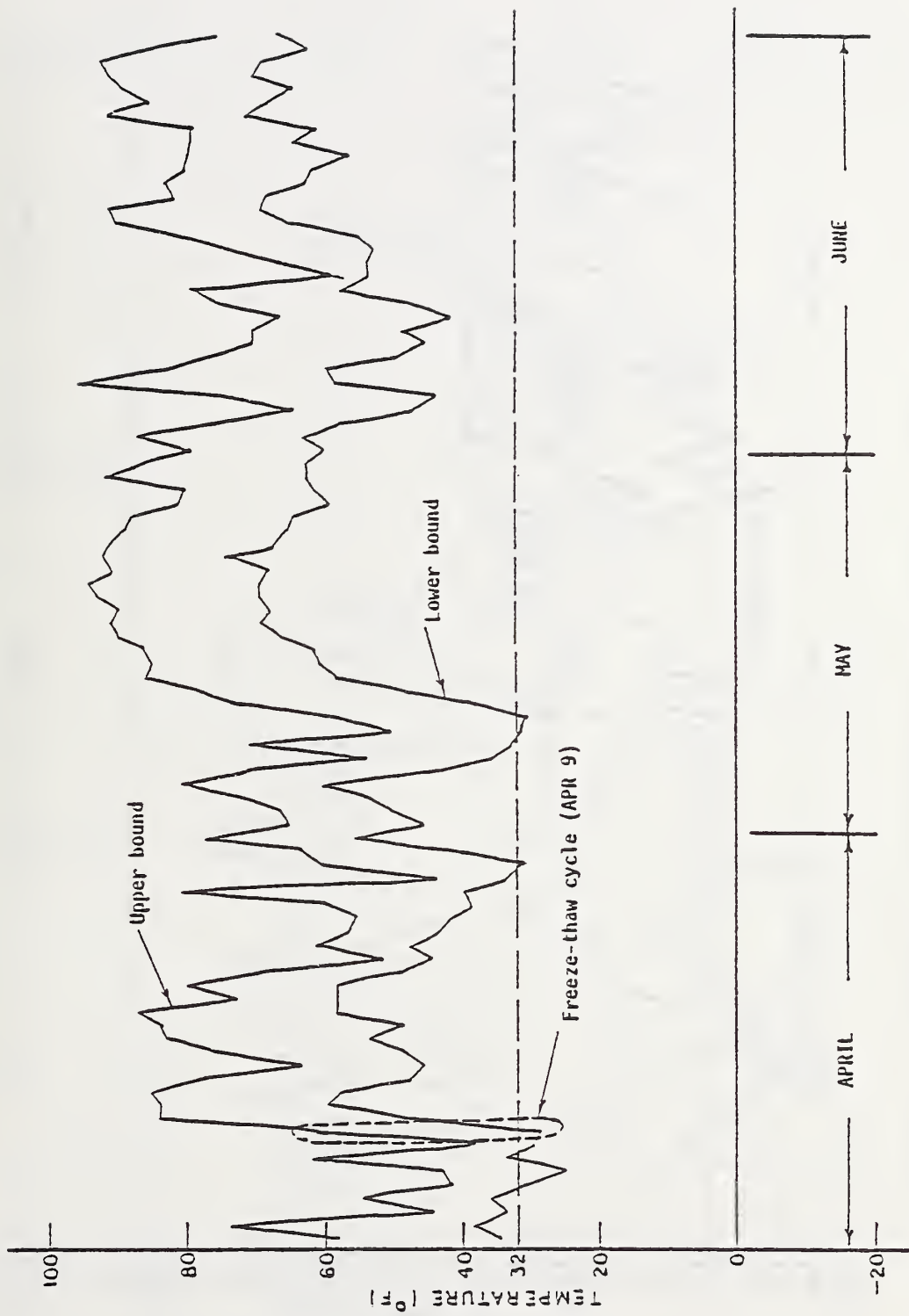


Figure 5. Temperature distribution during April, May, and June 1977 (Chicago)

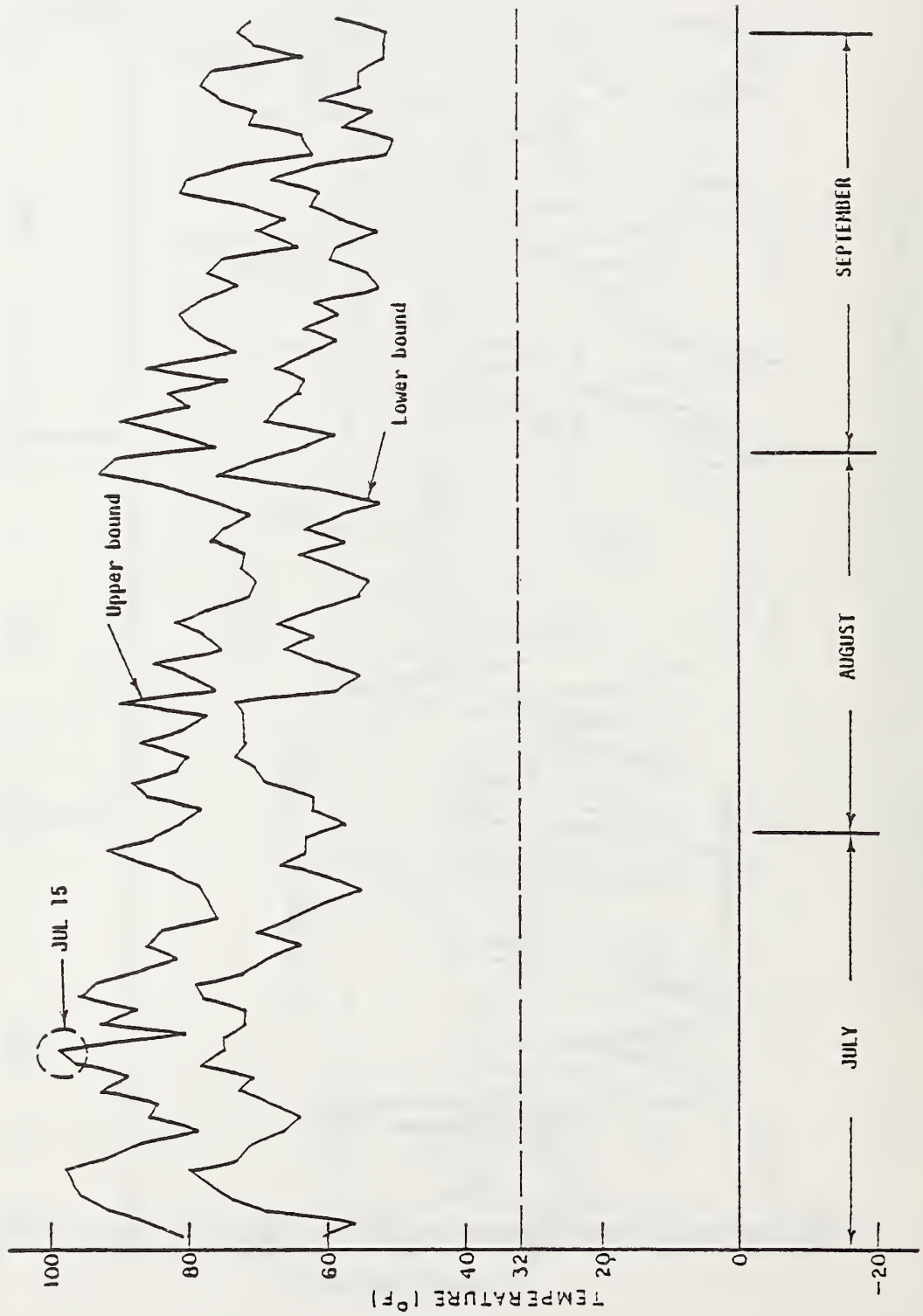


Figure 6. Temperature distribution during July, August, and September 1977 (Chicago)

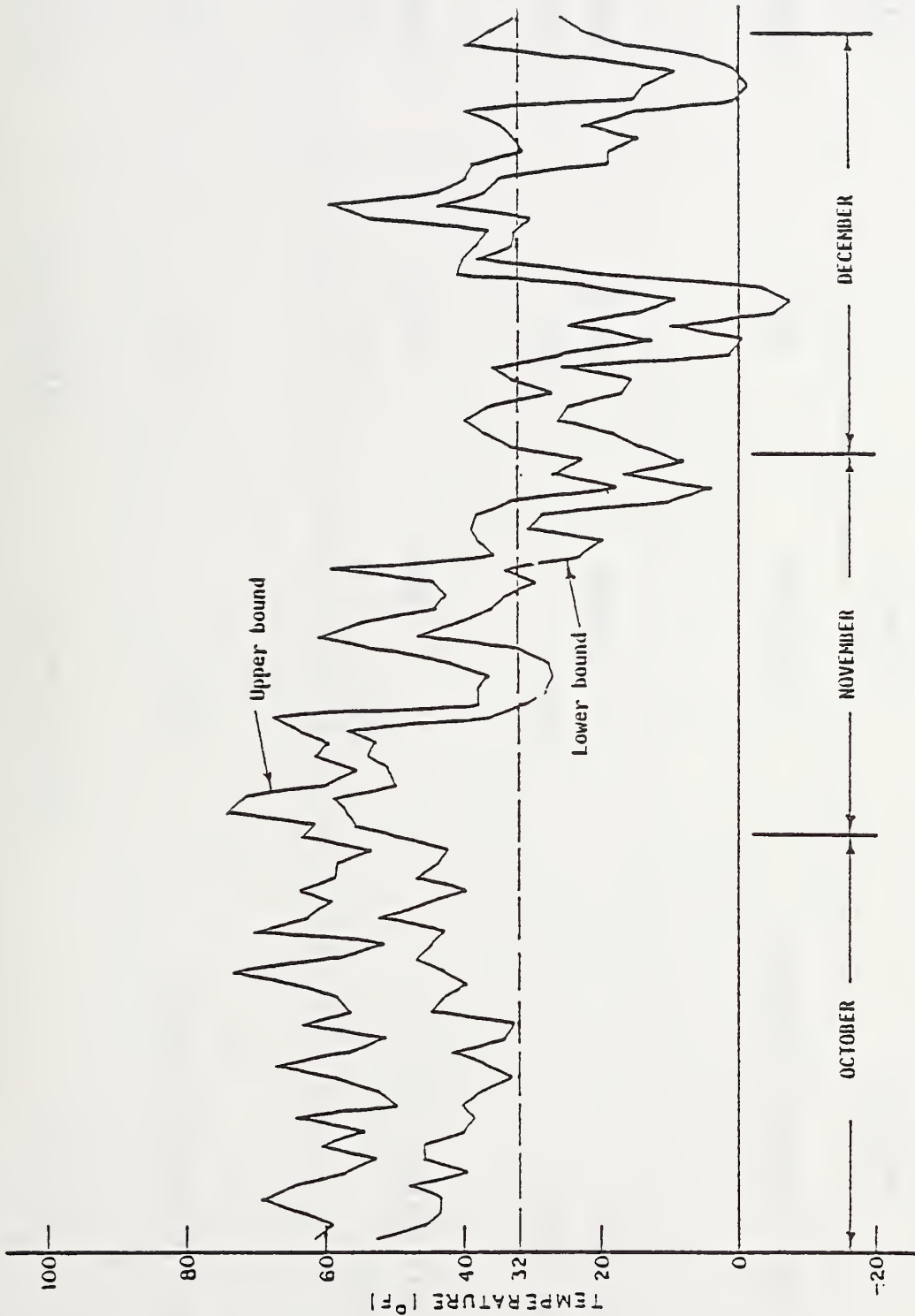


Figure 7. Temperature distribution during October, November, and December 1977 (Chicago)

Table 1. Material properties used in the static analysis

Material	E (psi)	$\alpha(1/^\circ\text{F})$
Fiber reinforced concrete	5,000,000	0.0000055
Ballast	25,000	0.0000075
Soil (Clay)	500	0.0000090

Table 2. Material properties used in the heat transfer model

Material	$K(\text{BTU}/\text{HR}-\text{IN}-^\circ\text{F})$	$c_v(\text{BTU}/\text{LBM}-^\circ\text{F})$	$\gamma(\text{LB}/\text{IN}^3)$
Fiber reinforced concrete	0.073	0.160	0.082
Ballast	0.093	0.267	0.075
Soil (Clay)	0.059	0.345	0.067

Mechanical strength properties of the materials used within pavement systems vary with temperature. This temperature dependence is important during a thermal stress analysis and reflects material behavior of the system that may be greatly different over different temperature ranges. The temperature dependent strength properties used in this investigation are the elastic modulus (E), the Poisson's ratio (ν), and the coefficient of linear expansion of the material under a uniform temperature gradient (Table 3).

Table 3. Material properties used in the thermal stress analysis

Material	Temperature (°F)	E (psf)	ν	α (1/°F)
Fiber reinforced concrete	-22	8,000,000	0.20	0.0000055
	0	*	*	*
	32	*	*	*
	70	5,000,000	0.20	0.0000055
Ballast	70	25,000	0.35	0.0000075
Soil (Clay)	-22	3,500	0.35	0.0000060
	0	3,300	0.38	0.0000090
	32	.600	0.40	*
	70	500	0.45	0.0000090
	120	400	0.45	0.0005000

CHAPTER 3 LOAD CHARACTERIZATION

3.1 MECHANICAL LOADS

Pavements are subject to axle weight distributions produced by the traffic volume. Vehicle speed and load duration are not included in this analysis. The load input consists only of the static weight of vehicular traffic, and the corresponding response is evaluated. Static load can be input as nodal forces or element surface pressures. The nodal forces were used, in order to minimize the elements of the mesh, and therefore, the computer cost.

Two kinds of vehicles were used: a truck and a passenger car (Fig. 8). The five-axle truck is 30 feet long, 7 feet wide, and weights 85,000 lbs. The two-axle passenger car is 9 feet long, 5 feet wide, and weights 4,000 lbs.

3.2 THERMAL LOADS

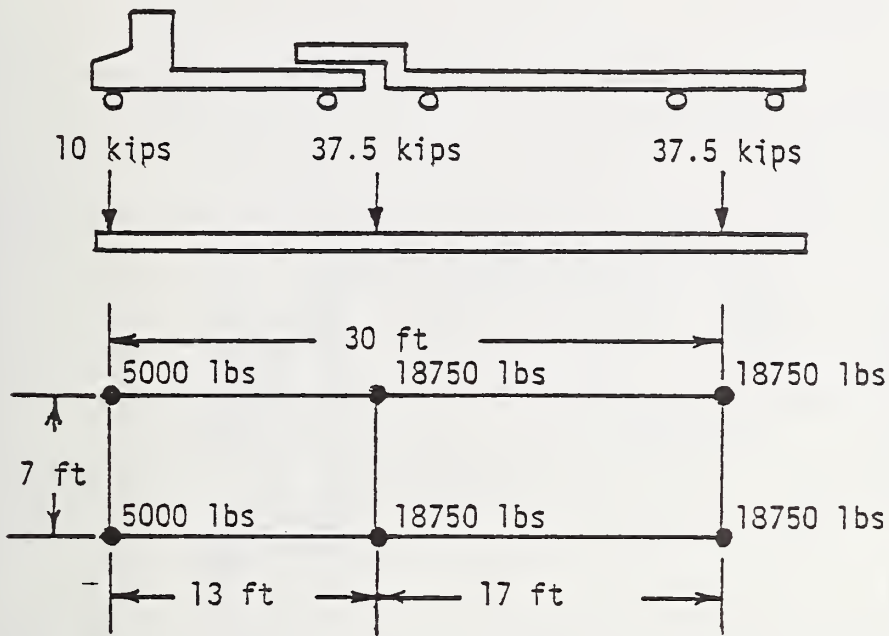
Surface temperature is closely linked to the ambient air temperature. As air temperature increases, surface temperature increases with very little, if any, phase difference or time lag. But, there is a difference between the soil and the pavement surface temperature, the latter being 20% higher (in absolute value) than the former.

Usually, the soil surface temperature is taken equal to the air temperature. Summer and winter daily temperature histories are shown in Figure 9 for both soil and pavement surfaces. The winter model attempts to generate a freeze-thaw cycle within the system, most of the temperature history being subfreezing.

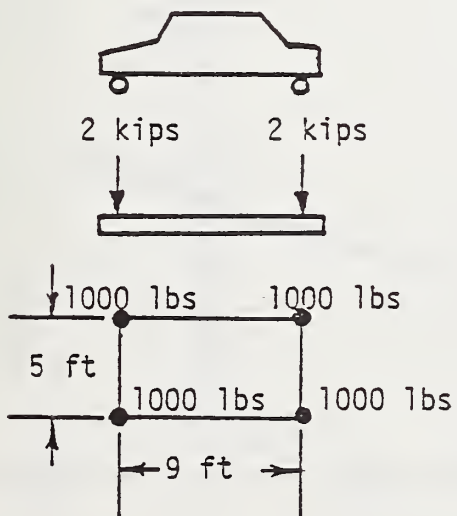
3.3 EFFECT OF CHANGING MOISTURE

The changing distribution of moisture within the load bearing layers of pavement systems result in variable behavior of the system under applied loads. Mechanical and thermal properties of soil depend significantly upon moisture content. The moisture content of the clay is altered when the pavement is constructed. Figure 10 shows the variation in water content of a soil subgrade before and after 80 days of traffic. The pounding of the pavement by the dynamic vehicle loads as well as the alternation in thermal behavior of the system creates the increase in moisture content near the surface, in this case, within three to four feet.

In sensitive clays, small changes in water content greatly alter the strength characteristics. Moisture content in freeze/thaw areas is greatest in the thaw period, then the critical condition to study is the period of rapid strength loss in spring with a higher moisture content and lower strength. Modulus of the clay decreases under such conditions, and Poisson's ratio approaches a value of 0.5. For that case (April 9, 1977) the modulus of elasticity of the "compressible clay" is reduced to 100 psi for the top four feet.



Truck loading



Passenger car loading

Figure 8. Vehicle loading

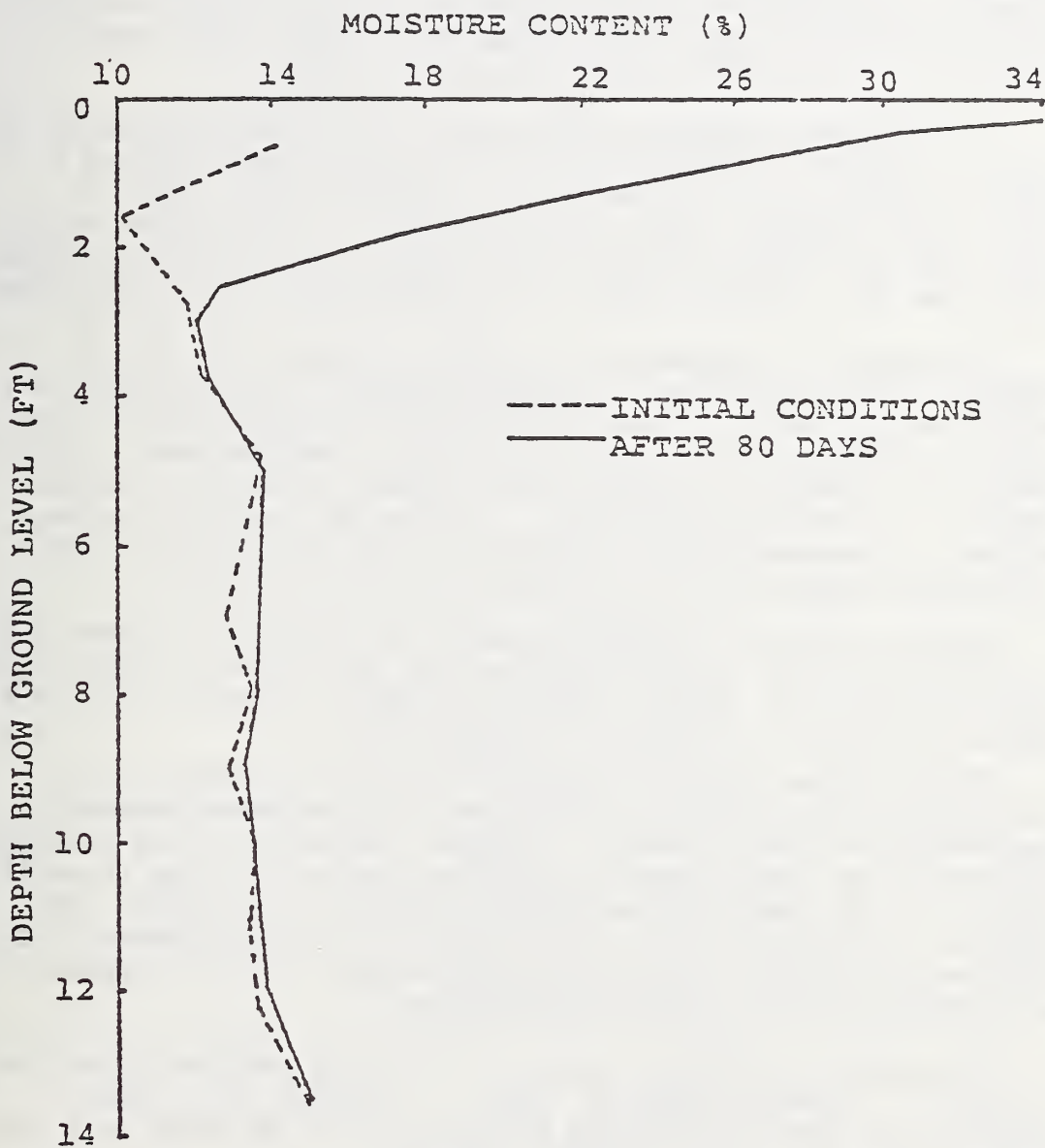


Figure 10. Effect of traffic on moisture content of subgrade soils (Lytton and Kher 1970)

CHAPTER 4
FINITE ELEMENT MESH GENERATION

4.1 EDENS EXPRESSWAY

The part of the Interstate 94 or Edens Expressway under consideration in this report starts from the north-east (about the intersection of Montrose Avenue and Cicero Avenue) to the north-west (about the intersection of Clavey Road and Skokie Road) of Chicago. The geometric configuration of the north bound of Edens Expressway is identical to the south one. Thus, it was considered necessary that only one of the bounds be analyzed. Each bound consists of three traffic lanes and two shoulders.

The anchored pavement configuration of the Edens Expressway is shown in Figure 11. Each traffic lane and the right shoulder is 12 feet wide, while the left shoulder is 9 feet wide. There are totally four anchors, which are 4 feet deep. The two right anchors are 2 feet wide, while the two left anchors are 1 foot wide. Each anchor has two capitals, which are 10 inches wide and 6 inches deep.

The material recommended for use in pavement construction is the steel fiber reinforced concrete, because of its high tensile and ultimate strength. A ballast subbase is recommended for two reasons. First, it distributes the vehicle pressure over a large area of soil mass and relieves a great amount of stress from the top layer of the soil. Secondly, it serves as a natural drainage device. The mechanical and the thermal properties of the fiber reinforced concrete and the ballast are given in Chapter 2.

Tables 4 through 10 are discussed in the following sections and are shown at the end of Chapter 4 (see page 28 for Table 4, page 29 for Table 5, page 30 for Table 6, page 31 for Table 7, page 41 for Table 8, page 50 for Table 9, and page 51 for Table 10).

Table 4 shows the dimensions of the finite elements of the mesh which simulates the cross-section of the anchored pavement, the subbase and the subgrade. The gross dimensions of the anchored pavement of the Edens Expressway are the same as the ones shown in Figure 11. The depth of the subbase (ballast) is 6 inches. The subgrade is 57.5 feet deep and 317 feet wide. The thickness of the interface elements, which connect the pavement with the subbase, was adopted as 0.001 inches in the analysis.

The material property numbers in the cross-sectional are given in Table 5. Material property number "1" through "5" is the "compressible clay," "6" is the ballast, "7" is the fiber reinforced concrete, and "8" is the interface elements.

Table 6 outlines the change of the modulus of elasticity (E) and the Poisson's ratio (ν) of the "compressible clay" with depth. It may be noted that as depth increases, the modulus of elasticity increases and the Poisson's ratio decreases.

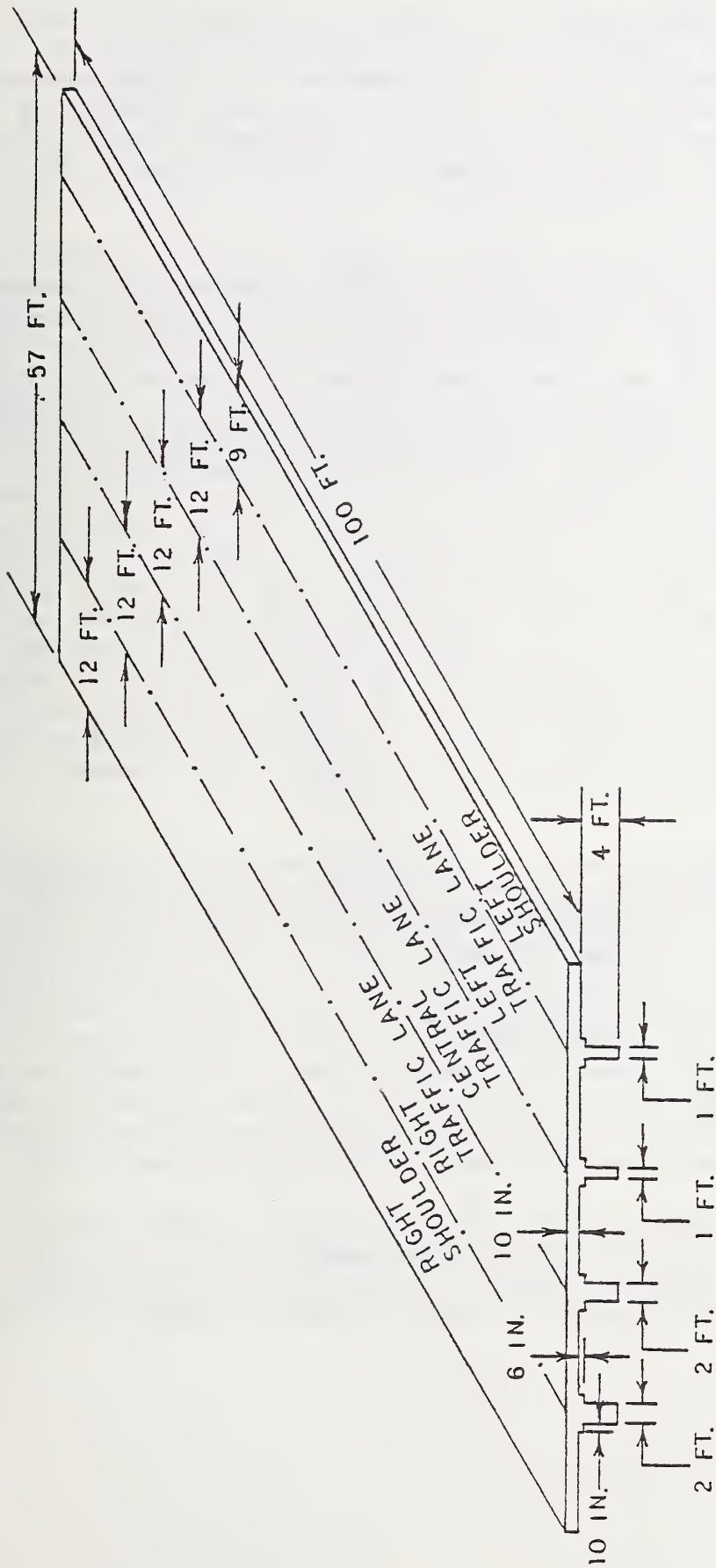


Figure 11. Dimensions of Edens expressway as an anchored pavement

4.2 THREE-DIMENSIONAL MESH

The finite element method was chosen for the analysis because of its versatility. Figure 12 shows a perspective view of the three-dimensional mesh of Eden's expressway as an anchored pavement. A total of 2,440 nodes and 1,745 elements were used to model the pavement/soil system. Three-dimensional isoparametric solid elements (STIF45) were used to simulate the concrete pavement, the ballast subbase and the clay subgrade.

From the ANSYS element library, it was felt that the three-dimensional interface elements (STIF52) best represent the pavement/soil interaction. The three-dimensional interface element represents two parallel surfaces in space which may maintain or break physical contact and may slide relative to each other. The element is capable of supporting only compression in the direction normal to the surfaces (it breaks physical contact on tension) and shear (Coulomb friction) in the tangential directions. The element has three degrees of freedom at each node: translations in the nodal x, y, and z directions. The element may be initially preloaded in the normal direction or it may be given a gap specification. A specified stiffness acts in the normal and tangential directions when the gap is closed and not sliding. Because of its nonlinearity of the element, an iterative solution is required. The interface elements were used to connect the concrete pavement with the ballast subbase. The gap is initially close, the coefficient of friction is 0.6 and the specified stiffness is 10,000 lbs./in. The primary purpose of this study is to investigate the effects of vehicle loads - termed mechanical loads.

Figure 13 shows the vehicle load configuration and the transverse lines (T1-R1, T2-R2, T3,R3, T4,R4) where deflections are plotted. Two identical trucks and a passenger car were used on the right, central, and left traffic lane correspondingly. Each tire was simulated by a single concentrated load (See Fig. 8). It is realized that vehicle loads are distributed over several square inches of area, but this poses a problem in three-dimensional analysis. A huge number of additional elements would be required and the analysis would be extremely costly. The single concentrated load does represent a worse case and stresses in the immediate vicinity of the load will tend to be higher than those resulting from a distributed pressure load.

The program "FEMESH" (Saxena and Militsopoulos, 1979) was used to generate the nodes (F-cards) and the elements (E1-cards) of the three-dimensional mesh for "ANSYS." The reason being that "FEMESH" has the capability of generating specified material numbers by layers,

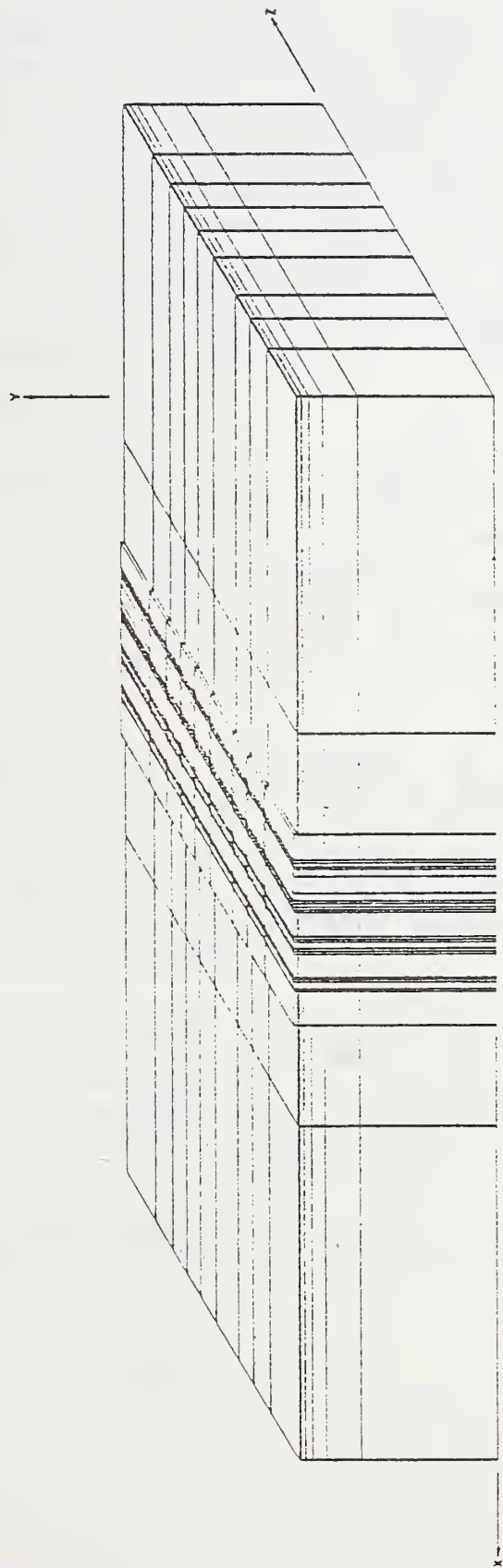


Figure 12. Perspective view of three-dimensional mesh

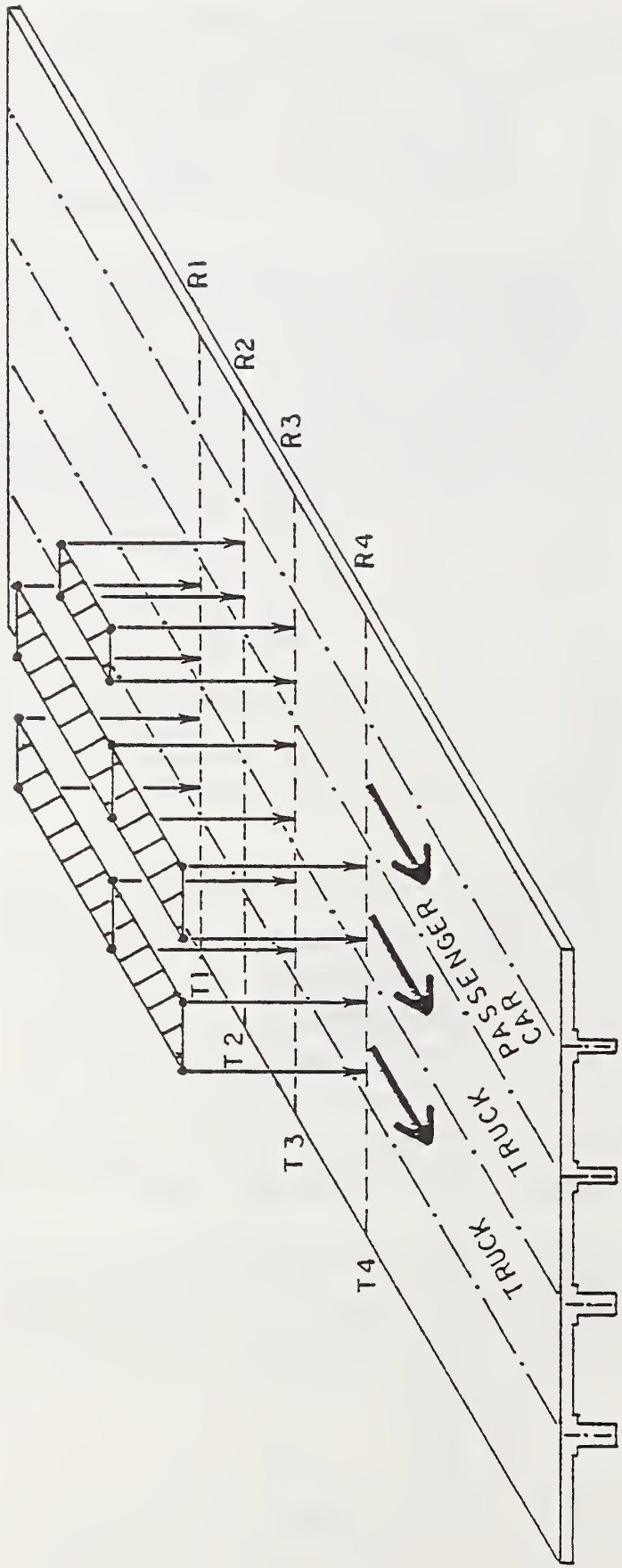


Figure 13. Static load configuration and transverse lines where deflections are plotted

in the increasing y-direction of the x-y plane. Second, note that the present restriction of ANSYS is that the maximum wave front size is 576. The wave front size is the product of the area of nodes of the wave front by the number of degrees of freedom per node.

Both the isoparametric solid elements and the three-dimensional interface elements have 3 degrees of freedom per node. The number of nodes in the x-direction is 28, in the y-direction is 9, and in the z-direction is 10. Thus, the wave front size for the x-y plane is 756 (28x9x3), for the y-z plane is 270 (9x10x3), and for z-x plane is 840 (10x28x3). Therefore, the only choice we have is to use the y-z plane as the wave front. The node ordering and the element reordering are given in Tables 7 and 8 respectively. Note that the nodes need not be reordered, because there is no "band width" limitation in the problem definition. The three-dimensional static analysis was used with both normal and weak (with increased moisture) subgrade.

4.3 TWO-DIMENSIONAL MESH

The two-dimensional mesh was used in the heat transfer analysis and the thermal stress analysis. The two-dimensional approach was used not only because the iterative heat transfer solution is extremely costly for a three-dimensional case, but because the temperature distribution is constant over the length of the pavement; and thus produces a constant deflection and stress contours over the length of a continuous pavement. Figure 14 shows the two-dimensional mesh configuration.

The program "FEMESH" was used again to generate the nodes (F-cards) and the elements (E1-cards) of the two-dimensional mesh for "ANSYS." A total of 244 nodes and 193 elements were used to model the soil/pavement system. The number of nodes in the x-direction is 28, and in the y-direction is 9; the geometry configuration being the same as the one of the cross-section (x-y plane) of the three-dimensional mesh.

For the heat transfer model, isoparametric quadrilateral temperature elements (STIF 55) were used to simulate the concrete pavement, the ballast subbase, and the clay subgrade. The two-dimensional conducting bar elements (STIF 32) best represent the pavement/soil interaction for the heat transfer analysis. The required real constant for the conducting bar is the area, which was set equal to

NOTE: However, changes are required for the generated element cards to confirm with the material properties.

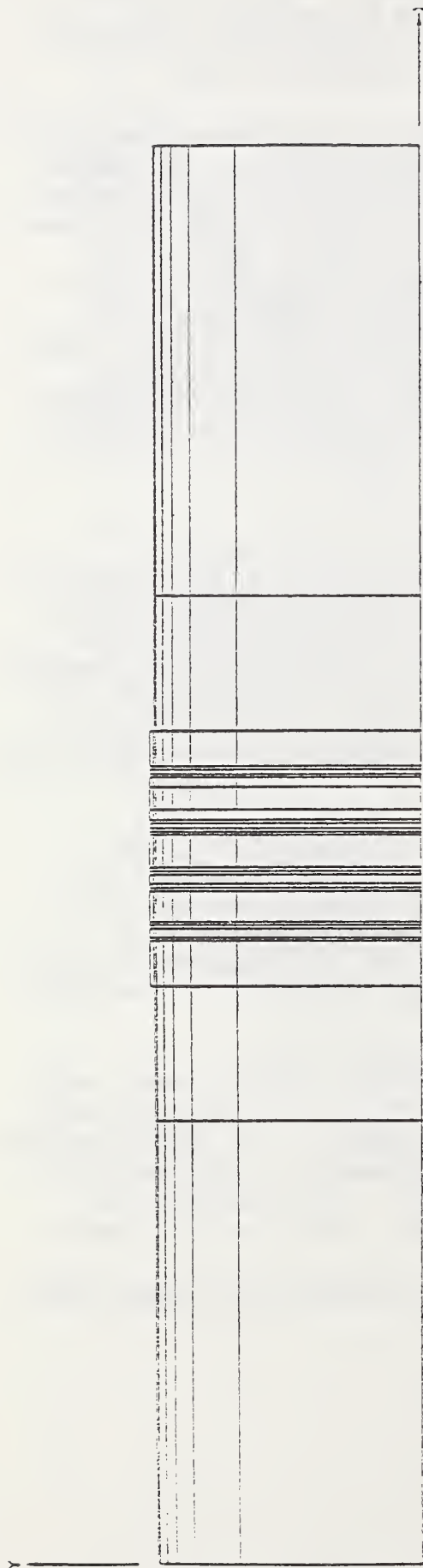


Figure 14. Two-dimensional mesh configuration

24 in.². Both the isoparametric quadrilateral elements and the conducting bar elements have 1 degree of freedom per node. The wave front size is the product of the line of nodes of the wave by the number of degrees of freedom per node. Thus, the wave front size for z-direction is 28 (28x1), and for the y-direction is 9 (9x1). The output wave front of "FEMESH" is in the y-direction, which coincides with the optimum wave front.

For the thermal stress model, two-dimensional isoparametric elements (STIF 42) were used to simulate the concrete pavement, the ballast subbase, and the subgrade. The two-dimensional interface element (STIF 12) best represents the pavement/soil interaction for the thermal stress analysis. Both the two-dimensional isoparametric elements and the two-dimensional interface elements have 2 degrees of freedom per node. Therefore, the wave front size for x-direction is 56 (28x2), and for the y-direction is 18 (9x2). The output wave front of "FEMESH" (same as in heat transfer analysis) is in the y-direction, which coincides with the optimum wave front. The node and the element ordering are given in Tables 9 and 10 respectively.

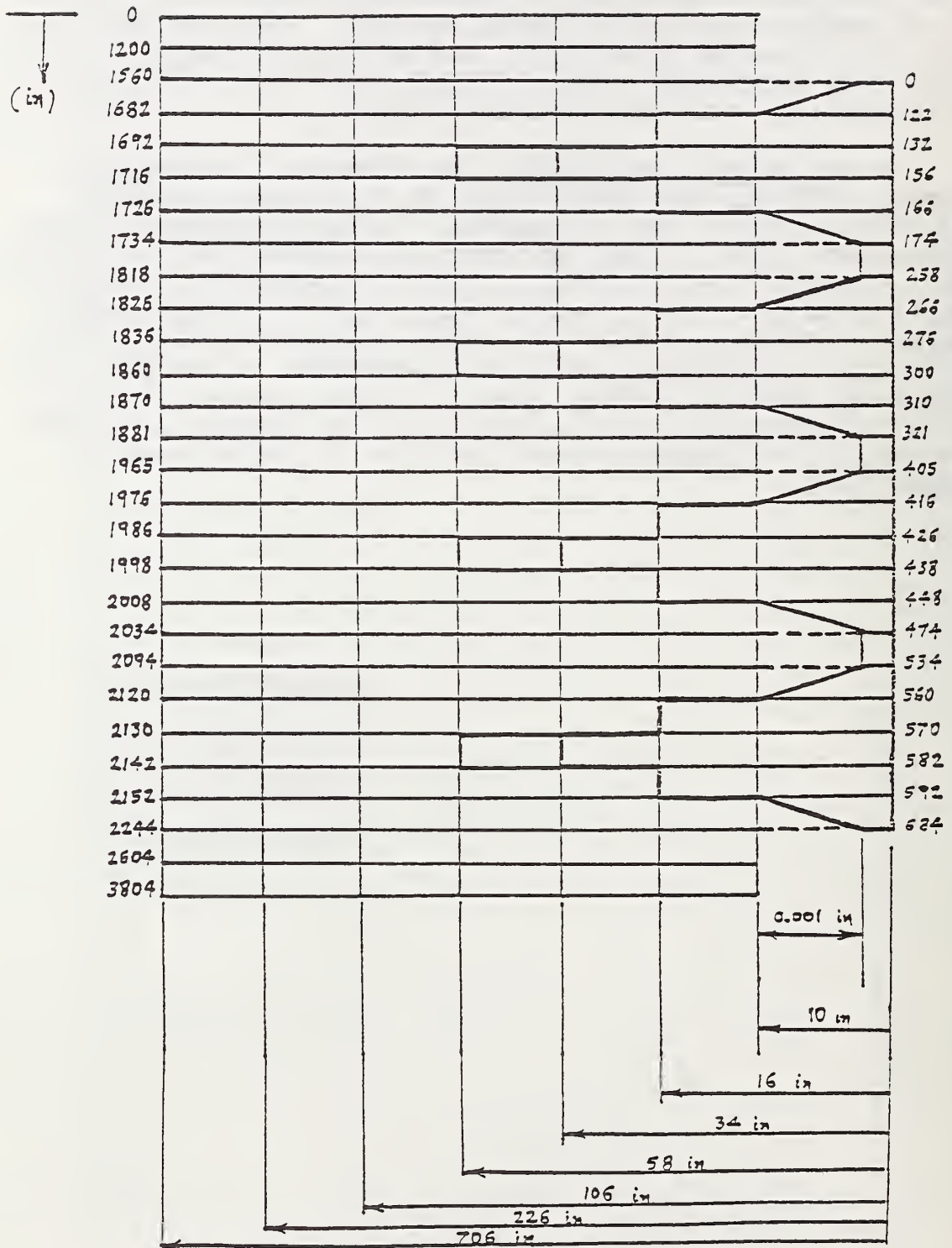


Table 4. Mesh dimensions in x-y plane

Table 6. Clay properties at different layers used in the finite element analysis

Layer	E (psi)	ν
1	3000	0.38
2	2000	0.38
3	1000	0.40
4	500*	0.42
5	500*	0.45

*Use 100 psi during thaw time (considerable moisture change).

Table 7. Node ordering in three-dimensional mesh

190	191	192	193	194	195	196	
183	184	185	186	187	188	189	
176	177	178	179	180	181	182	2007
169	170	171	172	173	174	175	2008
162	163	164	165	166	167	168	2006
155	156	157	158	159	160	161	2004
148	149	150	151	152	153	154	2002
141	142	143	144	145	146	147	2000
134	135	136	137	138	139	140	1997
127	128	129	130	131	132	133	1998
120	121	122	123	124	125	126	1996
113	114	115	116	117	118	119	1994
106	107	108	109	110	111	112	1992
99	100	101	102	103	104	105	1990
92	93	94	95	96	97	98	1988
85	86	87	88	89	90	91	1985
78	79	80	81	82	83	84	1986
71	72	73	74	75	76	77	1984
64	65	66	67	68	69	70	1983
57	58	59	60	61	62	63	1982
50	51	52	53	54	55	56	1980
43	44	45	46	47	48	49	1978
36	37	38	39	40	41	42	1976
29	30	31	32	33	34	35	1974
22	23	24	25	26	27	28	1973
15	16	17	18	19	20	21	1972
8	9	10	11	12	13	14	1971
1	2	3	4	5	6	7	1970
							1968
							1966
							1964
							1962
							1961

$Z = 0.$

Table 7. Node ordering in three-dimensional mesh (cont'd)

386	387	388	389	390	391	392		
379	380	381	382	383	384	385		
372	373	374	375	376	377	378	2055	2056
365	366	367	368	369	370	371		2054
358	359	360	361	362	363	364		2052
351	352	353	354	355	356	357		2050
344	345	346	347	348	349	350		2048
337	338	339	340	341	342	343	2045	2046
330	331	332	333	334	335	336		2044
323	324	325	326	327	328	329	2043	2042
316	317	318	319	320	321	322		2040
309	310	311	312	313	314	315		2038
302	303	304	305	306	307	308		2036
295	296	297	298	299	300	301	2033	2034
288	289	290	291	292	293	294		2032
281	282	283	284	285	286	287	2031	2030
274	275	276	277	278	279	280		2028
267	268	269	270	271	272	273		2026
260	261	262	263	264	265	266		2024
253	254	255	256	257	258	259	2021	2022
246	247	248	249	250	251	252		2020
239	240	241	242	243	244	245	2019	2018
232	233	234	235	236	237	238		2016
225	226	227	228	229	230	231		2014
218	219	220	221	222	223	224		2012
211	212	213	214	215	216	217		2010
204	205	206	207	208	209	210	2009	
197	198	199	200	201	202	203		

Z = 200.

Table 7. Node ordering in three-dimensional mesh (cont'd)

582	583	584	585	586	587	588	
575	576	577	578	579	580	581	
568	569	570	571	572	573	574	2103
561	562	563	564	565	566	567	2104
554	555	556	557	558	559	560	2102
547	548	549	550	551	552	553	2100
540	541	542	543	544	545	546	2098
533	534	535	536	537	538	539	2096
526	527	528	529	530	531	532	2094
519	520	521	522	523	524	525	2092
512	513	514	515	516	517	518	2091
505	506	507	508	509	510	511	2090
498	499	500	501	502	503	504	2088
491	492	493	494	495	496	497	2086
484	485	486	487	488	489	490	2084
477	478	479	480	481	482	483	2082
470	471	472	473	474	475	476	2081
463	464	465	466	467	468	469	2080
456	457	458	459	460	461	462	2079
449	450	451	452	453	454	455	2078
442	443	444	445	446	447	448	2076
435	436	437	438	439	440	441	2074
428	429	430	431	432	433	434	2072
421	422	423	424	425	426	427	2070
414	415	416	417	418	419	420	2069
407	408	409	410	411	412	413	2068
400	401	402	403	404	405	406	2067
393	394	395	396	397	398	399	2066
							2064
							2062
							2060
							2058
							2057

Z = 320.

Table 7. Node ordering in three-dimensional mesh (cont'd)

778	779	780	781	782	783	784		
771	772	773	774	775	776	777		
764	765	766	767	768	769	770	2151	2152
757	758	759	760	761	762	763		2150
750	751	752	753	754	755	756		2148
743	744	745	746	747	748	749		2146
736	737	738	739	740	741	742		2144
729	730	731	732	733	734	735	2141	2142
722	723	724	725	726	727	728		2140
715	716	717	718	719	720	721	2139	2138
708	709	710	711	712	713	714		2136
701	702	703	704	705	706	707		2134
694	695	696	697	698	699	700		2132
687	688	689	690	691	692	693	2129	2130
680	681	682	683	684	685	686		2128
673	674	675	676	677	678	679	2127	2126
666	667	668	669	670	671	672		2124
659	660	661	662	663	664	665		2122
652	653	654	655	656	657	658		2120
645	646	647	648	649	650	651	2117	2118
638	639	640	641	642	643	644		2116
631	632	633	634	635	636	637	2115	2114
624	625	626	627	628	629	630		2112
617	618	619	620	621	622	623		2110
610	611	612	613	614	615	616		2108
603	604	605	606	607	608	609		2106
596	597	598	599	600	601	602	2105	
589	590	591	592	593	594	595		

$Z = 420.$

Table 7. Node ordering in three-dimensional mesh (cont'd)

974	975	976	977	978	979	980		
967	968	969	970	971	972	973		
960	961	962	963	964	965	966	2199	2200
953	954	955	956	957	958	959		2198
946	947	948	949	950	951	952		2196
939	940	941	942	943	944	945		2194
932	933	934	935	936	937	938		2192
925	926	927	928	929	930	931	2189	2190
918	919	920	921	922	923	924		2188
911	912	913	914	915	916	917	2187	2186
904	905	906	907	908	909	910		2184
897	898	899	900	901	902	903		2182
890	891	892	893	894	895	896		2180
883	884	885	886	887	888	889	2177	2178
876	877	878	879	880	881	882		2176
869	870	871	872	873	874	875	2175	2174
862	863	864	865	866	867	868		2172
855	856	857	858	859	860	861		2170
848	849	850	851	852	853	854		2168
841	842	843	844	845	846	847	2165	2166
834	835	836	837	838	839	840		2164
827	828	829	830	831	832	833	2163	2162
820	821	822	823	824	825	826		2160
813	814	815	816	817	818	819		2158
806	807	808	809	810	811	812		2156
799	800	801	802	803	804	805		2154
792	793	794	795	796	797	798	2153	
785	786	787	788	789	790	791		

$z = 576.$

Table 7. Node ordering in three-dimensional mesh (cont'd)

1170	1171	1172	1173	1174	1175	1176		
1163	1164	1165	1166	1167	1168	1169		
1156	1157	1158	1159	1160	1161	1162	2247	2248
1149	1150	1151	1152	1153	1154	1155		2246
1142	1143	1144	1145	1146	1147	1148		2244
1135	1136	1137	1138	1139	1140	1141		2242
1128	1129	1130	1131	1132	1133	1134		2240
1121	1122	1123	1124	1125	1126	1127	2237	2238
1114	1115	1116	1117	1118	1119	1120		2236
1107	1108	1109	1110	1111	1112	1113	2235	2234
1100	1101	1102	1103	1104	1105	1106		2232
1093	1094	1095	1096	1097	1098	1099		2230
1086	1087	1088	1089	1090	1091	1092		2228
1079	1080	1081	1082	1083	1084	1085	2225	2226
1072	1073	1074	1075	1076	1077	1078		2224
1065	1066	1067	1068	1069	1070	1071	2223	2222
1058	1059	1060	1061	1062	1063	1064		2220
1051	1052	1053	1054	1055	1056	1057		2218
1044	1045	1046	1047	1048	1049	1050		2216
1037	1038	1039	1040	1041	1042	1043	2213	2214
1030	1031	1032	1033	1034	1035	1036		2212
1023	1024	1025	1026	1027	1028	1029	2211	2210
1016	1017	1018	1019	1020	1021	1022		2208
1009	1010	1011	1012	1013	1014	1015		2206
1002	1003	1004	1005	1006	1007	1008		2204
995	996	997	998	999	1000	1001		2202
988	989	990	991	992	993	994	2201	
981	982	983	984	985	986	987		

$Z = 684.$

Table 7. Node ordering in three-dimensional mesh (cont'd)

1366	1367	1368	1369	1370	1371	1372		
1359	1360	1361	1362	1363	1364	1365		
1352	1353	1354	1355	1356	1357	1358	2295	2296
1345	1346	1347	1348	1349	1350	1351		2294
1338	1339	1340	1341	1342	1343	1344		2292
1331	1332	1333	1334	1335	1336	1337		2290
1324	1325	1326	1327	1328	1329	1330		2288
1317	1318	1319	1320	1321	1322	1323	2285	2286
1310	1311	1312	1313	1314	1315	1316		2284
1303	1304	1305	1306	1307	1308	1309	2283	2282
1296	1297	1298	1299	1300	1301	1302		2280
1289	1290	1291	1292	1293	1294	1295		2278
1282	1283	1284	1285	1286	1287	1288		2276
1275	1276	1277	1278	1279	1280	1281	2273	2274
1268	1269	1270	1271	1272	1273	1274		2272
1261	1262	1263	1264	1265	1266	1267	2271	2270
1254	1255	1256	1257	1258	1259	1260		2268
1247	1248	1249	1250	1251	1252	1253		2266
1240	1241	1242	1243	1244	1245	1246		2264
1233	1234	1235	1236	1237	1238	1239	2261	2262
1226	1227	1228	1229	1230	1231	1232		2260
1219	1220	1221	1222	1223	1224	1225	2259	2258
1212	1213	1214	1215	1216	1217	1218		2256
1205	1206	1207	1208	1209	1210	1211		2254
1198	1199	1200	1201	1202	1203	1204		2252
1191	1192	1193	1194	1195	1196	1197		2250
1184	1185	1186	1187	1188	1189	1190	2249	
1177	1178	1179	1180	1181	1182	1183		

Z = 780.

Table 7. Node ordering in three-dimensional mesh (cont'd)

1562	1563	1564	1565	1566	1567	1568		
1555	1556	1557	1558	1559	1560	1561		
1548	1549	1550	1551	1552	1553	1554	2343	2344
1541	1542	1543	1544	1545	1546	1547		2342
1534	1535	1536	1537	1538	1539	1540		2340
1527	1528	1529	1530	1531	1532	1533		2338
1520	1521	1522	1523	1524	1525	1526		2336
1513	1514	1515	1516	1517	1518	1519	2333	2334
1506	1507	1508	1509	1510	1511	1512		2332
1499	1500	1501	1502	1503	1504	1505	2331	2330
1492	1493	1494	1495	1496	1497	1498		2328
1485	1486	1487	1488	1489	1490	1491		2326
1478	1479	1480	1481	1482	1483	1484		2324
1471	1472	1473	1474	1475	1476	1477	2321	2322
1464	1465	1466	1467	1468	1469	1470		2320
1457	1458	1459	1460	1461	1462	1463	2319	2318
1450	1451	1452	1453	1454	1455	1456		2316
1443	1444	1445	1446	1447	1448	1449		2314
1436	1437	1438	1439	1440	1441	1442		2312
1429	1430	1431	1432	1433	1434	1435	2309	2310
1422	1423	1424	1425	1426	1427	1428		2308
1415	1416	1417	1418	1419	1420	1421	2307	2306
1408	1409	1410	1411	1412	1413	1414		2304
1401	1402	1403	1404	1405	1406	1407		2302
1394	1395	1396	1397	1398	1399	1400		2300
1387	1388	1389	1390	1391	1392	1393		2298
1380	1381	1382	1383	1384	1385	1386	2297	
1373	1374	1375	1376	1377	1378	1379		

Z = 880.

Table 7. Node ordering in three-dimensional mesh (cont'd)

1758	1759	1760	1761	1762	1763	1764		
1751	1752	1753	1754	1755	1756	1757		
1744	1745	1746	1747	1748	1749	1750	2391	2392
1737	1738	1739	1740	1741	1742	1743		2390
1730	1731	1732	1733	1734	1735	1736		2388
1723	1724	1725	1726	1727	1728	1729		2386
1716	1717	1718	1719	1720	1721	1722		2384
1709	1710	1711	1712	1713	1714	1715	2381	2382
1702	1703	1704	1705	1706	1707	1708		2380
1695	1696	1697	1698	1699	1700	1701	2379	2378
1688	1689	1690	1691	1692	1693	1694		2376
1681	1682	1683	1684	1685	1686	1687		2374
1674	1675	1676	1677	1678	1679	1680		2372
1667	1668	1669	1670	1671	1672	1673	2369	2370
1660	1661	1662	1663	1664	1665	1666		2368
1653	1654	1655	1656	1657	1658	1659	2367	2366
1646	1647	1648	1649	1650	1651	1652		2364
1639	1640	1641	1642	1643	1644	1645		2362
1632	1633	1634	1635	1636	1637	1638		2360
1625	1626	1627	1628	1629	1630	1631	2357	2358
1618	1619	1620	1621	1622	1623	1624		2356
1611	1612	1613	1614	1615	1616	1617	2355	2354
1604	1605	1606	1607	1608	1609	1610		2352
1597	1598	1599	1600	1601	1602	1603		2350
1590	1591	1592	1593	1594	1595	1596		2348
1583	1584	1585	1586	1587	1588	1589		2346
1576	1577	1578	1579	1580	1581	1582	2345	2346
1569	1570	1571	1572	1573	1574	1575		

Z = 1000.

Table 7. Node ordering in three-dimensional mesh (cont'd)

1954	1955	1956	1957	1958	1959	1960		
1947	1948	1949	1950	1951	1952	1953		
1940	1941	1942	1943	1944	1945	1946	2439	2440
1933	1934	1935	1936	1937	1938	1939		2438
1926	1927	1928	1929	1930	1931	1932		2436
1919	1920	1921	1922	1923	1924	1925		2434
1912	1913	1914	1915	1916	1917	1918		2432
1905	1906	1907	1908	1909	1910	1911	2429	2430
1898	1899	1900	1901	1902	1903	1904		2428
1891	1892	1893	1894	1895	1896	1897	2427	2426
1884	1885	1886	1887	1888	1889	1890		2424
1877	1878	1879	1880	1881	1882	1883		2422
1870	1871	1872	1873	1874	1875	1876		2420
1863	1864	1865	1866	1867	1868	1869	2417	2418
1856	1857	1858	1859	1860	1861	1862		2416
1849	1850	1851	1852	1853	1854	1855	2415	2414
1842	1843	1844	1845	1846	1847	1848		2412
1835	1836	1837	1838	1839	1840	1841		2410
1828	1829	1830	1831	1832	1833	1834		2408
1821	1822	1823	1824	1825	1826	1827	2405	2406
1814	1815	1816	1817	1818	1819	1820		2404
1807	1808	1809	1810	1811	1812	1813	2403	2402
1800	1801	1802	1803	1804	1805	1806		2400
1793	1794	1795	1796	1797	1798	1799		2398
1786	1787	1788	1789	1790	1791	1792		2396
1779	1780	1781	1782	1783	1784	1785		2394
1772	1773	1774	1775	1776	1777	1778	2393	2394
1765	1766	1767	1768	1769	1770	1771		

Z = 1200.

Table 8. Element reordering in three-dimensional mesh

1740	1741	1742	1743	1744	1745		
1686	1687	1688	1689	1690	1691		
1630	1631	1632	1633	1634	1635	1636	1637
1558	1559	1560	1561	1562	1563		1564
1495	1496	1497	1498	1499	1500		1501
1432	1433	1434	1435	1436	1437		1438
1369	1370	1371	1372	1373	1374		1375
1305	1306	1307	1308	1309	1310	1311	1312
1232	1233	1234	1235	1236	1237	1238	1239
1160	1161	1162	1163	1164	1165		1166
1097	1098	1099	1100	1101	1102		1103
1034	1035	1036	1037	1038	1039		1040
971	972	973	974	975	976		977
907	908	909	910	911	912	913	914
834	835	836	837	838	839	840	841
762	763	764	765	766	767		768
699	700	701	702	703	704		705
636	637	638	639	640	641		642
573	574	575	576	577	578		579
509	510	511	512	513	514	515	516
436	437	438	439	440	441	442	443
364	365	366	367	368	369		370
301	302	303	304	305	306		307
238	239	240	241	242	243		244
175	176	177	178	179	180		181
112	113	114	115	116	117	118	
49	50	51	52	53	54		

$$0. \leq Z \leq 200.$$

Table 8. Element reordering in three-dimensional mesh (cont'd)

1734	1735	1736	1737	1738	1739		
1680	1681	1682	1683	1684	1685		
1622	1623	1624	1625	1626	1627	1628	1629
1551	1552	1553	1554	1555	1556	1557	
1488	1489	1490	1491	1492	1493	1494	
1425	1426	1427	1428	1429	1430	1431	
1362	1363	1364	1365	1366	1367	1368	
1297	1298	1299	1300	1301	1302	1303	1304
1224	1225	1226	1227	1228	1229	1230	1231
1153	1154	1155	1156	1157	1158	1159	
1090	1091	1092	1093	1094	1095	1096	
1027	1028	1029	1030	1031	1032	1033	
964	965	966	967	968	969	970	
899	900	901	902	903	904	905	906
826	827	828	829	830	831	832	833
755	756	757	758	759	760	761	
692	693	694	695	696	697	698	
629	630	631	632	633	634	635	
566	567	568	569	570	571	572	
501	502	503	504	505	506	507	508
428	429	430	431	432	433	434	435
357	358	359	360	361	362	363	
294	295	296	297	298	299	300	
231	232	233	234	235	236	237	
168	169	170	171	172	173	174	
105	106	107	108	109	110	111	
43	44	45	46	47	48		

$$200. \leq Z \leq 320.$$

Table 8. Element reordering in three-dimensional mesh (cont'd)

1728	1729	1730	1731	1732	1733		
1674	1675	1676	1677	1678	1679		
1614	1615	1616	1617	1618	1619	1620	1621
1544	1545	1546	1547	1548	1549	1550	
1481	1482	1483	1484	1485	1486	1487	
1418	1419	1420	1421	1422	1423	1424	
1355	1356	1357	1358	1359	1360	1361	
1289	1290	1291	1292	1293	1294	1295	1296
1216	1217	1218	1219	1220	1221	1222	1223
1146	1147	1148	1149	1150	1151	1152	
1083	1084	1085	1086	1087	1088	1089	
1020	1021	1022	1023	1024	1025	1026	
957	958	959	960	961	962	963	
891	892	893	894	895	896	897	898
818	819	820	821	822	823	824	825
748	749	750	751	752	753	754	
685	686	687	688	689	690	691	
622	623	624	625	626	627	628	
559	560	561	562	563	564	565	
493	494	495	496	497	498	499	500
420	421	422	423	424	425	426	427
350	351	352	353	354	355	356	
287	288	289	290	291	292	293	
224	225	226	227	228	229	230	
161	162	163	164	165	166	167	
98	99	100	101	102	103	104	
37	38	39	40	41	42		

$$320. \leq z \leq 420.$$

Table 8. Element reordering in three-dimensional mesh (cont'd)

1722	1723	1724	1725	1726	1727		
1668	1669	1670	1671	1672	1673		
1606	1607	1608	1609	1610	1611	1612	1613
1537	1538	1539	1540	1541	1542		1543
1474	1475	1476	1477	1478	1479		1480
1411	1412	1413	1414	1415	1416		1417
1348	1349	1350	1351	1352	1353		1354
1281	1282	1283	1284	1285	1286	1287	↖ 1288
1208	1209	1210	1211	1212	1213	1214	1215
1139	1140	1141	1142	1143	1144		1145
1076	1077	1078	1079	1080	1081		1082
1013	1014	1015	1016	1017	1018		1019
950	951	952	953	954	955		956
883	884	885	886	887	888	889	↖ 890
810	811	812	813	814	815	816	817
741	742	743	744	745	746		747
678	679	680	681	682	683		684
615	616	617	618	619	620		621
552	553	554	555	556	557		558
485	486	487	488	489	490	491	↖ 492
412	413	414	415	416	417	418	419
343	344	345	346	347	348		349
280	281	282	283	284	285		286
217	218	219	220	221	222		223
154	155	156	157	158	159		160
91	92	93	94	95	96	97	
31	32	33	34	35	36		

$$420. \leq z \leq 576.$$

Table 8. Element reordering in three-dimensional mesh (cont'd)

1716	1717	1718	1719	1720	1721		
1662	1663	1664	1665	1666	1667		
1598	1599	1600	1601	1602	1603	1604	1605
1530	1531	1532	1533	1534	1535	1536	
1467	1468	1469	1470	1471	1472	1473	
1404	1405	1406	1407	1408	1409	1410	
1341	1342	1343	1342	1345	1346	1347	
1273	1274	1275	1276	1277	1278	1279	→ 1280
1200	1201	1202	1203	1204	1205	1206	1207
1132	1133	1134	1135	1136	1137	1138	
1069	1070	1071	1072	1073	1074	1075	
1006	1007	1008	1009	1010	1011	1012	
943	944	945	946	947	948	949	
875	876	877	878	879	880	881	→ 882
802	803	804	805	806	807	808	809
734	735	736	737	738	739	740	
671	672	673	674	675	676	677	
608	609	610	611	612	613	614	
545	546	547	548	549	550	551	
477	478	479	480	481	482	483	→ 484
404	405	406	407	408	409	410	411
336	337	338	339	340	341	342	
273	274	275	276	277	278	279	
210	211	212	213	214	215	216	
147	148	149	150	151	152	153	
84	85	86	87	88	89	90	
25	26	27	28	29	30		

576. $\leq z \leq$ 684.

Table 8. Element reordering in three-dimensional mesh (cont'd)

1710	1711	1712	1713	1714	1715		
1656	1657	1658	1659	1660	1661		
1590	1591	1592	1593	1594	1595	1596	1597
1523	1524	1525	1526	1527	1528		1529
1460	1461	1462	1463	1464	1465		1466
1397	1398	1399	1400	1401	1402		1403
1334	1335	1336	1337	1338	1339		1340
1265	1266	1267	1268	1269	1270	1271	1272
1192	1193	1194	1195	1196	1197	1198	1199
1125	1126	1127	1128	1129	1130		1131
1062	1063	1064	1065	1066	1067		1068
999	1000	1001	1002	1003	1004		1005
936	937	938	939	940	941		942
867	868	869	870	871	872	873	874
794	795	796	797	798	799	800	801
727	728	729	730	731	732		733
664	665	666	667	668	669		670
601	602	603	604	605	606		607
538	539	540	541	542	543		544
469	470	471	472	473	474	475	476
396	397	398	399	400	401	402	403
329	330	331	332	333	334		335
266	267	268	269	270	271		272
203	204	205	206	207	208		209
140	141	142	143	144	145		146
77	78	79	80	81	82	83	
19	20	21	22	23	24		

684. $\leq Z \leq 780.$

Table 8. Element reordering in three-dimensional mesh (cont'd)

1704	1705	1706	1707	1708	1709		
1650	1651	1652	1653	1654	1655		
1582	1583	1584	1585	1586	1587	1588	1589
1516	1517	1518	1519	1520	1521	1522	
1453	1454	1455	1456	1457	1458	1459	
1390	1391	1392	1393	1394	1395	1396	
1327	1328	1329	1330	1331	1332	1333	
1257	1258	1259	1260	1261	1262	1263	→ 1264
1184	1185	1186	1187	1188	1189	1190	1191
1118	1119	1120	1121	1122	1123	1124	
1055	1056	1057	1058	1059	1060	1061	
992	993	994	995	996	997	998	
929	930	931	932	933	934	935	
859	860	861	862	863	864	865	→ 866
786	787	788	789	790	791	792	793
720	721	722	723	724	725	726	
657	658	659	660	661	662	663	
594	595	596	597	598	599	600	
531	532	533	534	535	536	537	
461	462	463	464	465	466	467	→ 468
388	389	390	391	392	393	394	395
322	323	324	325	326	327	328	
259	260	261	262	263	264	265	
196	197	198	199	200	201	202	
133	134	135	136	137	138	139	
70	71	72	73	74	75	76	
13	14	15	16	17	18		

$$780. \quad \begin{matrix} < Z < 880. \\ = & = \end{matrix}$$

Table 8. Element reordering in three-dimensional mesh (cont'd)

1698	1699	1700	1701	1702	1703		
1644	1645	1646	1647	1648	1649		
1574	1575	1576	1577	1578	1579	1580	1581
1509	1510	1511	1512	1513	1514		1515
1446	1447	1448	1449	1450	1451		1452
1383	1384	1385	1386	1387	1388		1389
1320	1321	1322	1323	1324	1325		1326
1249	1250	1251	1252	1253	1254	1255	← 1256
1176	1177	1178	1179	1180	1181	1182	1183
1111	1112	1113	1114	1115	1116		1117
1048	1049	1050	1051	1052	1053		1054
985	986	987	988	989	990		991
922	923	924	925	926	927		928
851	852	853	854	855	856	857	← 858
778	779	780	781	782	783	784	785
713	714	715	716	717	718		719
650	651	652	653	654	655		656
587	588	589	590	591	592		593
524	525	526	527	528	529		530
453	454	455	456	457	458	459	← 460
380	381	382	383	384	385	386	387
315	316	317	318	319	320		321
252	253	254	255	256	257		258
189	190	191	192	193	194		195
126	127	128	129	130	131		132
63	64	65	66	67	68	69	
7	8	9	10	11	12		

880. $\leq z \leq 1000.$

Table 8. Element reordering in three-dimensional mesh (cont'd)

1692	1693	1694	1695	1696	1697		
1638	1639	1640	1641	1642	1643	1572	
1565	1566	1567	1568	1569	1570	1571	1573
1502	1503	1504	1505	1506	1507		1508
1439	1440	1441	1442	1443	1444		1445
1376	1377	1378	1379	1380	1381		1382
1313	1314	1315	1316	1317	1318	1247	1319
1240	1241	1242	1243	1244	1245	1246 1174	1248
1167	1168	1169	1170	1171	1172	1173	1175
1104	1105	1106	1107	1108	1109		1110
1041	1042	1043	1044	1045	1046		1047
978	979	980	981	982	983		984
915	916	917	918	919	920	849	921
842	843	844	845	846	847	848 776	850
769	770	771	772	773	774	775	777
706	707	708	709	710	711		712
643	644	645	646	647	648		649
580	581	582	583	584	585		586
517	518	519	520	521	522	451	523
444	445	446	447	448	449	450 378	452
371	372	373	374	375	376	377	379
308	309	310	311	312	313		314
245	246	247	248	249	250		251
182	183	184	185	186	187		188
119	120	121	122	123	124	62	125
55	56	57	58	59	60	61	
1	2	3	4	5	6		

$$\underline{1000.} < Z < \underline{1200.}$$

Table 9. Node ordering in two-dimensional mesh

1	2	3	4	5	6	7		
8	9	10	11	12	13	14		
15	16	17	18	19	20	21	197	198
22	23	24	25	26	27	28		200
29	30	31	32	33	34	35		202
36	37	38	39	40	41	42		204
43	44	45	46	47	48	49		206
50	51	52	53	54	55	56	207	208
57	58	59	60	61	62	63	209	210
64	65	66	67	68	69	70		212
71	72	73	74	75	76	77		214
78	79	80	81	82	83	84		216
85	86	87	88	89	90	91		218
92	93	94	95	96	97	98	219	220
99	100	101	102	103	104	105	221	222
106	107	108	109	110	111	112		224
113	114	115	116	117	118	119		226
120	121	122	123	124	125	126		228
127	128	129	130	131	132	133		230
134	135	136	137	138	139	140	231	232
141	142	143	144	145	146	147	233	234
148	149	150	151	152	153	154		236
155	156	157	158	159	160	161		238
162	163	164	165	166	167	168		240
169	170	171	172	173	174	175		242
176	177	178	179	180	181	182	243	244
183	184	185	186	187	188	189		
190	191	192	193	194	195	196		

Table 10. Element ordering in two-dimensional mesh

1	2	3	4	5	6		
7	8	9	10	11	12	186	
13	14	15	16	17	18	163	
19	20	21	22	23	24	164	
25	26	27	28	29	30	165	
31	32	33	34	35	36	166	
37	38	39	40	41	42	187	167
43	44	45	46	47	48	188	168
49	50	51	52	53	54	169	
55	56	57	58	59	60	170	
61	62	63	64	65	66	171	
67	68	69	70	71	72	172	
73	74	75	76	77	78	189	173
79	80	81	82	83	84	190	174
85	86	87	88	89	90	175	
91	92	93	94	95	96	176	
97	98	99	100	101	102	177	
103	104	105	106	107	108	178	
109	110	111	112	113	114	191	179
115	116	117	118	119	120	192	180
121	122	123	124	125	126	181	
127	128	129	130	131	132	182	
133	134	135	136	137	138	183	
139	140	141	142	143	144	184	
145	146	147	148	149	150	193	185
151	152	153	154	155	156		
157	158	159	160	161	162		

CHAPTER 5 ANALYSIS OF LOADS

5.1 ANALYSIS OF MECHANICAL LOADS

The vehicle loads were imposed on the x-z plane (-y-direction) of the three-dimensional mesh, and a static analysis was performed. An analysis required the geometry (as described in Section 4.2), the material properties of the physical prototype (Section 2.2), and the boundary conditions. All boundaries were considered to be rollers except the bottom which was assumed fixed. The rollers simulate not only the continuity of the concrete pavement and the ballast subbase longitudinally, but also the lateral (both longitudinal and transverse) continuity of the soil mass. The fixed bottom boundary plane simulates the decrease of pressure distribution with depth in the soil subgrade. (Recall Fig. 13 which shows the transverse lines where deflections are plotted).

Transverse surface deflections along sections T1-R1, T2-R2, T3-R3, and T4-R4 are shown in Figures 15 through 18. Any conventional pavement exhibits the typical concentric contour basin, while the anchored pavement of the Edens Expressway (as seen from the above mentioned figures) tends to "barrel" and produce more cylindrical rather than spherical deflection patterns. That particular deflection shape is due to the four anchors which produce a high longitudinal rigidity. The value of the highest deflection reported was 0.075 inches at section T3-R3.

Stress contours are singled out in order to predict the vehicle's weight distribution into the different materials which constitute the pavement/soil system. The longitudinal bending stresses of the concrete slab, anchors, and capital are given in Figure 19. It may be noted that the maximum compressive bending stress in the slab is 42.64 psi, while in the anchors is 14.60 psi. Also, the maximum tensile bending stress in the slab is 2.00 psi, while in the anchors is 116.34 psi.

The pressure distribution through the ballast subbase reduces considerably the stress in the top layer of subgrade. Figures 20 and 21 give the vertical and the maximum shear stresses in the ballast respectively. The maximum compressive vertical stress is 0.12 psi, while the maximum value of the maximum shear stress is 1.83 psi.

The stresses introduced into the soil subgrade give further insight for understanding the soil/structure interaction. The vertical stress contours are shown in Figure 22. The maximum compressive vertical stress occurs underneath the second anchor, and its value is 0.95 psi. Figure 23 shows the maximum shear stress

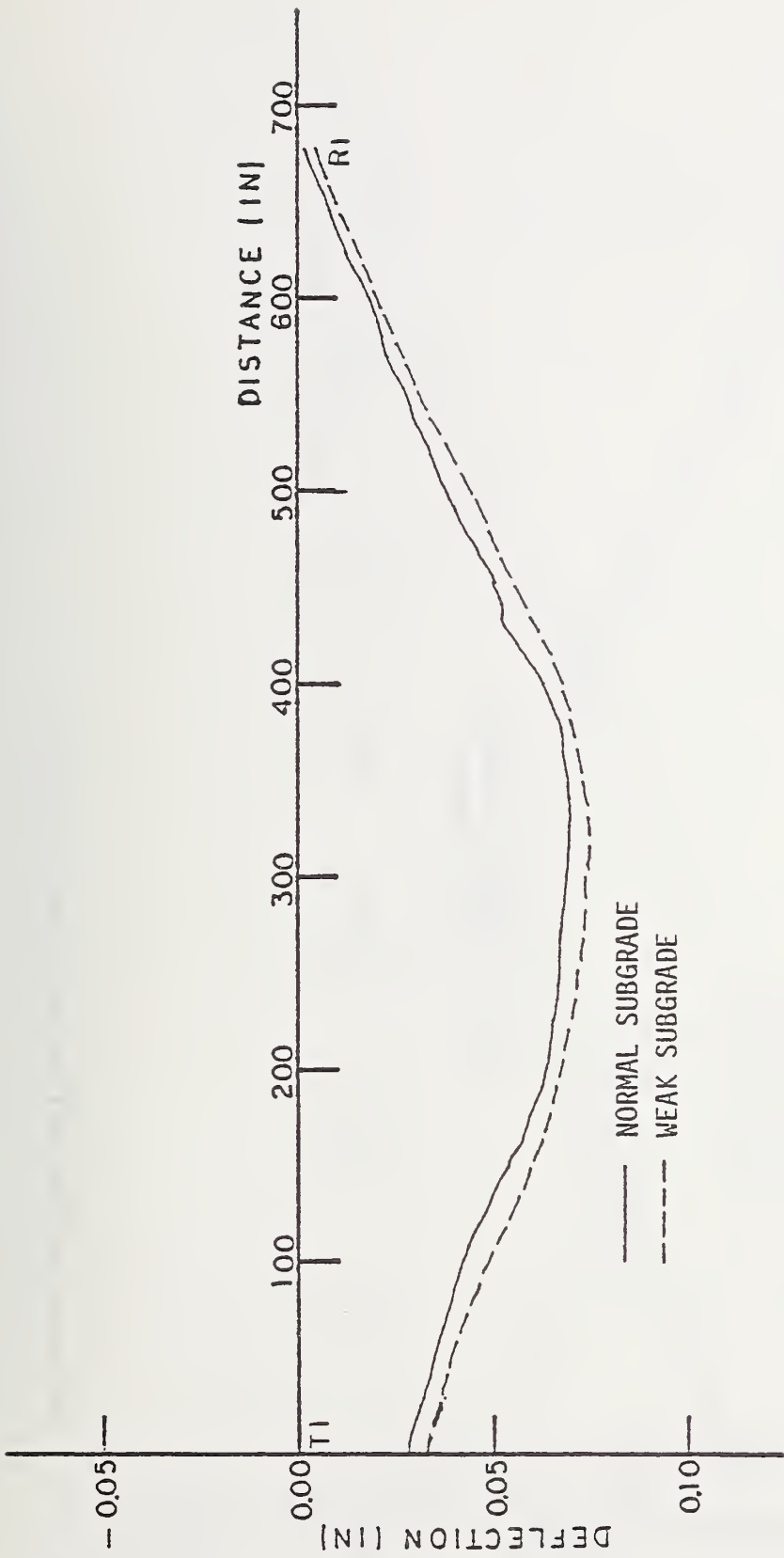


Figure 15. Transverse deflection along line T1-R1

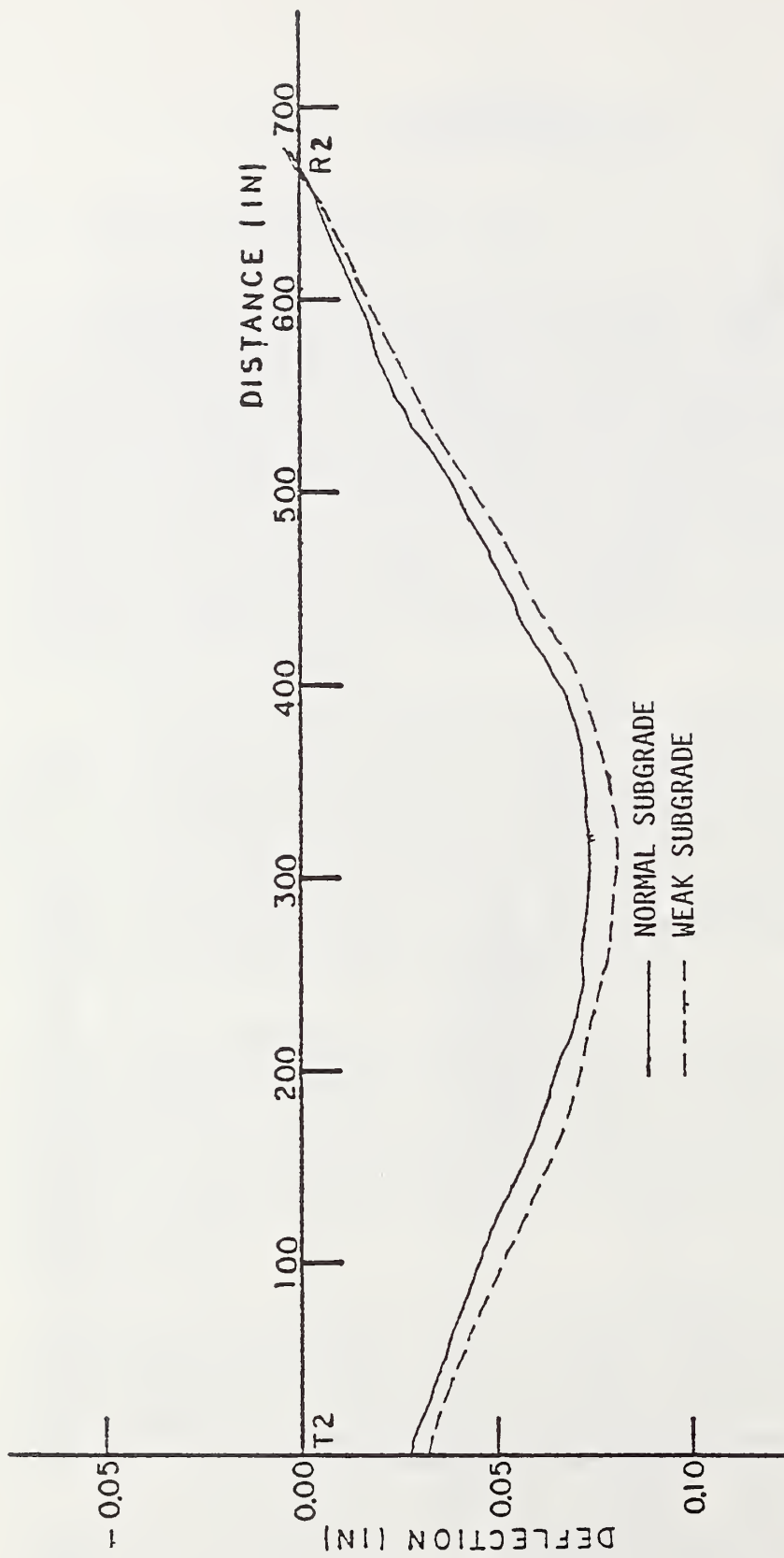


Figure 16. Transverse surface deflection along line T2-R2

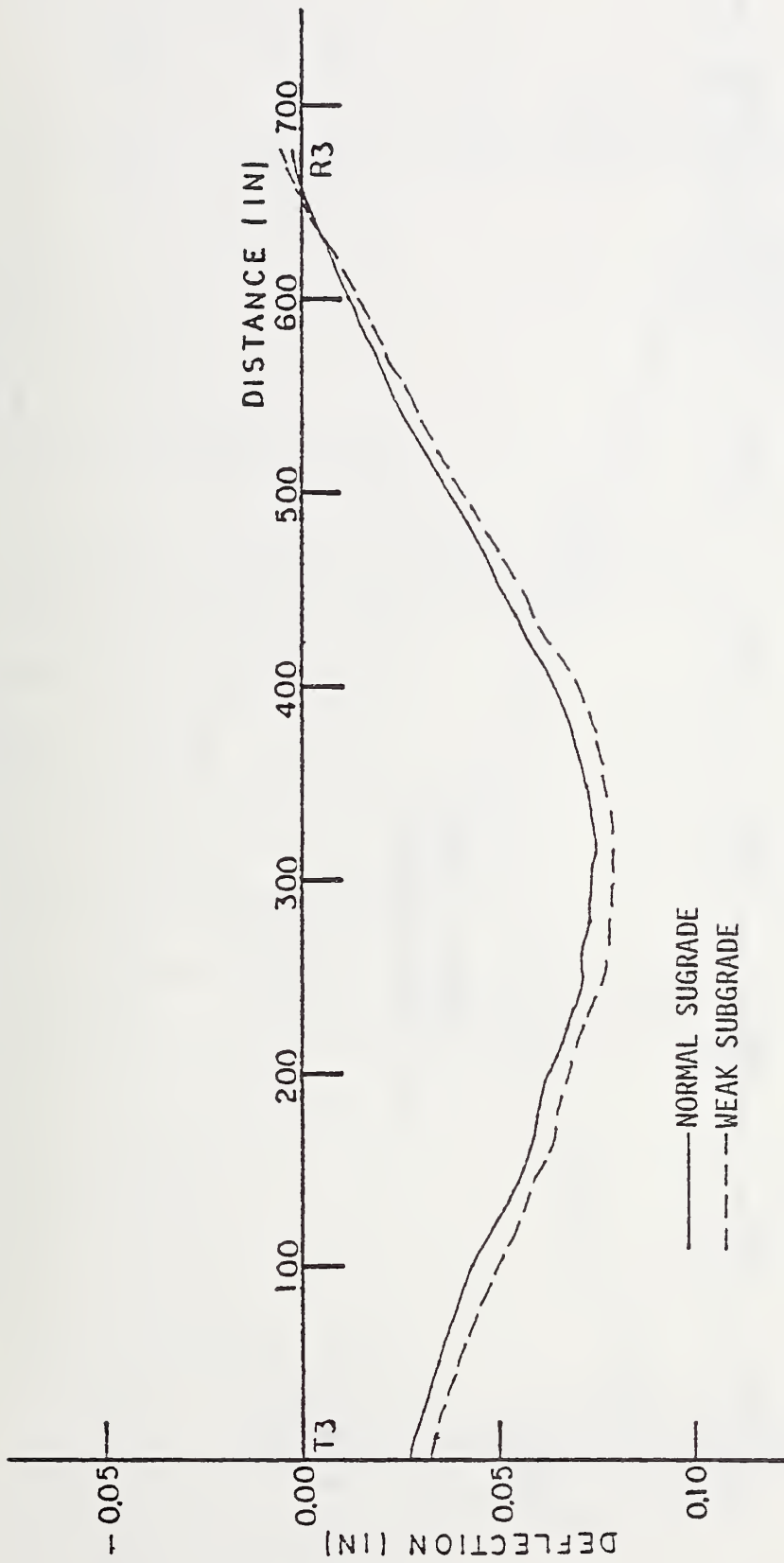


Figure 17. Transverse surface deflection along line T3-R3

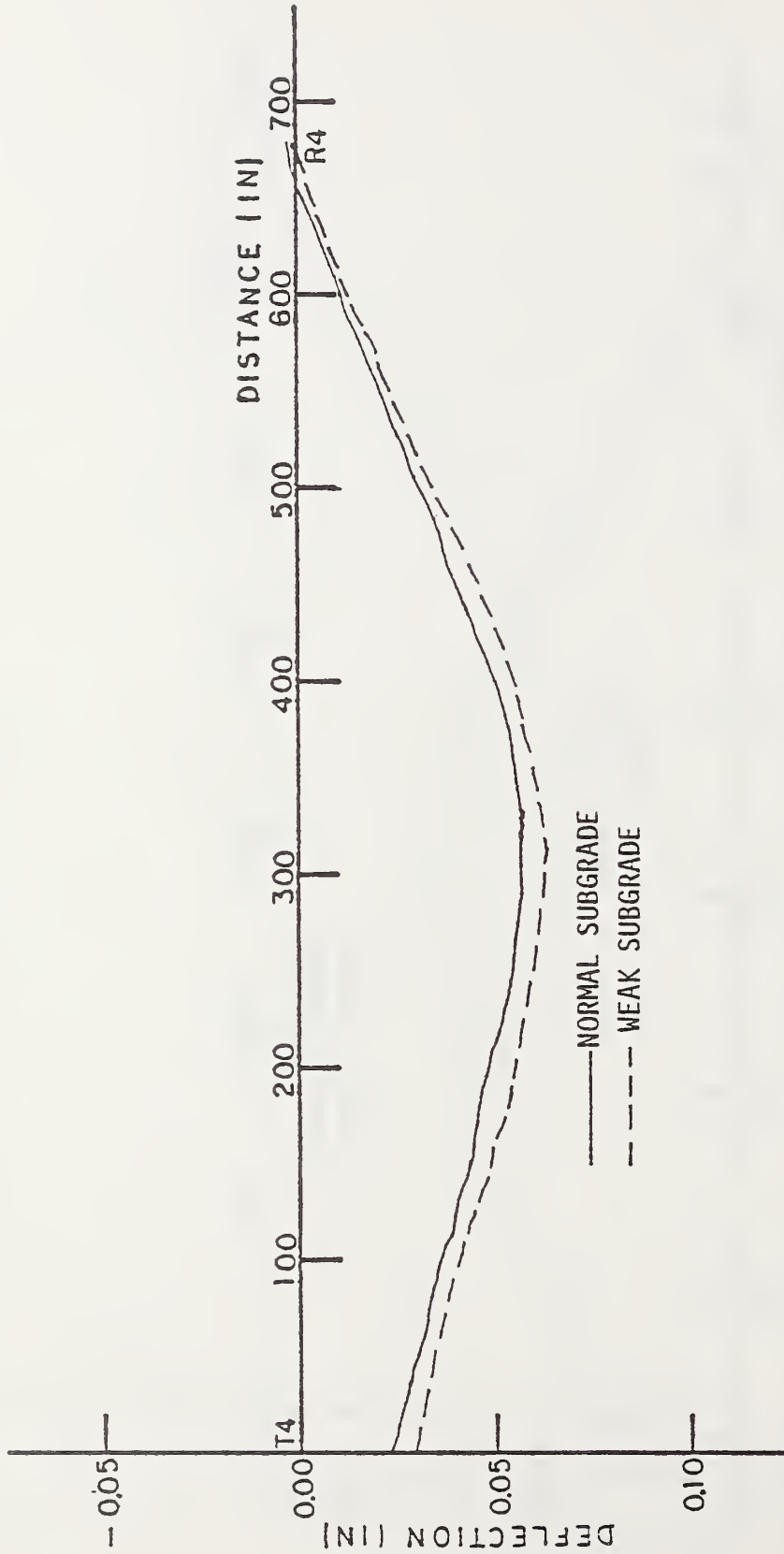


Figure 18. Transverse surface deflection along line T4-R4

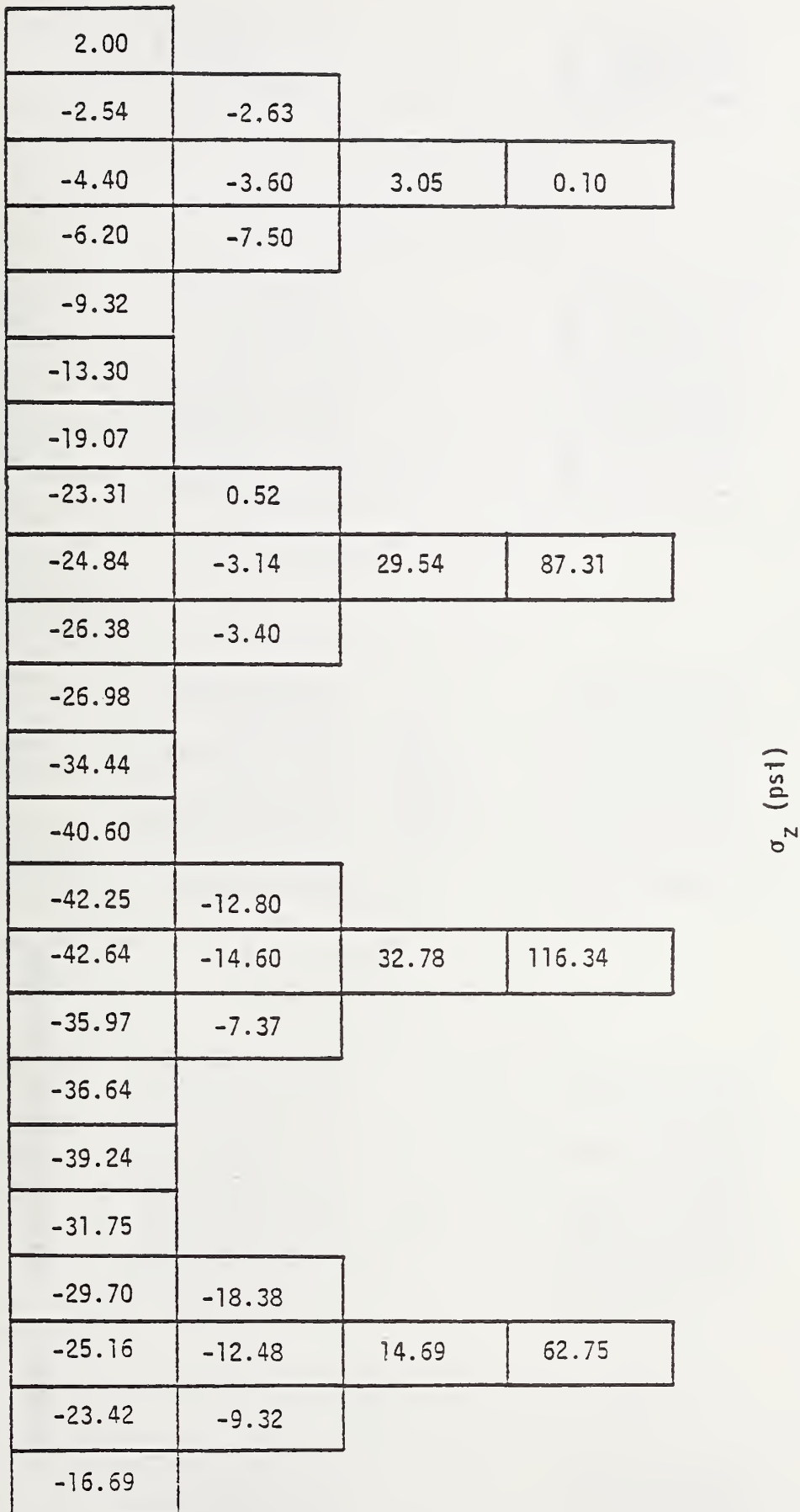


Figure 19. Concrete bending stresses in Z-direction

-0.08

-0.12
-0.02
-0.11

-0.05
-0.12
-0.05

-0.07
-0.12
-0.10

-0.01

σ_y (psf)

Figure 20. Ballast vertical stresses

0.09

0.29
0.06
0.51

1.73
0.41
1.79

1.83
0.26
1.75

0.89

τ_{\max} (psi)

Figure 21. Ballast maximum shear stresses

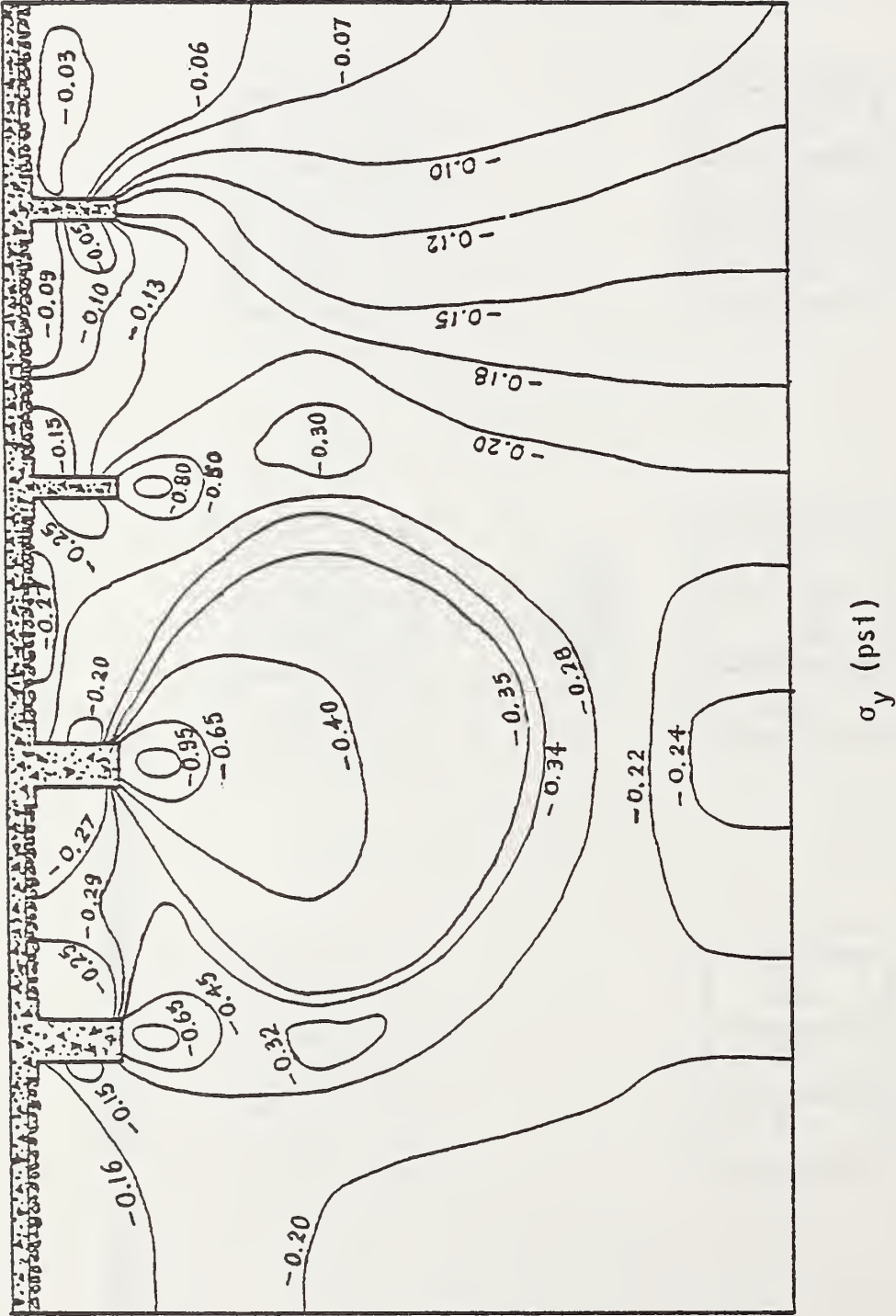
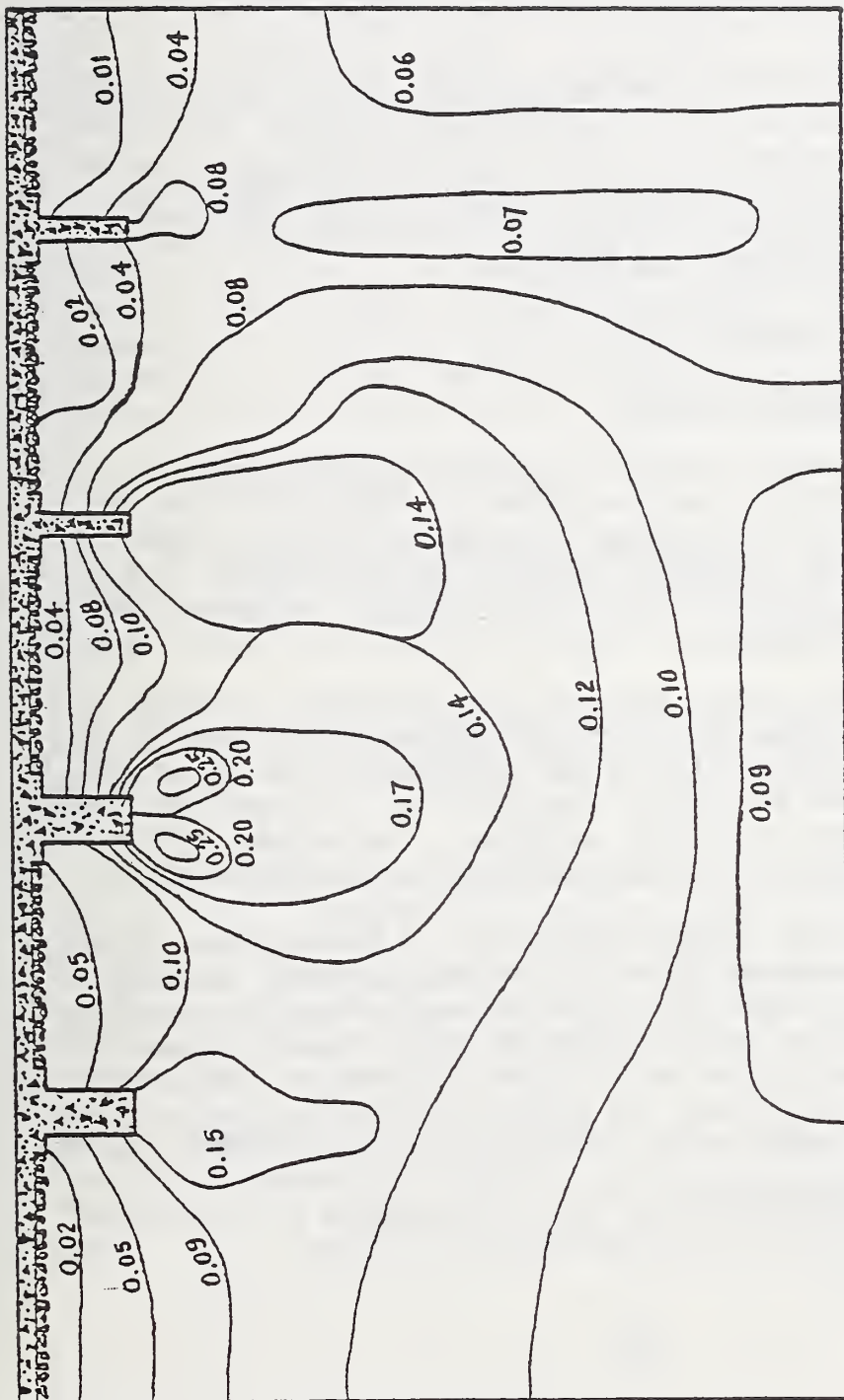


Figure 22. Soil vertical stress contours



τ_{\max} (psi)

Figure 23. Soil maximum shear stress contours

distribution in the subgrade. The maximum value of the maximum shear stress is 0.20 psi, and its location is underneath the second anchor. As could be intuitively forethought, the localized stress intensification in the soil is underneath the anchors, the main stress path going through the anchors to the lower layers of soil. This particular stress path relieves the pressure in the top four feet of the subgrade. However, the advantage is that the strength of the subgrade increases with depth to the point that the localized stress intensity does not produce any failure modes underneath the anchors.

It may be noted that the observed maximum value of the tensile bending stress of 116.34 psi in the second anchor causes no problem. The fiber reinforced concrete can stand tensile stress of the order of 1000 psi (depending on the amount of steel fibers), before it starts cracking. The stresses are not significant in the ballast due to the stress path through the anchors..

5.2 ANALYSIS OF ENVIRONMENTAL LOADS

5.2.1 Moisture in Pavement System

The variation in water content of a soil subgrade during a period of 80 days of traffic has been shown in Figure 10. The increase in moisture content is primarily due to the vehicle loads as well as in the change in thermal behavior of the system. The increase of moisture within the load bearing layers decreases the strength of the clay subgrade.

A three-dimensional static analysis was performed. Figures 15 through 18 show the transverse surface deflection along lines T1-R1, T2-R2, T3-R3, and T4-R4 (See Fig. 13 for transverse line locations). As expected, deflections are higher compared with the ones from the static analysis performed on normal subgrade. The maximum deflection was observed at section T3-R3, and its value is 0.080 inches.

The difference in net maximum deflection of the anchored pavement with the normal subgrade and with the weak subgrade is 0.005 inches. A difference of only 6% in the deflection despite the 80% decrease in modulus of the top four feet of soil, clearly shows the importance of the depth of anchors. If the anchors are deep enough to be just below the frost line, the significant spring thaw weakening would not adversely effect the deflection of the pavement system.

NOTE: Since no available data was found, the modulus of elasticity for the top four feet of soil was decreased to 100 psi.

5.2.2 Heat Transfer Results

Surface temperature histories for both extreme summer and winter conditions (See Fig. 9) were input in the two-dimensional model, and a heat transfer analysis was performed. The geometry has been described in Section 4.3 and the material properties in Section 2.3. A detailed view of the slab-soil interface reveals conduction elements to thermally link the slab and the soil. Iso-parametric quadrilateral temperature elements are used to decrease the required finess of the mesh (number of degrees of freedom) and still maintain accuracy. The results of transient state heat transfer analysis are used to generate temperature distributions within the pavement and the soil.

The temperature profiles at various positions and times are called tautochrones. Summer tautochrones at pavement traffic lane, at pavement shoulder, and in subgrade are presented in Figures 24 through 26. Figures 27 through 29 show the winter tautochrones at pavement traffic lane, at pavement shoulder, and in subgrade correspondingly. The time used for the tautochrones is 1 day and increment is 6 hours. No significant change of the temperature is noticed below 45 inches from the top of the grade.

5.2.3 Thermal Stress Analysis

The temperatures generated in the heat transfer model were input in a two-dimensional stress model and the resulting stresses and strains were computed. The output of the heat transfer analysis was assigned as an input to thermal stress analysis.

Note that at time 00 hours, a steady heat transfer analysis was performed (1 iteration) and pavement temperatures were set equal to 50°F, while subbase and subgrade temperatures were set equal to 45°F.

Sliding interface elements that cannot sustain tensile loads and at certain shear stress begin to slide with an irrecoverable displacement were used. With this type of interface behavior, it is possible to simulate curling of the anchored slab with the associated loss of subgrade contact and also simulate penetration of the anchored slab into the soil. If no penetration is desired, a constraint limiting the compressive deflection of the anchored

NOTE: "KTEMP" was set equal to -7 (read temperatures from 7th iteration of previous transient heat transfer solution from file "TAPE 4"). The 7th iteration is the last iteration at time 06 hours. hours.

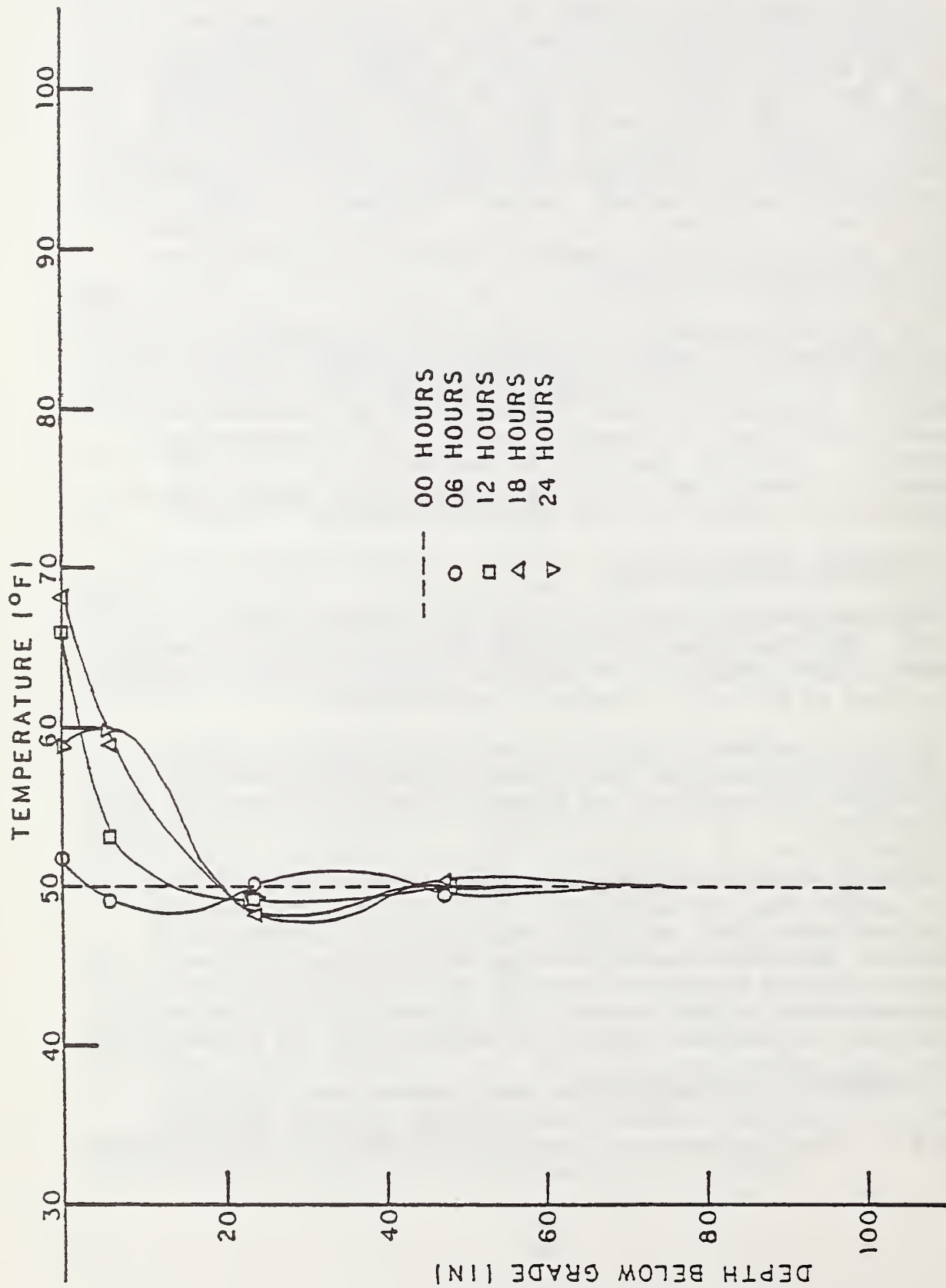


Figure 24. Summer tautochrones at pavement traffic lane

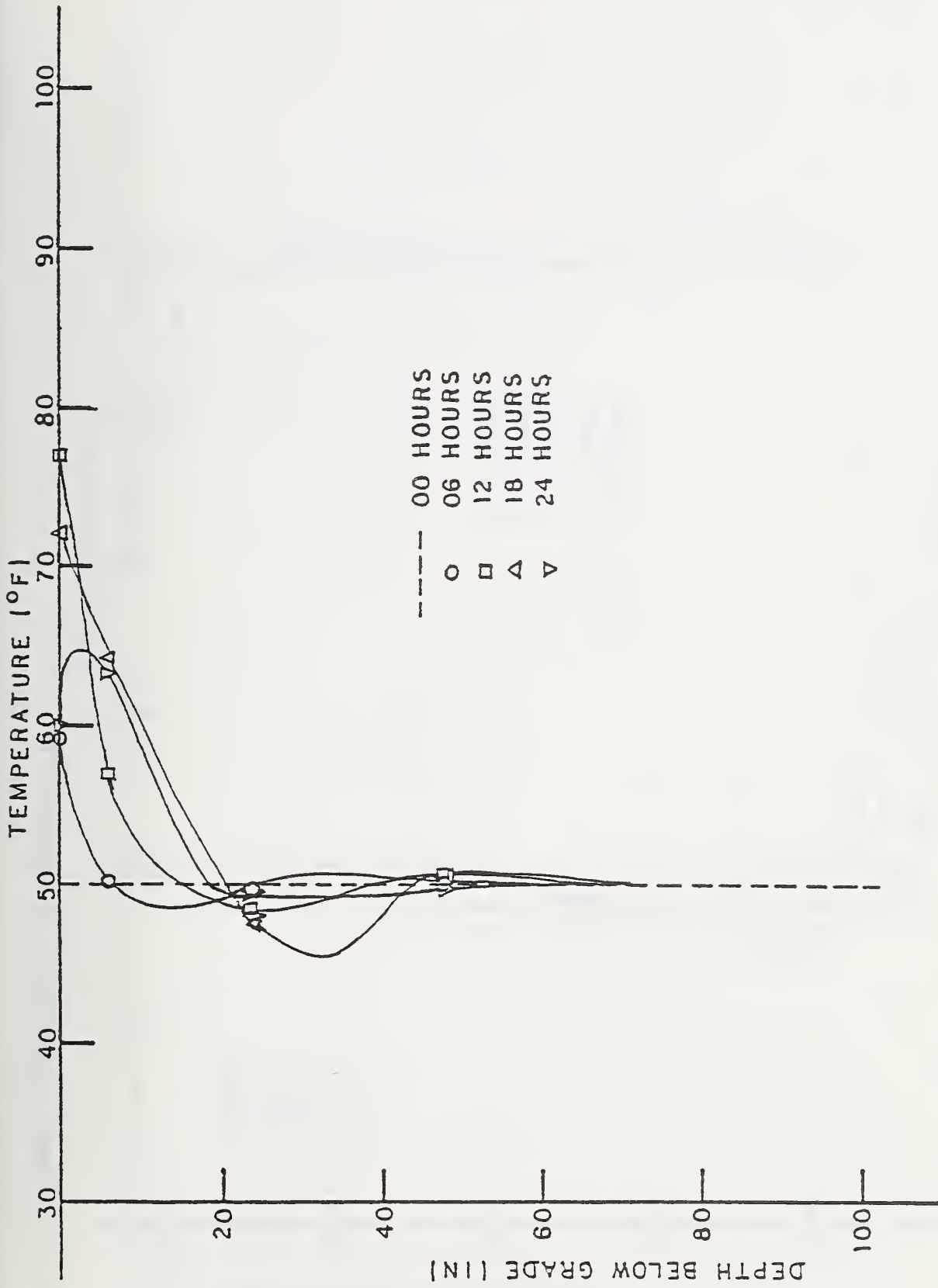


Figure 25. Summer tautochrones at pavement shoulder

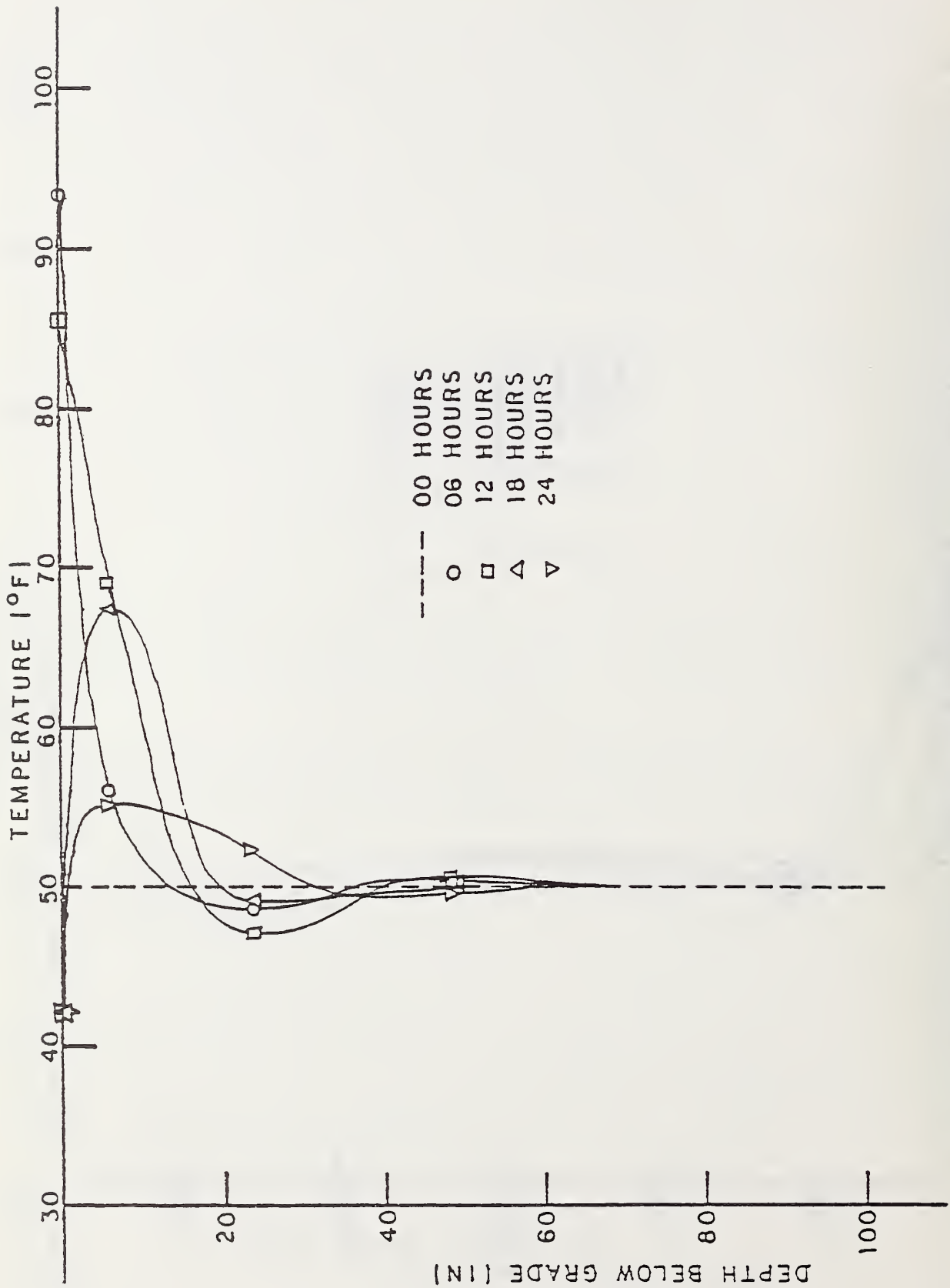


Figure 26. Summer tautochrones in natural soil

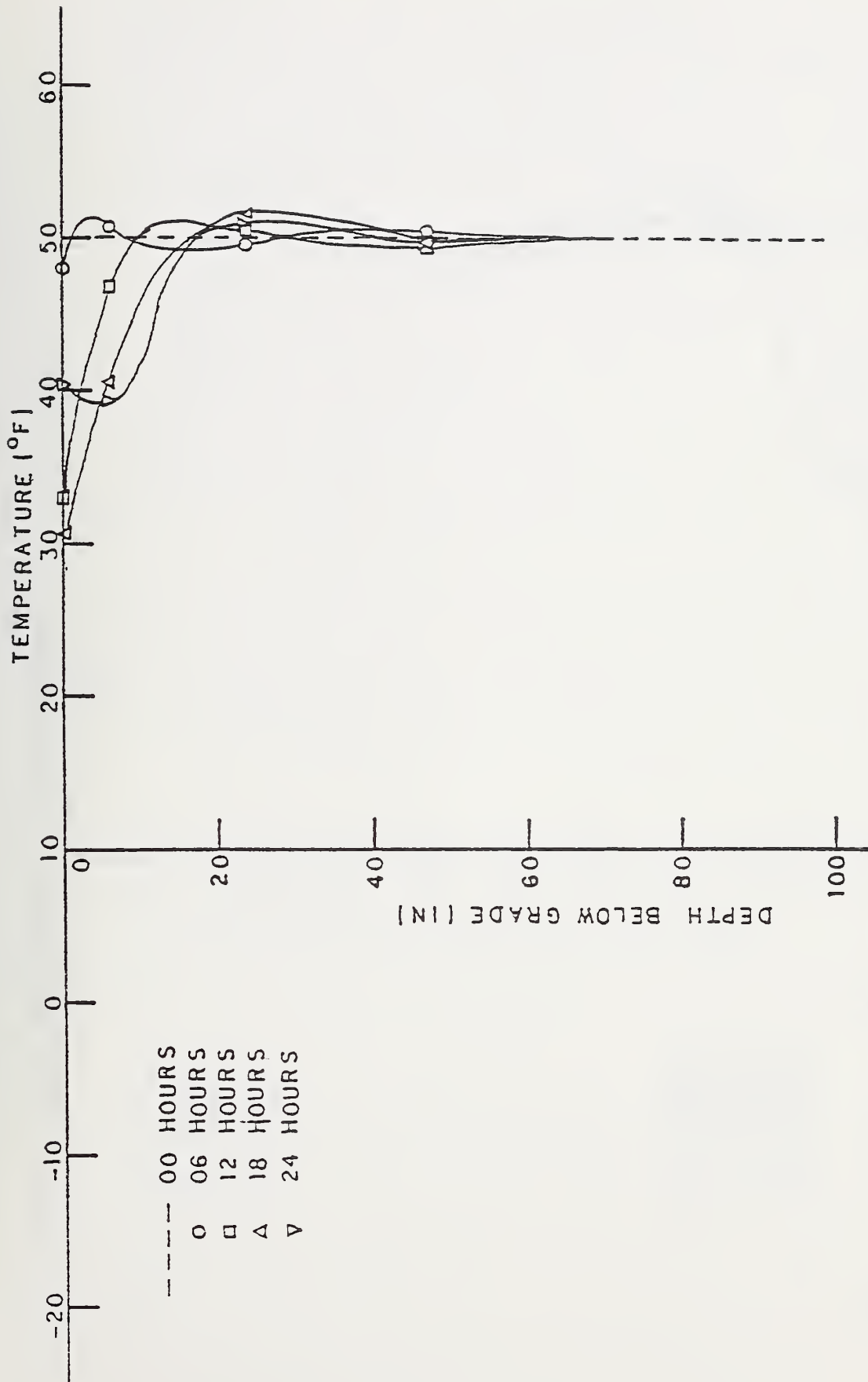


Figure 27. Winter tautochrones at pavement traffic lane

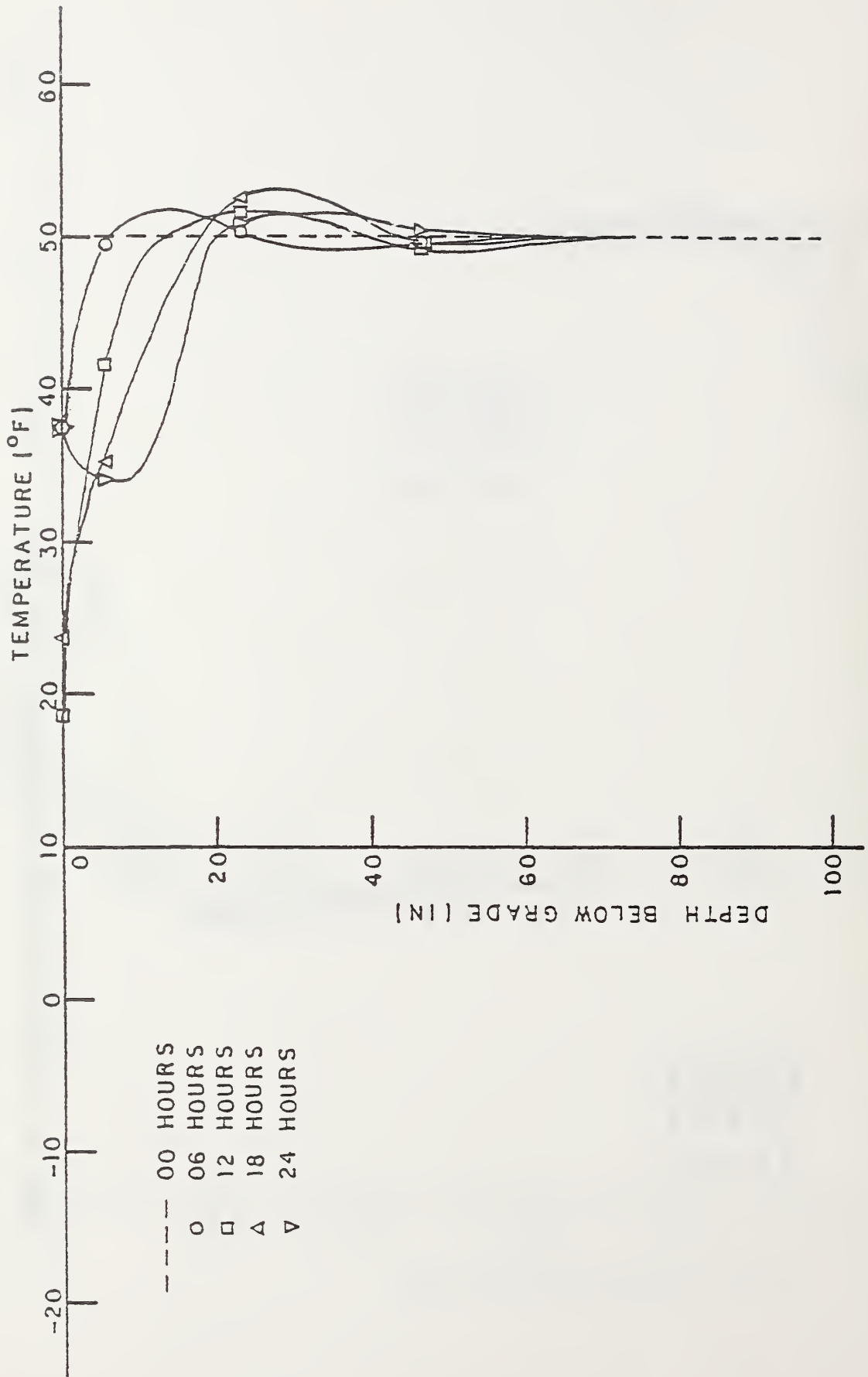


Figure 28. Winter tautochrones at pavement shoulder

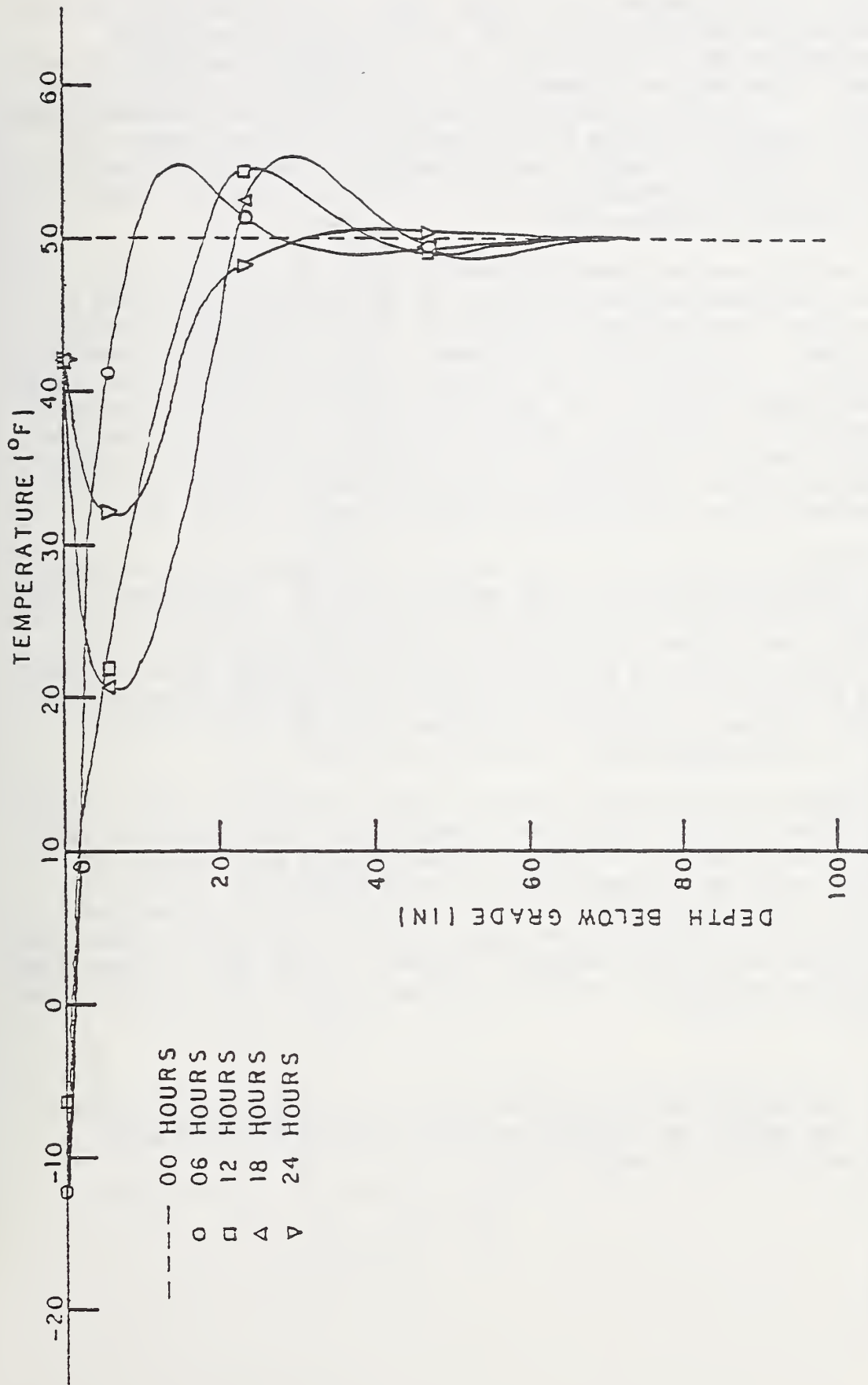


Figure 29. Winter tautochrones in natural soil

slab can be established by choosing a sufficient large value for K.

Surface deflections for extreme summer conditions (Fig. 30) and extreme winter conditions (Fig. 36) at 06 hours are presented. Winter deflections are lower than in the summer because there is not as great a temperature differential between the slab top and bottom surfaces. The anchors greatly reduce curling near the pavement edges with only moderate curling of the shoulders at extreme winter conditions. Stresses, however, are increased and the size of the slab-anchor joint was increased by adding fillets to lower any stress concentrations that may occur.

From the various generated contour plots of stress in the system, some observations pertaining to the nature of the state of stress within and the gross behavior of the soil/structure system can be made. In the concrete pavement, transverse bending stresses are given in Figures 31 and 37 for both summer and winter conditions. For the summer condition, the maximum value of the compressive bending stresses is 145.02 psi, while the maximum value of the tensile bending stresses is 192.50 psi. For the winter condition, the maximum value of the compressive bending stresses is 206.34 psi, while the maximum value of the tensile bending stresses is 127.53 psi.

Figures 32 and 33 give the vertical and maximum shear stresses in the ballast material for the summer condition. The maximum value of the vertical stresses is 0.88 psi in compression and 0.47 psi in tension. The maximum value of the maximum shear stresses is 8.45 psi. Figures 38 and 39 give the vertical and maximum shear stresses in the ballast for the winter condition. The maximum value of the vertical stresses is 2.99 psi in compression, while the maximum value of the maximum shear stresses is 9.18 psi.

Figures 34 and 35 show vertical stress and maximum shear stress in subgrade for summer condition respectively. The maximum value of the vertical stresses is 0.20 psi in compression and 1.00 psi in tension, while the maximum value of the maximum shear stresses is 0.75 psi. For winter condition, the vertical stress and maximum shear contours in subgrade are shown in Figures 40 and 41 respectively. The maximum value of the vertical stresses is 0.65 psi in compression and 0.06 psi in tension, while the maximum value of the maximum shear stresses is 0.65 psi.

NOTE: The values for μ , the coefficient of static sliding friction, and K, the modulus of subgrade reaction, were obtained from the tests done by G. W. Clough (1974).

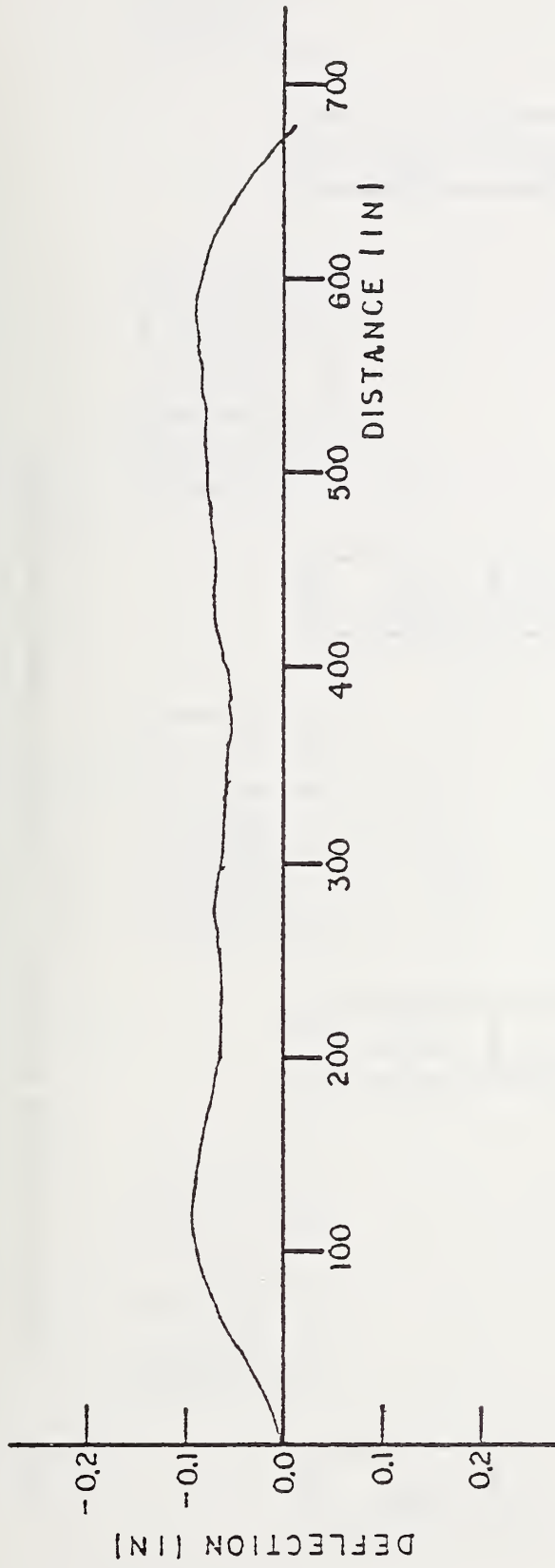


Figure 30. Deflected shape of the pavement surface (summer condition)

-11.99			
-70.79	94.74		
-89.64	140.40	-7.55	0.75
-80.84	104.54		
-19.10			
-19.71			
-20.12			
-127.17	181.00		
-135.86	171.99	9.30	-1.63
-124.03	172.08		
-22.85			
-22.83			
-22.98			
-132.86	186.83		
-145.02	180.55	11.92	-2.06
-134.82	192.50		
-21.33			
-21.13			
-20.93			
-105.88	144.49		
-116.78	161.26	2.54	-0.85
-94.87	134.89		
-12.62			

σ_x (psi)

Figure 31. Concrete bending stresses in X-direction (summer condition)

0.21

-0.88
0.36
-0.63

-0.59
0.08
-0.54

-0.59
0.12
-0.76

0.47

σ_y (psi)

Figure 32. Ballast vertical stresses (summer condition)

8.45

1.06
0.67
1.46

1.87
1.48
1.96

1.84
1.31
1.67

7.17

τ_{\max} (psi)

Figure 33. Ballast maximum shear stresses (summer condition)

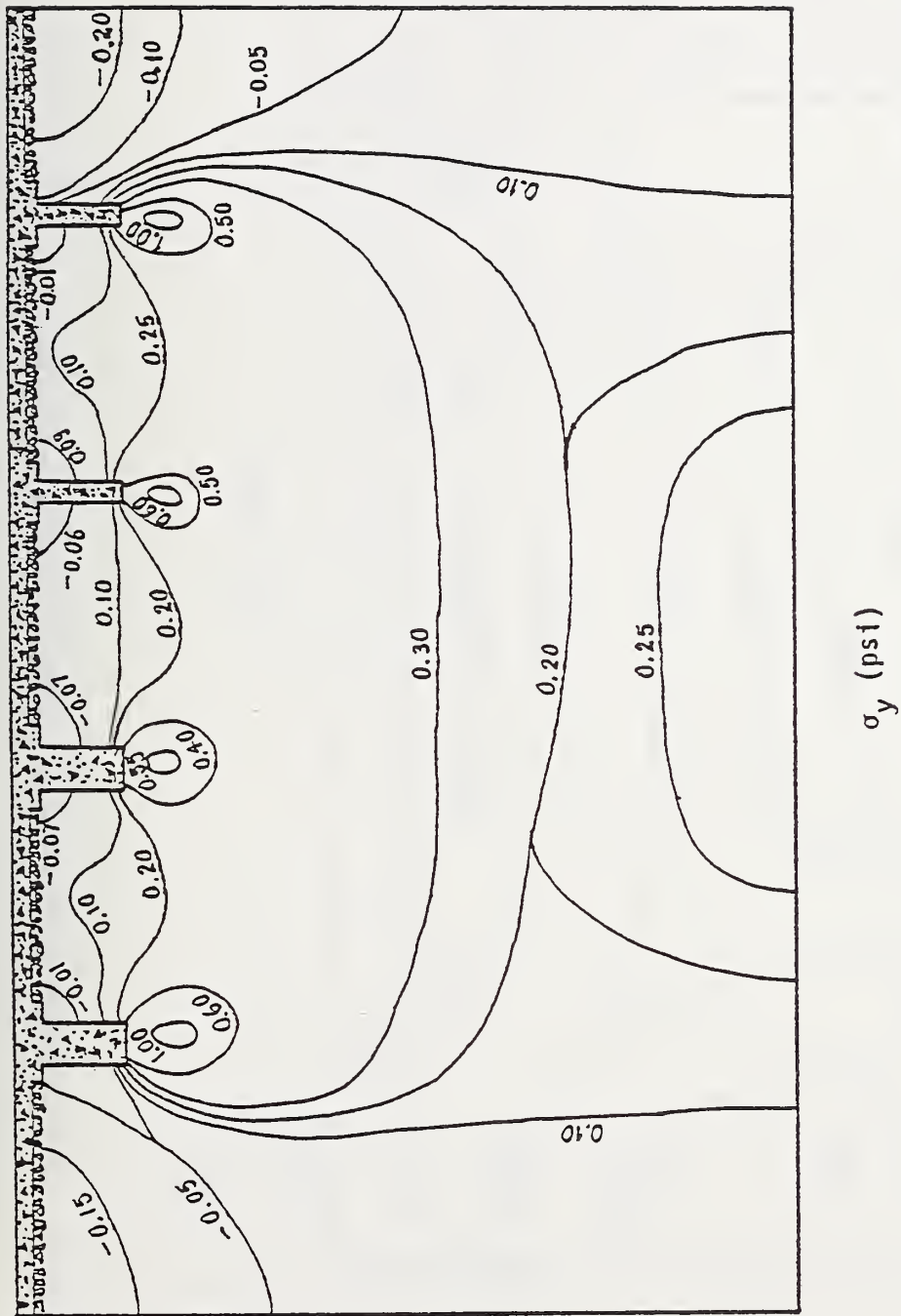
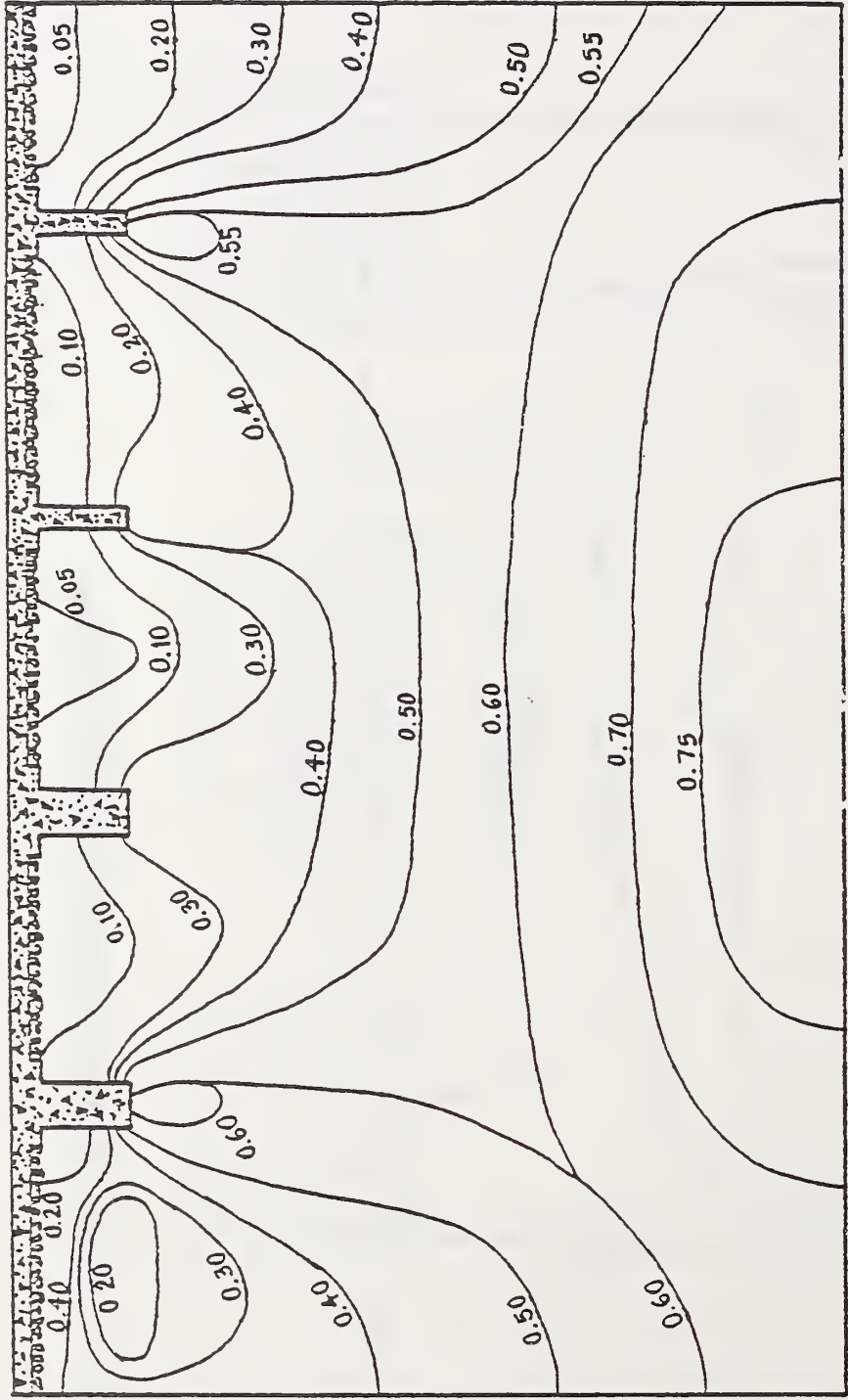


Figure 34. Soil vertical stress contours (summer condition)



τ_{max} (psi)

Figure 35. Soil maximum shear stress contours (summer condition)

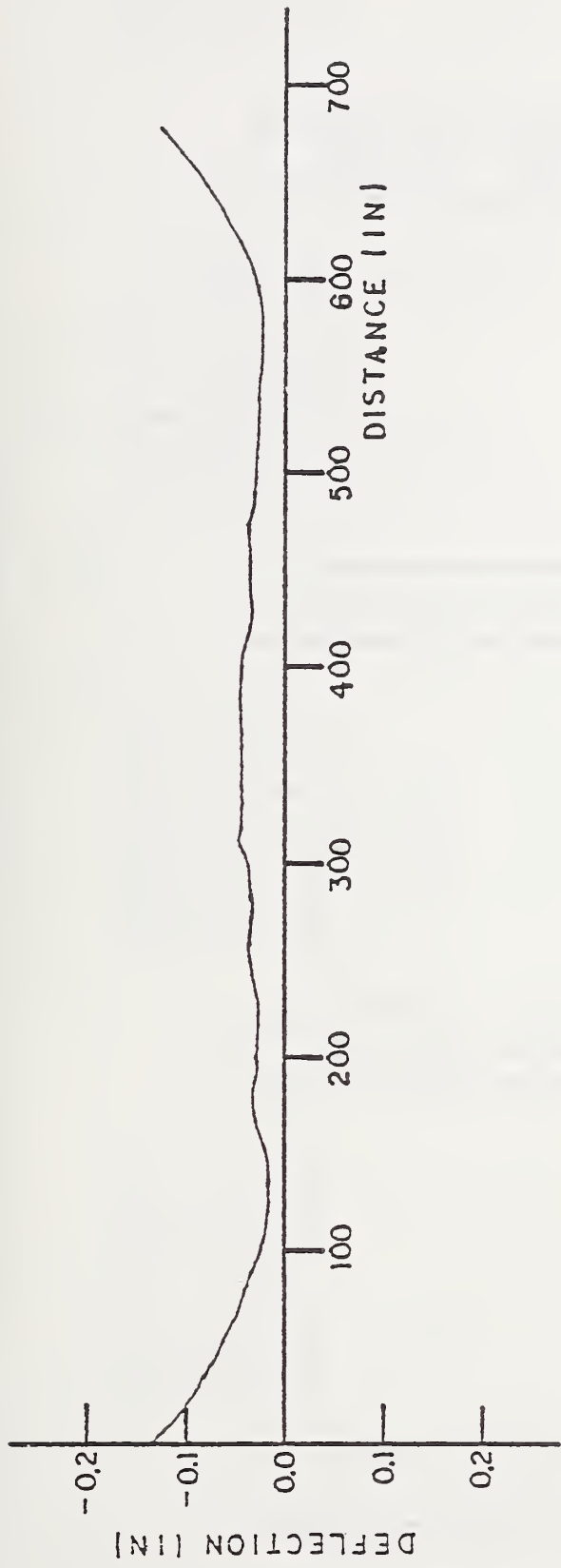


Figure 36. Deflected shape of the pavement surface (winter condition)

-2.49			
48.86	-93.03		
75.02	-154.32	7.00	-1.42
72.57	-134.36		
-3.37			
-3.35			
-2.66			
108.17	-193.50		
118.97	-187.58	-10.22	1.21
108.88	-193.70		
-1.68			
-1.98			
-1.57			
116.42	-206.34		
127.53	-196.03	-12.64	1.57
116.10	-206.26		
-2.10			
-2.44			
-2.37			
95.33	-171.72		
101.13	-175.19	-2.97	0.20
72.62	-134.35		
-2.97			

σ_x (psi)

Figure 37. Concrete bending stresses in X-direction (winter condition)

-1.12

-2.40
0.38
-2.67

-2.93
0.08
-2.99

-2.96
-0.06
-2.81

-1.18

σ_y (psi)

Figure 38. Ballast vertical stresses (winter condition)

9.18

2.56
3.88
2.94

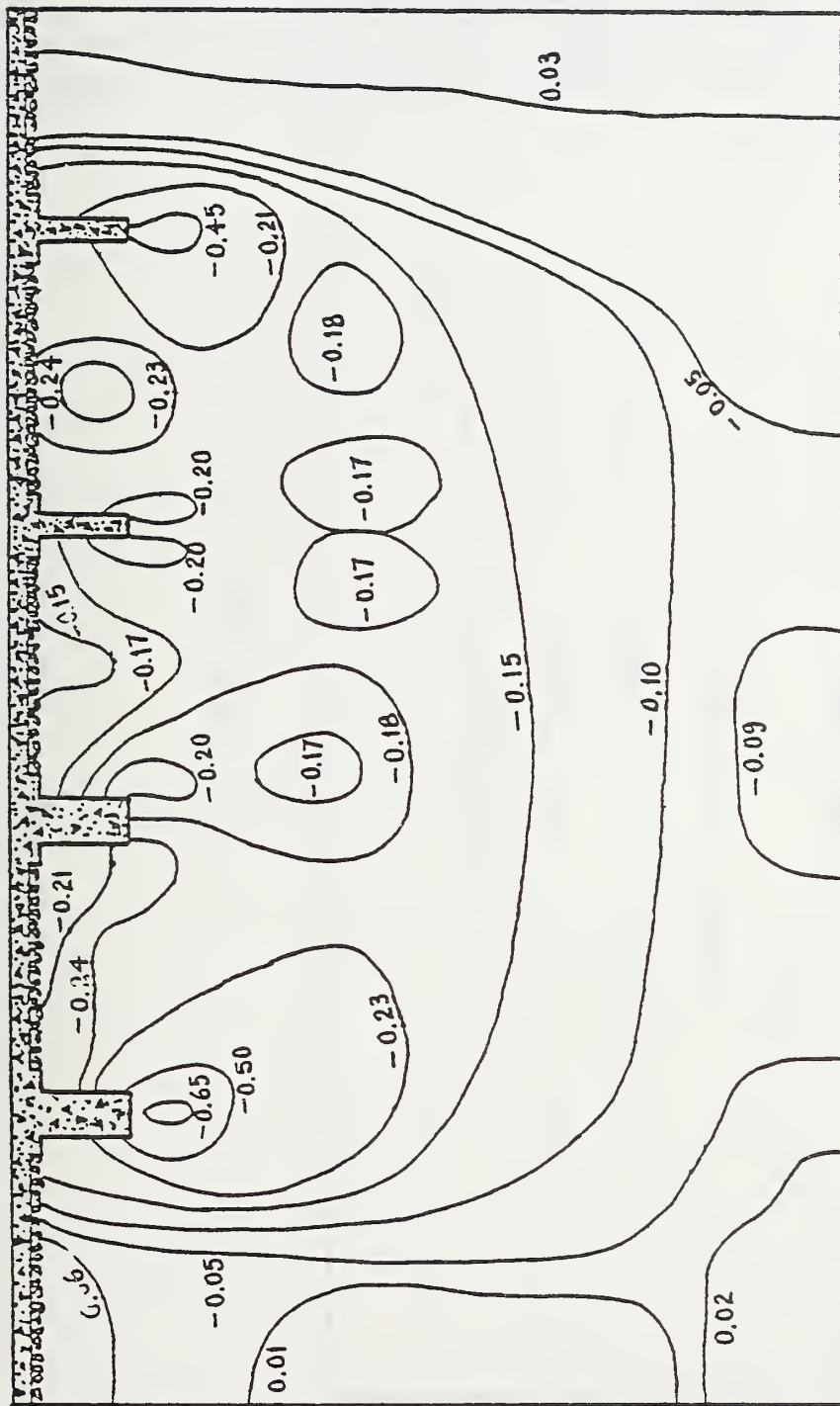
3.17
4.40
3.25

3.05
4.91
2.92

8.22

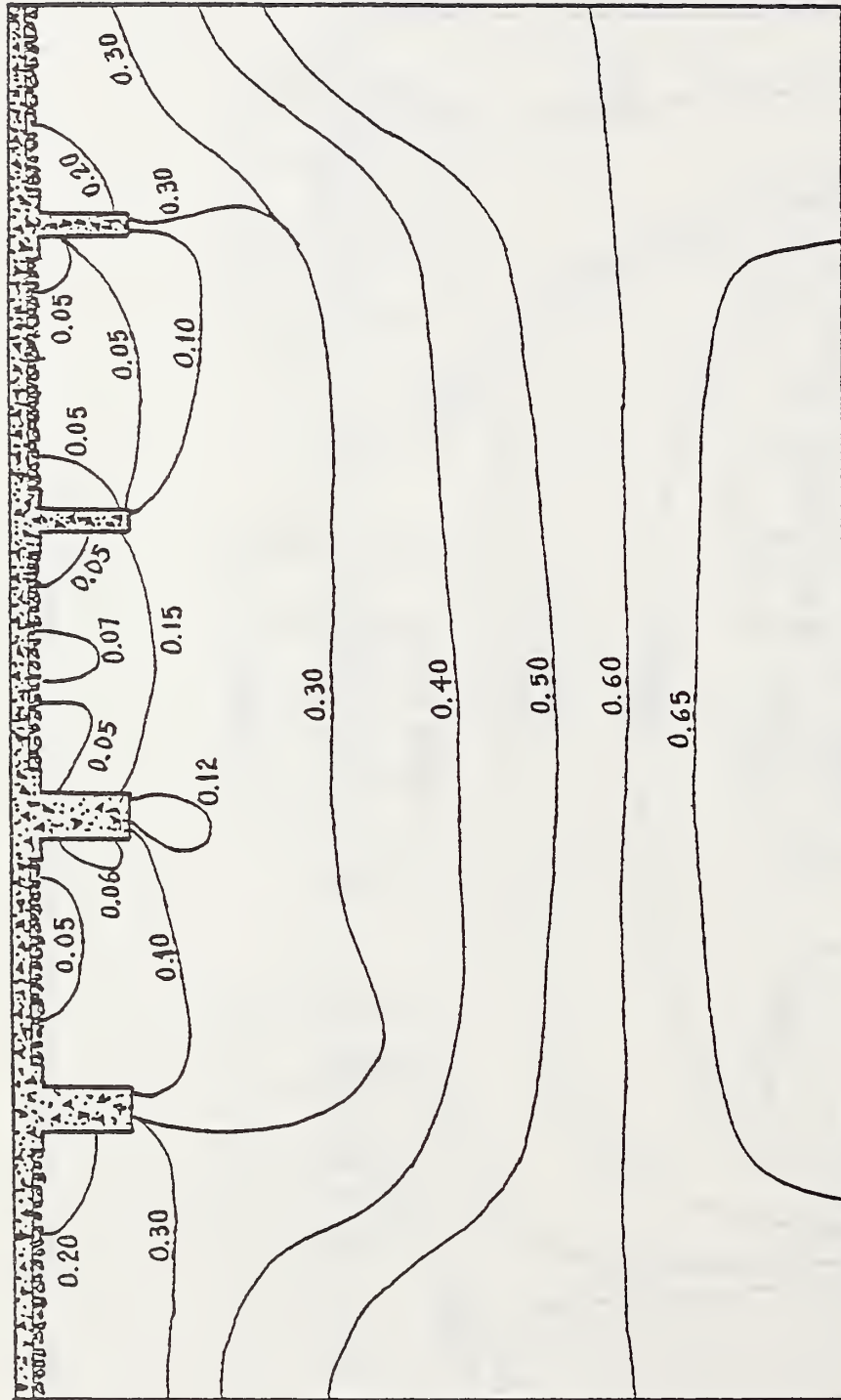
τ_{\max} (psi)

Figure 39. Ballast maximum shear stresses (winter condition)



σ_y (psi)

Figure 40. Soil vertical stress contours (winter condition)



τ_{max} (psi)

Figure 41. Soil maximum shear stress contours (winter condition)

5.3 SUPERPOSITION OF LOADS

For evaluating the general response of the Edens Expressway, the superposition of vehicle loads and environmental loadings was done. This section combines the effects of the previous analyses for a more complete description of the soil/pavement system. The results of the superposition of summer (or winter) extreme conditions with vehicle loads are shown in Figure 42. The results clearly show the significance of the environmentally (thermally) induced deflections - curling. Deflections from curling can be as much as an order of magnitude larger than vehicle imposed deflections.

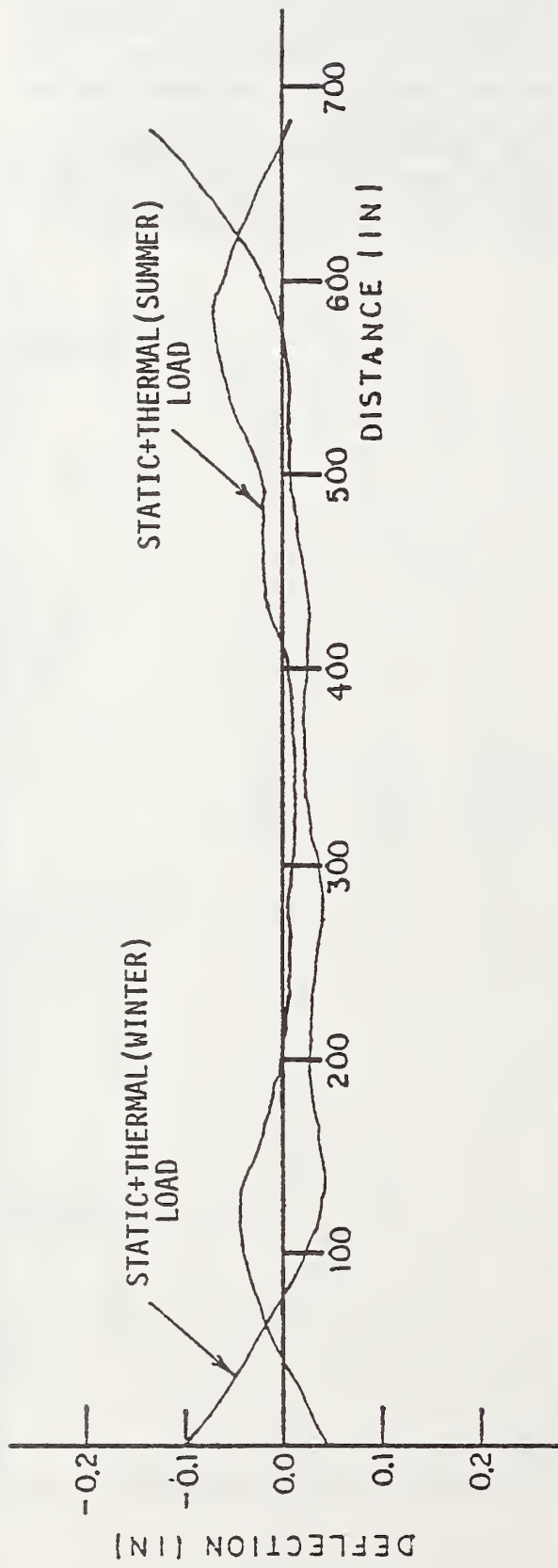


Figure 42. Results of surface deflection load superposition

CHAPTER 6 GUIDELINES FOR CONSTRUCTION

6.1 THE SUBGRADE AND BASE COURSE

This section will deal with excavation and preparation of subgrade and the material selection and layout of crushed stone base course. It may be noted that the intent is not to provide detailed specifications, but only guidelines. Local codes should invariably be used where applicable.

6.1.1 EXCAVATION

The natural subgrade should be excavated to depths required for the installation of permanent construction in such a manner as not to disturb subbase below such depths. Where any other structures, which may cause hard spots are encountered, they should be removed at least two feet below subgrade for pavement or anchors. In case the bottom of excavation be disturbed or carried below required depths, the following procedure is recommended:

- a) under the anchors: compact bottom and replace with concrete (not fiber reinforced concrete);
- b) elsewhere, replace and compact as specified for fill.

The bottom of trenches for utilities, drains, and anchors must be graded to specified elevations. The contact between the anchors and the subgrade must be assured.

Where considered necessary, the sides of excavation should be secured against movement by means of sheeting held in place by means of waling, bracing, or other means. Excavation below the bottom of sheeting should not be performed except where necessary to place the sheeting. Voids in back of sheeting should be immediately back-filled with approved material.

During the excavation, efforts should be made to prevent water from entering the excavated area and if it enters, it should be disposed of immediately to maintain dry conditions at the time of construction. If water enters an excavation and disturbs or weakens the underlying soil, the disturbed material should be excavated, the bottom of excavation compacted, and backfilled. The best precaution is to lower the water in the area of construction to an elevation that is two feet below the elevation of the required excavation, and maintaining this condition until the construction is completed. Dewatering should be accomplished in such a manner so as to prevent the loss of ground due to the migration of soil fines into the excavation.

Where trench excavations are performed into cohesive soils, investigation must be made for heave. If the factor of safety against heave is unsatisfactory, measures as recommended by a local competent soils engineer should be taken.

6.1.2 PROOFROLLING AND TAMPING

After excavation has been performed to the elevation of pavement subgrade, proofrolling is recommended in the entire area in which such excavation has been performed by rolling two passes of a pneumatic tired roller. Under the anchors, instead of proofrolling, tamping may be necessary by mechanical tampers. Proofrolling or tamping may also be required before installing the drains.

6.1.3 BACKFILL

Backfill means the filling of excavations made for the purposes of installing anchors, utilities, and other structure (not including pavement). Backfill usually extends only up to existing grades or up to bottom of excavations, whichever is lower. The materials for backfill should consist of clean sand, gravel, or a mixture of these, with no organic matter, and should have no particles exceeding four inches in largest dimensions. No more than 30% (by weight) of the material shall be retained on a 3/4 inch sieve. The material passing the 3/4 inch sieve shall conform to the following gradation:

<u>Sieve Size</u>	<u>Percent Passing By Weight</u>
3/4 inch	100
No. 10	40-100
No. 40	20-50
No. 80	0-10
No. 200	0-3

Temporary structures such as sheeting, bracings, and forms (as well as organic matter and debris of every nature) should be removed during backfill operations, but care must be taken to remove sheeting in such a manner as not to cause movement of adjacent ground. Backfill should never be placed on a frozen subgrade. Backfill should be compacted by suitable mechanical tampers.

6.1.4 FILL

Fill in this connection shall mean placing of all material to meet grades required by detailed drawings, other than backfill.

Local codes often detail the fill and its placing methodology. However, for the zero-maintenance pavement system, the fill should be of the following gradation:

<u>Sieve Size</u>	<u>Percent Passing By Weight</u>
3/4 inch	100
No. 10	40-100
No. 40	20-85
No. 80	0-20
No. 200	0-3

The fill should be placed in uniform layers not more than eighteen inches and should be compacted to a firm hard surface by a minimum of six passes of a vibratory roller. The equipment should be such as to permit regulation of vibration frequency. The roller shall be operated at a speed not to exceed three miles per hour and at its maximum vibrating frequency. Passes shall overlap a minimum of six inches.

The top layer of fill to receive pavement should be tested with a sixteen foot straight edge and variations corrected.

6.1.5 CRUSHED STONE FOUNDATION COURSE

The most suitable stone for foundation course is quality controlled crushed dolomitic limestone or traprock, free from clay, loam, or other foreign matter. Suitable replacement depending upon local availability can be made. The crushed stone, however, should conform to the following gradation:

<u>Sieve Size</u>	<u>Percent Passing By Weight</u>
1.5 inch	100
3/4 inch	60-100
3/8 inch	40-80
No. 4	25-60
No. 40	10-30
No. 200	2-12

The crushed stone should not be spread unless the subgrade is free of frost and water. The rolling of crushed stone should not be

performed when the water level is above a plane two feet below the bottom of the crushed stone.

The crushed stone should be spread evenly over prepared sub-grade by a suitable equipment capable of spreading stone without segregation of aggregate sizes. It should be spread to a level which will compact to the required top of course. Crushed stone must be spread at or near optimum moisture content. The stone should be compacted immediately, while at or near optimum moisture content by rolling with a minimum of six passes of a vibratory roller operated at a speed not to exceed 3 mp-bank at its maximum operating frequency. To obtain maximum compaction, further rolling by a pneumatic tired roller may be necessary. In areas where use of rollers is impractical, the stone must be compacted at or near optimum moisture content by mechanical tampers.

6.1.6 FILTER MATERIAL

Around the pipes, filter material should be used. The filter material should be a combination of broken stone, gravel and sand with individual particles of tough, rough surfaced grains, free of clay, loam, or other foreign material. It shall conform to the following gradation:

<u>Sieve Size</u>	<u>Percent Passing by Weight</u>
1.5 inch	-
3/4 inch	100
No. 4	70-100
No. 10	50-100
No. 40	20-50
No. 80	0-10
No. 200	0-3

Currently, the use of filter fabrics is prevalent and they have proved successful.

6.2 THE ANCHORED PAVEMENT

A section of the anchored pavement system with anchors, drains and other details, is shown in Fig.43. All dimensions are marked but the scales in vertical and horizontal directions are different to provide clarity. Though all concrete shown in the section is steel fiber reinforced, the portion of anchors below the crushed stone level can be of ordinary concrete (without steel fibers). In case such a scheme is utilized, bonding between the two sections will be required.

6.2.1 ANCHORS

Steel fiber reinforced concrete for the anchors (up to the top of the crushed stone layer) should be made from regular air-entrained Portland cement concrete meeting the requirement of ASTM C94. The cement factor should not be less than 1000 lbs. per cubic yard and the water cement ratio should be around 0.35. These requirements are only for the Chicago area and will have to be modified for other places. The fiber content of the material should be 1.5% by volume.

6.2.2 SLAB

Since the slab is restrained from movement by the anchors, there is a strong possibility of shrinkage cracks at the junction of anchors and slab. It is therefore specified that the slab utilize shrinkage compensating concrete. Shrinkage compensating concrete is an expansive cement concrete in which the expansion, if restrained, induces compressive stresses of high enough magnitude to result in a significant compression in the concrete after drying shrinkage has occurred. Expansive cement concrete is made with commercially available Type K, Type M, or Type S expansive cement. The shrinkage compensating concrete should be used as per the Recommended Practice - ACI Standard 223-77. For a state-of-the-art knowledge in expansive cement concrete, a report by ACI Committee 223 (ACI Journal - August 1970) is recommended. Steel fiber content in the slab should be 1.5% by volume. With this amount of reinforcement, the shrinkage stresses should be minimal.

The top two to three inches of this concrete will be sulphur impregnated. The amount of sulphur is specified to be 10% of the dry weight of concrete. The impregnation technique is similar to the polymer impregnation. Sulphur impregnation though done on minor scale, like bridge decks or so, has not been used in such a large scale.

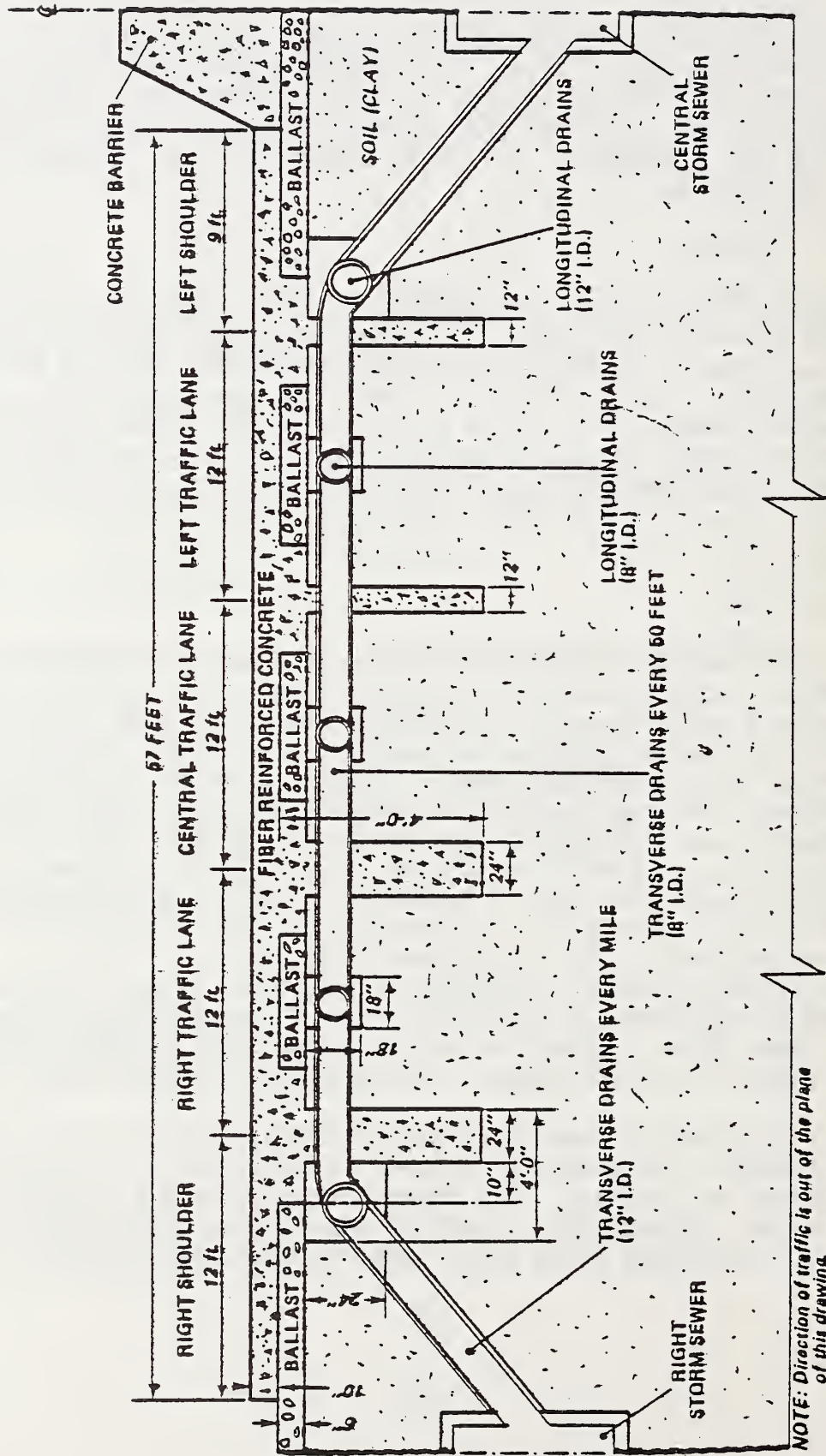


Figure 43. Edens Expressway as an Anchored Pavement Drainage Configuration (typical cross section)

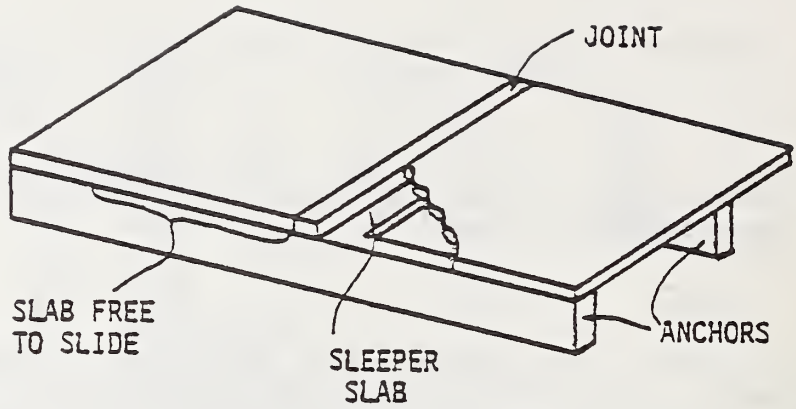
Alternatively, commercially available material like Sealcrete has been successfully used.

6.2.3 JOINT

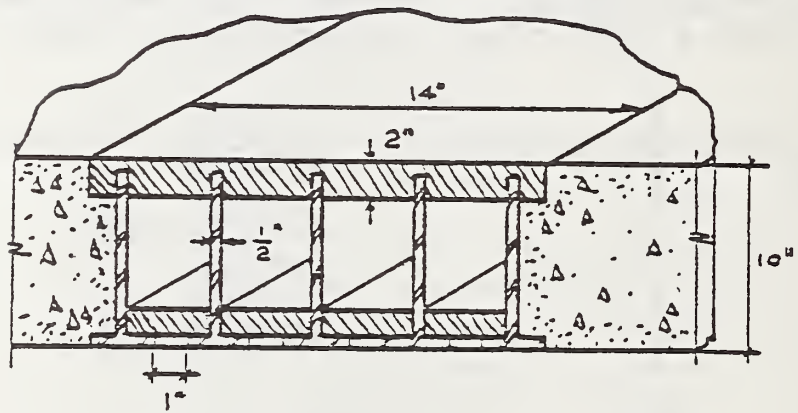
The joint concept cohesion is based upon a system reported by Mogilevich et al. (1976). The joint consists of a set of parallel vertical plates (Fig. 44) coupled together at the tops and bottoms by an elastomeric material to allow flexibility to deform at constant volume.

The joint is assumed to rest on a sleeper slab cast integrally with the anchors. This effectively inhibits water infiltration and should eliminate problems of pumping. The lower surface of the joint structure is frictionless and may freely slide on the sleeper slab.

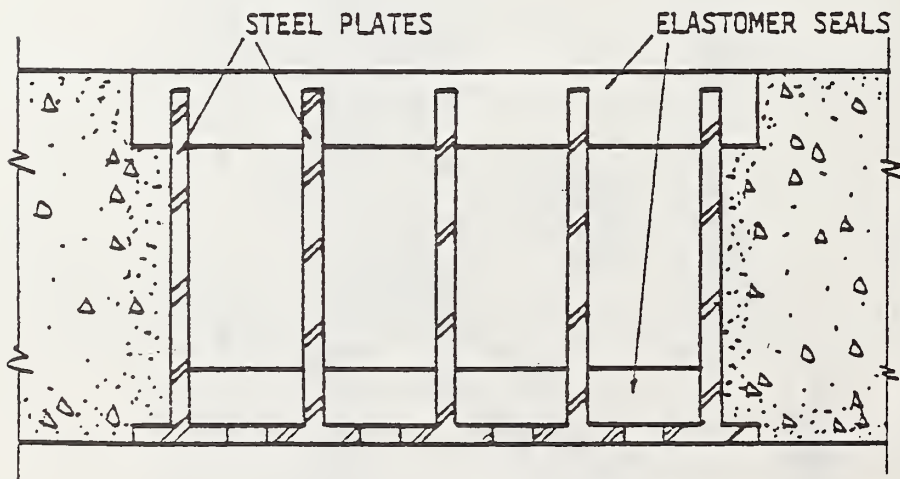
The joints are provided at every 500 ft. intervals for estimating purposes.



a) Overall joint construction of prototype joint in anchored pavement



b) Joint details



c) initial joint model

Figure 44. Results of joint response to slab movement analysis

CHAPTER 7 CONCLUSION

The "Anchored Pavement System" investigated previously by a laboratory model and also analytically by finite element method has been applied to a real life problem. A section of Edens Expressway of Chicago has been analyzed using the "Anchored Pavement System" as an example.

This example will assist an engineer in utilizing the anchored pavement concept to any of the heavily trafficked roads. The computer program used is called ANSYS.

The example problem provides the input parameters of materials and loads for the analysis, the generation of finite element mesh and the results of the analysis. The comparison of Anchored Pavement System with the traditional pavement has not been attempted in this example as the superiority of the anchored pavement (by comparison) has been demonstrated in Volume 1 of this series of reports, entitled Analytical and Experimental Studies of Anchored Pavement: A Candidate Zero-Maintenance Pavement (Saxena, Rosenkranz, and Militisopoulos, 1979). The behavior of the anchored pavement under induced temperature loads and due to weakening of subgrade (by thawing action) has been candidly demonstrated.

The construction guidelines are intended to provide the required background for preparation of detailed specifications for any specific site. Also included in this report are construction cost estimates for an anchored pavement system. These estimates are presented in Appendix C, and a total construction cost estimate is listed on page 112 of Appendix C.

REFERENCES

1. Branson, D. E., "Deformation of Concrete Structures," McGraw-Hill, N. Y., 1977.
2. DeSalvo, G. J. and Swanson, J. A., "ANSYS User's Manual (Rev. 2)," Swanson Analysis Systems, Inc., 1975.
3. DeSalvo, G. J. and Swanson, J. A., "ANSYS User's Manual (Rev. 3)," Swanson Analysis Systems, Inc., 1978.
4. Effects of Temperature and Heat on Engineering Behavior of Soils, Proceedings HRB, Special Report 103, January 1969.
5. "Expansive Cement Concretes - Present State of Knowledge," Report by ACI Committee 223, ACI Journal, August 1970.
6. Hanna, A. N., "Steel Fiber Reinforced Concrete Properties and Resurfacing Applications," PCA Research and Development Bulletin, 1977.
7. Mogilevich, V. M., (Editor), "Prefabricated Highway Pavement," Translated from Russian, Report No. FHWA-RD-76, 1976.
8. Nagataki, Shigeyoshi, "Shrinkage and Shrinkage Restraints in Concrete Pavements," Journal of Structural Division, ASCE, pp. 1333-1357, July 1970.
9. Pavement Analysis for Edens Expressway, Bureau of Design, Cook County Highway Department, 1978.
10. Peck, R. B. and Reed, W. C., "Engineering Properties of Chicago Subsoils," University of Illinois Engineering Experiment Station Bulletin No. 423, Vol. 51, No. 44, February 1954.
11. Plans of Edens Expressway Reconstruction, R.A.I. Rte. 94, Section 1978-006-R, Cook County Highway Department, 1978.
12. Ritter, L. J. and Paquette, R. J., "Highway Engineering," Ronald Press, 1967.
13. Russell, H.G., "Design of Shrinkage - Compensating Concrete Slabs," PCA Research and Development Bulletin, 1973.

REFERENCES (continued)

14. Saxena, S. K., Wang, J. W. H., Udari, J. J., and Rosenkranz, W. J., "Unique Concepts and Systems for Zero-Maintenance Pavements," FHWA-RD-77-76, July 1977.
15. Saxena, S. K. and Militsopoulos, S. G., "Model Study of an Anchored Pavement," M.S. Thesis, October 1978.
16. Saxena, S. K. and Rosenkranz, W. J., "Analysis of Pavement Response to Environmental and Mechanical Loads," M.S. Thesis, October 1978.
17. Saxena, S. K., W. J. Rosenkranz, and Militsopoulos, S. G., Volume 1: "Analytical and Experimental Studies of an Anchored Pavement: A Candidate Zero-Maintenance Pavement," December 1979 (not published yet).
18. Saxena, S. K. and Militsopoulos, S. G., Volume 2: "Analysis of Anchored Pavements Using ANSYS," December 1979 (not published yet).
19. Soils Profile, Section 1978-006-R, Cook County Highway Dept., 1947.
20. Traffic Volumes at Various Locations on Edens Expressway, Bureau of Design, Cook County Highway Department, 1978.

APPENDIX A: METRIC CONVERSION TABLE

Table 11. Metric Conversion Table

$$1 \text{ ton/ft}^2 = 2,205 \text{ lb/ft}^2 = 10,766 \text{ Kg/m}^2$$

$$1 \text{ in}^2/\text{min} = 2.54 \text{ cm}^2/\text{min}$$

$$1 \text{ psi} = 0.0703 \text{ Kg/cm}^2$$

$$1 \text{ }^\circ\text{F} = 1.8^\circ\text{C} + 32$$

$$1 \text{ lb/in}^3 = 27.68 \text{ gr/cm}^3$$

$$1 \text{ ft} = 0.3048 \text{ m}$$

$$1 \text{ in} = 2.54 \text{ cm}$$

$$1 \text{ lb} = 453.59 \text{ gr}$$

$$1 \frac{\text{Btu}}{(\text{hr})(\text{in})(^\circ\text{F})} = \frac{415.4 \text{ Joules}}{(\text{hr})(\text{cm})(1.8^\circ\text{C} + 32)}$$

$$1 \frac{\text{Btu}}{(\text{lb})(^\circ\text{F})} = \frac{2.33 \text{ Joules}}{(\text{gr})(1.8^\circ\text{C} + 32)}$$

APPENDIX B: SUMMARY OF JAPANESE INVESTIGATION OF SHRINKAGE EFFECTS

Investigation of shrinkage effects in concrete pavements in the laboratory and field has been more systematically done in Japan (Nagataki, 1970) than in the U.S.A. The research indicates that it is reasonable to divide the unrestrained unit linear shrinkage strain distribution, ϵ_z , into three strain components.

ϵ_{mean} = mean drying shrinkage strain over the full depth

ϵ_w = warping drying shrinkage strain due to curvature of slab

ϵ_{ij} = internal drying shrinkage strain to prevent distortion of plane section

Effectiveness of restraint in concrete pavement varies for these three strain components. The amount and distribution of drying shrinkage in concrete pavement varies with the local atmosphere, environment (temperature, relative humidity, wind), moisture conditions of subgrade, materials, and mix proportions of concrete, etc. Some observed numbers were

$\epsilon_{\text{mean}} = 110 \times 10^{-6}$ (contraction);

$\epsilon_w = 150 \times 10^{-6}$ (contraction at upper surface); and

$\epsilon_{ij} = 150 \times 10^{-6}$ (swelling strain at bottom of pavement).

It was also observed that most shrinkage stresses in concrete pavement are caused by restraint of ϵ_w and approximate values of these stresses are 230 psi tensile stresses at the surface and 230 psi compressive stresses at the bottom. Use of expansive concrete was found very effective in preventing cracking.

APPENDIX C: CONSTRUCTION COST ESTIMATES

Estimates for the construction costs of an anchored pavement system are given on the following pages. The estimates were prepared by Mr. R. Harnett. Mr. Harnett is a certified estimator and a member of the American Association of Estimators.

The conditions listed below were assumed for the preparation of these estimates.

1. All work will be accomplished during a standard work week for the crafts involved. Provisions for shift work or overtime have not been included.
2. The construction site is level and has been rough graded and compacted to an elevation of 1'-6" below the finished surface of the highway.
3. All construction equipment is available at the site. Provisions for move in and move out of equipment is not included.
4. All prices are essentially current day costs and provisions for escalation have not been included.
5. The cost of detailed engineering has not been included.
6. Contingencies for labor productivity, weather, material quantities, pricing or other unforeseen factors have not been included.
7. Contractors O. H. & P. not included.
8. Steel fiber reinforcement is based on U.S. Steel "Fibercon". The fibrous mix is based on approximately 200 lbs./cy. This equates to a 1-1/2% mix by volume.
9. The fibers are added to the concrete mix in the trucks at the site, not at the batch plant.
10. Concrete prices are based on "Ready-Mix", as phone quoted by Material Services Corp., not local site batch operations.
11. All work relating to storm sewers is not in the scope of this work.
12. Underground drain lines are based on perforated clay pipe.
13. The price of the elastomer seals are estimated due to the problems in obtaining phone quotes.
14. The Richardson Engineering Services, Construction Estimating Standards, 1979 Edition was used as the basis for material and labor subcontract prices.
15. The accuracy of this estimate is in the order of $\pm 15\%$.

ESTIMATE DETAILS

PROJECT Estimate No. 1: Concrete Work for Anchored Pavement, Edens Expressway (1 mile).
 ESTIMATE NO. 1
 SHEET NO. 1 of 5
 PREPARED BY: RJH
 CHECKED BY: _____
 DATE 8-23-79
 DATE _____

DESCRIPTION	QUANTITY	MATERIALS		LABOR		SUB-CONTRACT		TOTAL
		UNIT PRICE	AMOUNT	UNIT/MH	TOTAL MH	DATE	AMOUNT	
(Details for one side only)								
(001) Excavate for Anchors (Using Cleveland J5-36 Trencher)								
(2' x 3.5' x 52.80') 2 =	2738 CY			1.87 CY/MH	220			
(1' x 3.5' x 5280') 2 =	1369 CY			53 CY/MH	22			
Total Excavate	4107 CY				44			4400
(002) Forming for Anchor Pads SF Side Forms/mile = 5280 SF/PAD 2" x 6" = 2 BF/SF - 4000 SF Incl. nails, cleats, etc								
5280 SF/PAD x 4 PADS	21,180 SF	0.38/SF	8,000	1.45/LF	3062			61,200
(003) Sub-grade (Crushed Stone) 6" x 40' x 5280 = 126,720 CF ÷ 27 = 4700 SF	4700 SF							28,200
Fine grade w/12-G CAT & SP-51R Roller	248,200 SF				90			11,000

ESTIMATE DETAILS

PROJECT Estimate No. 1: Concrete Work (cont'd) ESTIMATE NO 1
 SHEET NO 2 of 5 PREPARED BY: RJH DATE 8-23-79
 CHECKED BY: _____ DATE _____

DESCRIPTION	QUANTITY	MATERIALS		LABOR		SUB-CONTRACT		TOTAL
		UNIT PRICE	AMOUNT	UNIT/HR	DATE	UNIT PRICE	AMOUNT	
(000) <u>Farming At Sleeper Joints</u> <u>Face Area/It. - Unformed</u>								
$[(3' \times 5') \times 2 + (2' \times 5') \times 2] \times 10$ $[(2' \times 2.5') \times 2 + (1' \times 3.5') \times 2] \times 10$ ITS = 100 SF = 420 SF 320 SF		2.50/SF	1,300	.15/SF	78	20/HR	1,600	
(002) <u>Farming for Anchors</u> <u>Assume Clean Cut w/ Trenches</u> <u>No Farming Req'd.</u>								
(002) <u>Form Sleepers</u> <u>(10 req'd)</u>								
SF Side forms/Sleeper $(57' \times 1') \times 2 + (2' \times 1') \times 2 = 118$ SF Face area forms sleepers $(57' \times 2') = 114$ SF	1180 SF 1140 SF	0.38/SF 2.50/SF	450 2900	.145/LF .15/SF	171 177	20/HR 20/HR	3400 3400	
(001) <u>Concrete (steel fiber reinf)</u> <u>Anchors</u> $(2 \times 3.5 \times 5.280') \times 2 = 73,920$ CF $(1 \times 3.5 \times 5.280') \times 2 = 36,960$ 110,880 CF @ 22'	4100 CF	-	-	0.25/Y	1230	20/HR	24,600	

ESTIMATE DETAILS

PROJECT Estimate No. 1, Concrete Work (cont'd)
 ESTIMATE NO. 1
 SHEET NO. 3 of 5
 PREPARED BY: JRH DATE 9-23-78
 CHECKED BY: _____ DATE _____

DESCRIPTION	QUANTITY	MATERIALS		LABOR			SUB-CONTRACT		TOTAL
		UNIT PRICE	AMOUNT	UNIT III	TOTAL HRS.	DATE	AMOUNT	UNIT PRICE	
Concrete (steel fiber reinf) cont'd									
Asobar Pads (3 X .5 X 52.80) 2 = 15840 CF (2 X .5 X 52.80) 2 = 10560 26,400 CF @ 27	980 CY	-	-	0.3 / CY	294			20 ⁰⁰ / HR	5,900
Sleepers (57' X 1' X 2') 10 = 1140 CF @ 27	45 CY	-	-	0.3 / CY	14			20 ⁰⁰ / HR	300
Main Roadway 57' X 10" X 52.80 = 250,800 CF @ 27	9300 CY								
Subtotal Concrete	14,425 CY								
Slop, Spills, etc. @ 19%	145 CY								
	14,570 CY	40 CY Ready mix	582,800						
(Using CMI Paver) Note: Assume Equip. @ site No move & out costs for trencher, scarper, paver									

ESTIMATE DETAILS

PROJECT Estimate No. 1: Concrete Work (cont'd)

ESTIMATE NO. 2
 SHEET NO. 4 of 5
 PREPARED BY: RJH
 CHECKED BY:
 DATE 8-21-28

DESCRIPTION	QUANTITY	MATERIALS		UNIT MH	TOTAL MH	LABOR		SUB-CONTRACT		TOTAL
		UNIT PRICE	AMOUNT			DATE	AMOUNT	UNIT PRICE	AMOUNT	
(004) Steel Fiber Reinforcing										
1 1/2" Dia. 30" Wl = 800 lb/cy										
300 lb/cy x 14,570 cy =	2,914,000 lb	0.265/lb	732,200		-					
F.O.B. Hammond, INVD										
FRT to Site										
8000 #/Pallet x 22/Pallet = 66 Truck loads		1.00/cwt	30,000		-					
Shaker Provided by U.S. Steel at no cost.										
Unload & Pour on Shaker										
50 lb. Boxes	58,280 Boxes				971			20/HR	19,500	
Assume 1 box/Min =										
(005) Concrete (Sulfer Impreg)										
Finish Surface - 2" T										
.57' x 9" x 580 = 50,160 CF (±)	1858 CY	40/CY Ready-Mix	74,300	.01/CY	18			350/HR	6,300	
Molten Sulfer										
Based on 10% dry weight of Conc.										
Dry Conc. ~ 500 lb/CY.										
∴ Sulfer = 50 lb/CY.										
50 lb/CY x 1858 CY = 92,900 lb = 2000	46.5 Short T.									
46.5 T.T. x 1.1 = 51.1 T	51 Long Ton	54/L.T.	2,800	.04/CY	743			20.00/HR	14,900	

ESTIMATE DETAILS

PROJECT Estimate No. 1: Concrete Work (cont'd)

ESTIMATE NO. 1

SHEET NO. 5 of 5

PREPARED BY: RJH DATE: 8-23-

CHECKED BY: _____ DATE: _____

DESCRIPTION	QUANTITY	MATERIALS		LABOR		SUB-CONTRACT		TOTAL
		UNIT PRICE	AMOUNT	UNIMH	TOTAL MH	DATE	UNIT PRICE	
(008) Strip Form Work Assume 10% of install time		-	-		350		20/HR	7000
(001) Haul Excavated Material 1.45 X 4102CY = 5955 CY @ 60 = 357300								
10CY Trucks @ 99 = 0.10 MIN SPOT " = 0.50 " DUMP " = 2.00 " Travel Time $\frac{7.00}{8.60}$ "								
60 @ 2.60 = 156 Loads/HR X 10 62.5 CY/HR								
30/HR @ 62.5 = 1875 CY	5299CY	-	-	82.5/HR	95		0.49/CY	2900
TOTAL CONCRETE WORK - 1	Side		4,424,750		7350			208,300
and	Side		1,434,750		7350			808,300
TOTAL			2,899,500		14,700			416,600
								3,266,1

ESTIMATE DETAILS

PROJECT Estimate No. 2; Draining Elbow for Anchored ESTIMATE NO. 2
Pavement, Edens Express way SITE NO. 1 of 4
(1 mile) PREPARED BY: RJH DATE 8-25-7
Vitrified Clay Pipe - Slip Joint Type, Rectangular CHECKED BY: DATE

DESCRIPTION	QUANTITY	MATERIALS		UNIT MI	TOTAL MI	DATE	AMOUNT	SUB-CONTRACT		TOTAL
		UNIT PRICE	AMOUNT					UNIT PRICE	AMOUNT	
(006)										
<u>Longitudinal Drains - 1 side</u>										
<u>(5'-0" bay lengths)</u>										
8" Pipe 5280' x 3 =	10,560 LF	2.53/LF	26,717	16,1000 LF (REW)	16.9			80/HR (REW)	13,530	
6" Pipe 5280' x 3 =	15,840 LF	1.81/LF	28,670	"	2.53				26,240	
8" Joints	812	-	-	Incl.	above			Incl.	above	
6" Joints	3168	-	-	"	"			"	"	
<u>Transverse Drains - 1 side</u>										
6" Pipe 30' x 105	3150 LF	1.11/LF	5,700	16,1000 LF (REW)	6.3			80/HR (REW)	5040	
6" WYE 6' x 105	630	12.10/EA	7,623	0.30/EA	1.89			25/EA	15750	
6" x 8" Increaser 3x2	6	13.25/EA	74	0.33/EA	2			30/EA	180	
8" Pipe 40' x 8	80 LF	2.53/LF	202	-	1.0			80/HR (REW)	800	
8" TEE 5' x 2	10	21.80/EA	218	0.33/EA	3			30/EA	300	
8' x 12" Increaser 4x2	8	27.40/EA	219	0.40/EA	3			37/EA	296	
12" TEE 8' x 2	0	52.30/EA	-	0.40/EA	-			37/EA	-	
12" PIPE 30' x 2	60 LF	5.50/LF	390	-	1.0			80/HR (REW)	800	
18" 1/2 Bends 2 x 2	4	27.40/EA	110	0.40/EA	2			37/EA	148	
16" Joints 6.30 x 3 + 6	1996	-	-	Incl.	above			Incl.	above	
8" Joints 16 + (6 x 3) + 6	42	-	-	"	"			"	"	
18" Joints 12 + 8 + (4 x 3) + 2	40	-	-	"	"			"	"	

(See Figure 45)

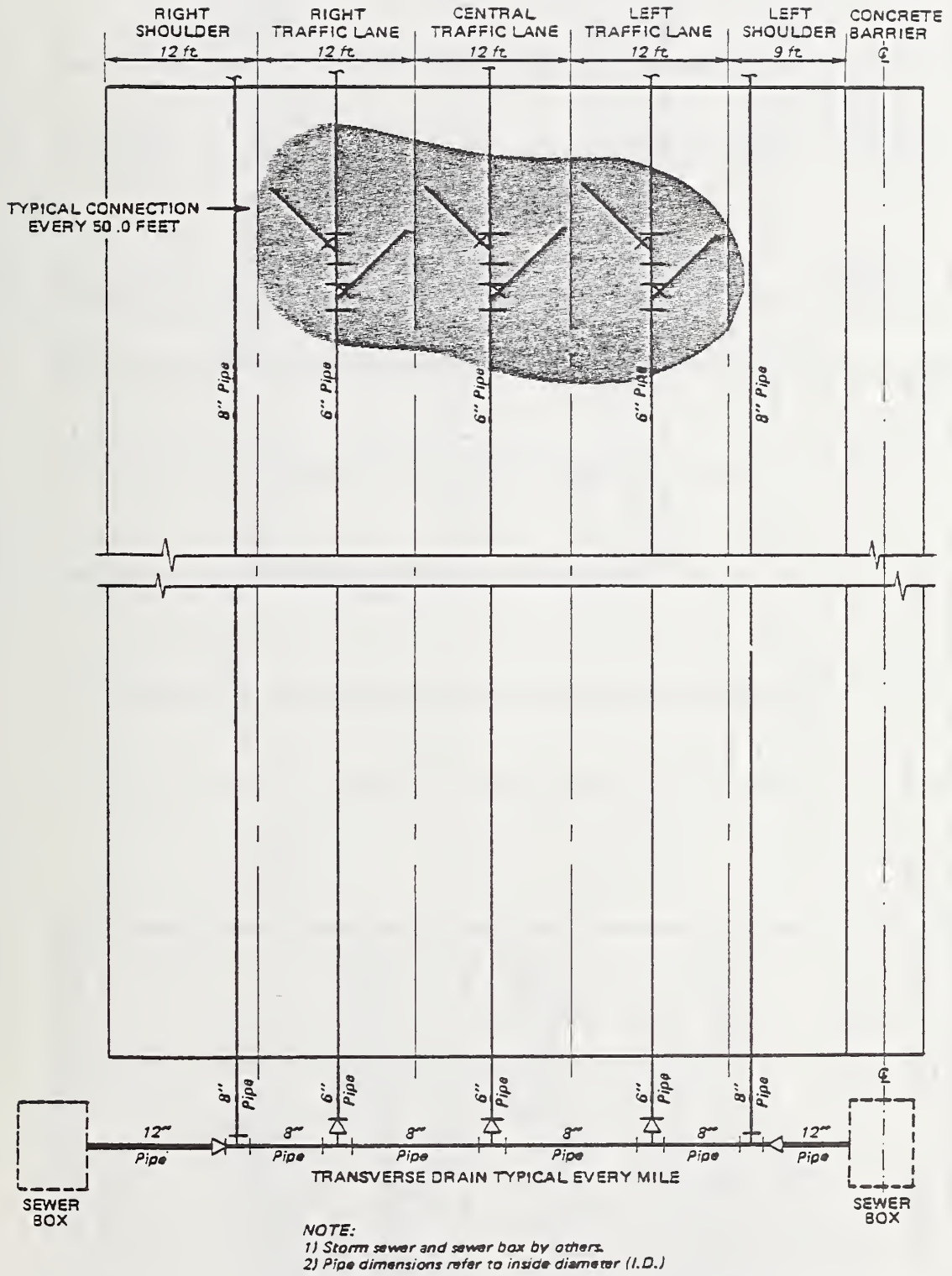


Figure 45. Drainage Work for Anchored Pavement, Edens Expressway

ESTIMATE DETAILS

PROJECT Estimate No. 2: Drainage Work (cont'd) ESTIMATE NO. 2
 SHEET NO. 3 of 4 PREPARED BY: PJA DATE 8-26-78
 CHECKED BY: _____ DATE _____

DESCRIPTION	QUANTITY	MATERIALS		LABOR		SUB-CONTRACT		TOTAL
		UNIT PRICE	AMOUNT	UNIT/HR	TOTAL HR	UNIT PRICE	AMOUNT	
<u>Trenching (Steelband JS-36 Trencher)</u>								
<u>6" Pipe. (5,240 + 3450) x 1.5' x 1.5'</u>	<u>1583 CY</u>	-	-	<u>110 CY/HR</u>	<u>15</u>	<u>180/HR.</u>	<u>1500</u>	
<u>8" Pipe. (20,560 + 10) x 2 x 2</u>	<u>1576 CY</u>	-	-	<u>118 CY/HR</u>	<u>11</u>	<u>185/HR.</u>	<u>1100</u>	
<u>Excavate for 12" Pipe (Case 580 Back hoe 60/18" Bucket)</u>								
<u>(10' x 10' x 6') 2 x 2 + (10' x 4' x 16') 4</u>	<u>163 CY</u>	-	-	<u>11.5 CY/HR</u>	<u>14</u>	<u>75/HR</u>	<u>1050</u>	
<u>Backfill for 12" Pipe (CAT 930 Loader & PANTIRE Compactor)</u>								
<u>Clean Sand</u>	<u>161 CY</u>	-	-	<u>40 CY/HR</u>	<u>4</u>	<u>5/CY</u>	<u>200</u>	
<u>163 CY - (181 x $\frac{1}{4}$ x $\frac{50}{27}$) =</u>	<u>161 CY</u>	-	-			<u>60/HR</u>	<u>240</u>	

ESTIMATE DETAILS

PROJECT Estimate No. 2: Drainage Work (cont'd) ESTIMATE NO. 2
 SHEET NO. 3 of 4 PREPARED BY: RJH DATE 8-2-77
 CHECKED BY: _____ DATE _____

DESCRIPTION	QUANTITY	MATERIALS		LABOR		SUB-CONTRACT UNIT PRICE	TOTAL
		UNIT PRICE	AMOUNT	UNIT/MIL	TOTAL MIL		
<u>Half Excavated Material - 1 mile</u>							
$1.45 (163 + 1583 + 1576) = 4817 \text{ CY} \div 60$	$= 80.3 \text{ CY/MIN}$						
$10 \text{ CY Truck} \div 80.3 = 0.12 \text{ MIN}$							
$\text{SPOT Truck} = 0.50 \text{ ''}$							
$\text{Dump returning} = 2.00 \text{ ''}$							
$\text{Travel time} = 7.00 \text{ ''}$							
9.52 ''							
$60 \div 9.52 = 6.28 \text{ Loads/HR}$							
$6.28 \times 10 = 62.8 \text{ CY/HR}$							
$4817 \text{ CY} / \text{HR} = 62.8 \text{ HR} = 62.8 \text{ CY/HR}$	4817 CY	-	-	62.8 CY/HR	77	6300	
<u>Ballast Around Pipe</u>							
$\left[\frac{15}{4} \left(\frac{9}{12} \right)^2 \right] \times 2 \times 280 = 38,54 \text{ HCF}$							
$\left[\frac{57}{4} \left(\frac{6}{12} \right)^2 \right] \times 1.5 \times 15 \times 2 \times 620 = 32,530$							
$\left[\frac{11}{4} \left(\frac{6}{12} \right)^2 \right] \times 1.5 \times 15 \times 3150 = 1,392$	2684 CY	-	-			$600/\text{CY}$	$16,100$
$72,466 \text{ CF} \div 27$							

ESTIMATE DETAILS

PROJECT Estimate No. 2: Drainage Work (cont'd)

ESTIMATE NO. 2
 SHEET NO. 2 of 4
 PREPARED BY: V RSH DATE 8-26-78
 CHECKED BY: _____ DATE _____

DESCRIPTION	QUANTITY	MATERIALS		TOTAL MH	LABOR DATE	AMOUNT	SUB-CONTRACT		TOTAL
		UNIT PRICE	AMOUNT				UNIT PRICE	AMOUNT	
Subtotal 1st side			69,923	825				80,164	
2nd side			69,923	825				80,164	
Add for perforated pipe 2 30% Misc.			41,954					172	
TOTAL PROJECT PIPING			181,800	1650				160,500	342,300

ESTIMATE DETAILS

PROJECT Estimate No. 3: Expansion Joints for Anchored
Pavement, Edens Expressway
 (1 mile)

ESTIMATE NO. 3
 SHEET NO. 1 of 2
 PREPARED BY: RLK DATE 9-4-78
 CHECKED BY: _____ DATE _____

DESCRIPTION	QUANTITY	MATERIALS		LABOR		SUB-CONTRACT		TOTAL
		UNIT PRICE	AMOUNT	UNIT PRICE	AMOUNT	UNIT PRICE	AMOUNT	
(001) (Details for 1 Side)								
Steel Plates (1/2 PL)								
$(9' \times 57') \times 5 \times 10 \text{ Jts.} = 2138 \text{ SF}$ $(2' \times 57') \times 5 \times 10 \text{ Jts.} = 475 \text{ SF}$ <u>2613 SF</u>								
$2613 \text{ SF} \times 204 \text{ SF} = 2000 \text{ 16/T}$ (Fabricated Cost/Ton)	26.7 T	2004/T	56,000					
<u>Elastomer Seals</u>								
$(2" T. \times 14" W.) \quad 57' \times 10 = 570 \text{ LF}$ $(2" T. \times 2.5" W.) \quad 57' \times 4 \times 10 = 2280 \text{ LF}$ (Estimated Costs)	665 SF 475 SF	10/SF 10/SF	6,650 4,750					
<u>Assemble Joint</u>								
$\text{Steel/SF} = 5.330^{\#}$ $\text{Seals/SF} = 2.85 \text{ LF}$	10 Jts 10 Jts							
<u>Install Joints</u>	30 ton							
$\sim 3T / \text{SF} \times 1034$								
				40/SF	400	25/HR	10,000	
				10/T	300	20/HR	6,000	

ESTIMATE DETAILS

PROJECT Estimate No. 3: Expansion Joints (cont'd) ESTIMATE NO. 3
 SHEET NO. 2 of 2
 PREPARED BY: RJH DATE 9-4-78
 CHECKED BY: _____ DATE _____

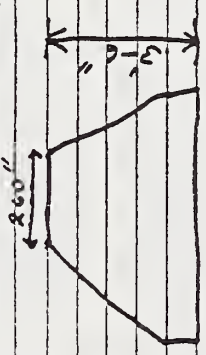
DESCRIPTION	QUANTITY	MATERIALS		LABOR		SUB-CONTRACT		TOTAL	
		UNIT PRICE	AMOUNT	UNIT MIL	TOTAL MIL	DATE	AMOUNT		UNIT PRICE
<u>Poly Filer Sheet liner</u>									
<u>1.5' x 57' x 10,15' = 855 SF + Waste</u>	<u>1000 SF</u>	<u>-</u>	<u>-</u>		<u>10</u>			<u>0.80/SF</u>	<u>800</u>
<u>Installed</u>									
<u>Subtotal</u>			<u>67,400</u>		<u>710</u>				<u>16,800</u>
			<u>67,400</u>		<u>710</u>				<u>16,800</u>
<u>TOTAL EXPANSION JOINTS</u>			<u>134,800</u>		<u>1420</u>				<u>33,600</u>
									<u>68,400</u>

ESTIMATE DETAILS

PROJECT Estimate No. 4: Concrete/Work - Center Barrier
for Anchored Pavement,
Edens Expressway (1 mile).

ESTIMATE NO. 4
 SHEET NO. 1 of 1
 PREPARED BY: RJA DATE 8-22-79
 CHECKED BY: _____ DATE _____

DESCRIPTION	QUANTITY	MATERIALS		LABOR		SUB-CONTRACT	TOTAL
		UNIT PRICE	AMOUNT	UNIT PRICE	AMOUNT		
<p><u>(00P) Central Barrier</u></p> <p><u>Based on Accast, Double</u></p> <p><u>Faced.</u></p> <p><u>340 LF/Day Output for 500' x 26" x 12" Barrier</u></p> <p><u>5280 ÷ 340 = 15.5 Days x 500' = 2640 LF</u></p>	<u>5280 LF</u>	<u>19/LF</u>	<u>100,300</u>	<u>0.164/1.5</u>	<u>868</u>	<u>50/LF</u>	<u>266,400</u>
							<u>126,700</u>



FEDERALLY COORDINATED PROGRAM (FCP) OF HIGHWAY RESEARCH AND DEVELOPMENT

The Offices of Research and Development (R&D) of the Federal Highway Administration (FHWA) are responsible for a broad program of staff and contract research and development and a Federal-aid program, conducted by or through the State highway transportation agencies, that includes the Highway Planning and Research (HP&R) program and the National Cooperative Highway Research Program (NCHRP) managed by the Transportation Research Board. The FCP is a carefully selected group of projects that uses research and development resources to obtain timely solutions to urgent national highway engineering problems.*

The diagonal double stripe on the cover of this report represents a highway and is color-coded to identify the FCP category that the report falls under. A red stripe is used for category 1, dark blue for category 2, light blue for category 3, brown for category 4, gray for category 5, green for categories 6 and 7, and an orange stripe identifies category 0.

FCP Category Descriptions

1. Improved Highway Design and Operation for Safety

Safety R&D addresses problems associated with the responsibilities of the FHWA under the Highway Safety Act and includes investigation of appropriate design standards, roadside hardware, signing, and physical and scientific data for the formulation of improved safety regulations.

2. Reduction of Traffic Congestion, and Improved Operational Efficiency

Traffic R&D is concerned with increasing the operational efficiency of existing highways by advancing technology, by improving designs for existing as well as new facilities, and by balancing the demand-capacity relationship through traffic management techniques such as bus and carpool preferential treatment, motorist information, and rerouting of traffic.

3. Environmental Considerations in Highway Design, Location, Construction, and Operation

Environmental R&D is directed toward identifying and evaluating highway elements that affect

the quality of the human environment. The goals are reduction of adverse highway and traffic impacts, and protection and enhancement of the environment.

4. Improved Materials Utilization and Durability

Materials R&D is concerned with expanding the knowledge and technology of materials properties, using available natural materials, improving structural foundation materials, recycling highway materials, converting industrial wastes into useful highway products, developing extender or substitute materials for those in short supply, and developing more rapid and reliable testing procedures. The goals are lower highway construction costs and extended maintenance-free operation.

5. Improved Design to Reduce Costs, Extend Life Expectancy, and Insure Structural Safety

Structural R&D is concerned with furthering the latest technological advances in structural and hydraulic designs, fabrication processes, and construction techniques to provide safe, efficient highways at reasonable costs.

6. Improved Technology for Highway Construction

This category is concerned with the research, development, and implementation of highway construction technology to increase productivity, reduce energy consumption, conserve dwindling resources, and reduce costs while improving the quality and methods of construction.

7. Improved Technology for Highway Maintenance

This category addresses problems in preserving the Nation's highways and includes activities in physical maintenance, traffic services, management, and equipment. The goal is to maximize operational efficiency and safety to the traveling public while conserving resources.

0. Other New Studies

This category, not included in the seven-volume official statement of the FCP, is concerned with HP&R and NCHRP studies not specifically related to FCP projects. These studies involve R&D support of other FHWA program office research.

* The complete seven-volume official statement of the FCP is available from the National Technical Information Service, Springfield, Va. 22161. Single copies of the introductory volume are available without charge from Program Analysis (HRD-3), Offices of Research and Development, Federal Highway Administration, Washington, D.C. 20590.

DOT LIBRARY



00056784

